An Overview of the Past, Present and Future of Gravity-Wave Drag Parametrization for Numerical Climate and Weather Prediction Models

Survey Article

Young-Joon Kim[1*], Stephen D. Eckermann[2] and Hye-Yeong Chun[3]

[1]*Naval Research Laboratory, Marine Meteorology Division*
7 Grace Hopper Ave., Stop 2
Monterey, CA 93943, USA
[2]*Naval Research Laboratory, Space Science Division*
E. O. Hulburt Center for Space Research
Washington, DC, USA
[3]*Yonsei University, Department of Atmospheric Sciences, Seoul, Korea*

[Original manuscript received 7 March 2002, in revised form 18 October 2002]

ABSTRACT *An overview of the parametrization of gravity wave drag in numerical weather prediction and climate simulation models is presented. The focus is primarily on understanding the current status of gravity wave drag parametrization as a step towards the new parametrizations that will be needed for the next generation of atmospheric models. Both the early history and latest developments in the field are discussed. Parametrizations developed specifically for orographic and convective sources of gravity waves are described separately, as are newer parametrizations that collectively treat a spectrum of gravity wave motions. The differences in issues in and approaches for the parametrization of the lower and upper atmospheres are highlighted. Various emerging issues are also discussed, such as explicitly resolved gravity waves and gravity wave drag in models, and a range of unparametrized gravity wave processes that may need attention for the next generation of gravity wave drag parametrizations in models.*

RÉSUMÉ *[Traduit par la rédaction] Le présent article donne un aperçu de la paramétrisation de la traînée due aux ondes de gravité dans les modèles numériques de prévision météorologique et de simulation du climat. Il est axé principalement sur la compréhension de l'état actuel de la paramétrisation de la traînée due aux ondes de gravité en vue des nouvelles paramétrisations qui seront nécessaires pour la prochaine génération de modèles de l'atmosphère. Les débuts ainsi que les développements les plus récents de la science sont examinés. Les paramétrisations développées expressément pour les ondes de gravité orographiques et les ondes de gravité résultant de la convection sont décrites, de même que les paramétrisations plus récentes visant collectivement une gamme de mouvements des ondes de gravité. Les différences dans les préoccupations et les méthodes propres à la paramétrisation de l'atmosphère inférieure et de l'atmosphère supérieure sont soulignées. Des préoccupations nouvelles sont examinées, notamment les ondes de gravité et la traînée due aux ondes de gravité explicitement résolues dans les modèles, ainsi qu'une gamme de processus associés aux ondes de gravité qui ne sont pas paramétrisés mais dont il faudra éventuellement tenir compte dans la prochaine génération de paramétrisations de la traînée due aux ondes de gravité dans les modèles.*

1 Introduction

There have been considerable advances in the numerical prediction of weather ever since Lewis Fry Richardson attempted the first weather prediction during World War I. With the advance of human knowledge and the advent of state-of-the-art computing technologies, it is becoming more feasible to tackle the formidable problem of accurate numerical weather and climate prediction.

Although the efforts to solve the problem of numerical weather prediction (NWP) are severely hindered by limitations in physical theories, mathematical techniques and computational expense, significant developments have been achieved in all the areas of the atmospheric sciences. Many concurrent efforts are being made to represent the physical processes of the atmosphere more accurately and more efficiently, along with parallel efforts to solve the system of equations governing the atmosphere more accurately and more efficiently in NWP and general circulation models (GCMs). Contemporary NWP and climate models are now

*Corresponding author's e-mail: kimyj@nrlmry.navy.mil

© Canadian Meteorological and Oceanographic Society

Report Documentation Page

Form Approved
OMB No. 0704-0188

Public reporting burden for the collection of information is estimated to average 1 hour per response, including the time for reviewing instructions, searching existing data sources, gathering and maintaining the data needed, and completing and reviewing the collection of information. Send comments regarding this burden estimate or any other aspect of this collection of information, including suggestions for reducing this burden, to Washington Headquarters Services, Directorate for Information Operations and Reports, 1215 Jefferson Davis Highway, Suite 1204, Arlington VA 22202-4302. Respondents should be aware that notwithstanding any other provision of law, no person shall be subject to a penalty for failing to comply with a collection of information if it does not display a currently valid OMB control number.

1. REPORT DATE	2. REPORT TYPE	3. DATES COVERED
18 OCT 2002		**00-00-2002 to 00-00-2002**

4. TITLE AND SUBTITLE	5a. CONTRACT NUMBER
An Overview of the Past, Present and Future of Gravity-Wave Drag Parametrization for Numerical Climate and Weather Prediction Models	5b. GRANT NUMBER
	5c. PROGRAM ELEMENT NUMBER
6. AUTHOR(S)	5d. PROJECT NUMBER
	5e. TASK NUMBER
	5f. WORK UNIT NUMBER
7. PERFORMING ORGANIZATION NAME(S) AND ADDRESS(ES) **Naval Research Laboratory,E.O. Hulburt Center for Space Research,Washington,DC,20375**	8. PERFORMING ORGANIZATION REPORT NUMBER
9. SPONSORING/MONITORING AGENCY NAME(S) AND ADDRESS(ES)	10. SPONSOR/MONITOR'S ACRONYM(S)
	11. SPONSOR/MONITOR'S REPORT NUMBER(S)

12. DISTRIBUTION/AVAILABILITY STATEMENT
Approved for public release; distribution unlimited

13. SUPPLEMENTARY NOTES

14. ABSTRACT
see report

15. SUBJECT TERMS

16. SECURITY CLASSIFICATION OF:			17. LIMITATION OF ABSTRACT	18. NUMBER OF PAGES	19a. NAME OF RESPONSIBLE PERSON
a. REPORT **unclassified**	b. ABSTRACT **unclassified**	c. THIS PAGE **unclassified**	**Same as Report (SAR)**	**34**	

successful in simulating major observed mean features of the atmosphere. However, even the most up-to-date models often suffer from some unrealistic aspects of their simulated atmospheres. Notable examples are the "cold-pole" problems associated with an unrealistically strong polar night jet in the stratosphere (e.g., Shepherd, 2000) which is closely linked to excessively zonal and strong surface westerlies (also called the "westerly bias"), as first noted in the northern hemisphere winter (e.g., Palmer et al., 1986).

Aside from the theoretical deficiencies, even the most powerful available computing architectures still cannot run typical NWP or climate models fast enough to resolve all relevant scales of atmospheric motion. At present, global models must, in practice, be run with horizontal resolutions that cannot typically resolve atmospheric phenomena shorter than ~10–100 km or greater for weather prediction and ~100–1000 km or greater for climate prediction. Many atmospheric processes have shorter horizontal scales than these, and some of these "subgrid-scale" processes interact with and affect the larger-scale atmosphere in important ways. Since they cannot be resolved, large-scale models must resort to "parametrizations" that capture the salient effects on the resolved atmosphere.

Atmospheric gravity waves are one such unresolved process. These waves are generated by lower atmospheric sources, e.g., flow over irregularities at the Earth's surface such as mountains and valleys, uneven distribution of diabatic heat sources associated with convective systems, and highly dynamic atmospheric processes such as jet streams and fronts. The dissipation of these waves produces synoptic-scale body forces on the atmospheric flow, known as "gravity-wave drag" (GWD), which affects both short-term evolution of weather systems and long-term climate. However, the spatial scales of these waves (in the range of ~5–500 km horizontally) are too short to be fully captured in models, and so GWD must be parametrized. It is now generally agreed that the westerly bias in models can be alleviated, to some extent, with a suitable parametrization of GWD (e.g., Boville, 1995). While the adequacy of some aspects of the formulations (and even the necessity of such a parametrization for westerly bias) is still in debate (Pawson et al., 1998; Newman et al., 2001), the role of GWD in driving the global middle atmosphere circulation and thus global mean wind/temperature structure is well established. Thus, GWD parametrizations are now critical components of virtually all large-scale atmospheric models.

The parametrization of the effects of atmospheric gravity waves has evolved into branches with their own (interrelated) backgrounds, histories and communities. This paper attempts to provide a global overview of the past, present and foreseeable future in the parametrization of gravity wave effects in NWP and climate models, with the emphasis on GWD. Throughout this paper we will continue to use the common term "gravity wave drag" to describe the forces exerted on the atmosphere by gravity wave dissipation, despite its shortcomings: "drag" implies a deceleration of the flow, whereas the body forces on the flow produced by gravity wave dissipation can either accelerate or decelerate (retard or reverse) atmospheric winds. This broader definition of GWD should be kept in mind throughout this article (Appendix Ad3 has further details).

Section 2 discusses the early history of and motivations behind GWD parametrization. Section 3 reviews parametrizations of gravity waves from two important sources: mountains and convection. Section 4 discusses newer parametrizations originally designed for middle atmospheric models that are now being applied more widely. Methods of evaluating these parametrization schemes are discussed in Section 5. Since some gravity waves are being resolved in new high-resolution models, we review some of these findings in Section 6. Section 7 discusses a number of specific issues that may need to be considered in future development work. The overall situation is briefly summarized in Section 8.

Given that this is an overview paper, many details will necessarily be omitted. Appendix A provides a brief tour through common nomenclature, concepts and dynamical theories of gravity waves relevant to GWD parametrization. Those readers who are new to this topic may wish to read this Appendix before proceeding to the next section. In addition, references are provided to the relevant parts of Appendix A in the following sections, to aid readers who may need theoretical background on certain topics. Readers needing more detailed background on atmospheric gravity waves can find it in various texts (e.g., Gossard and Hooke, 1975; Gill, 1982; Andrews et al., 1987; Baines, 1995) and review articles (Smith, 1979, 2001; Fritts, 1984; Hamilton, 1998; Fritts and Alexander, 2003). Additionally, the basic ways in which GWD drives global atmospheric circulation features have been described quite well in a number of review articles (e.g., Andrews, 1987; Holton and Alexander, 2000; McIntyre, 2001). Subsequent sections and Appendix A also provide citations to key review papers on specific subject matter in greater detail. Finally, Appendix B lists the acronyms and symbols used in this paper.

2 Birth of gravity wave drag parametrization

a *Misrepresented Damping Mechanisms in Models*

The earliest large-scale models with relatively low resolutions and low model tops seemed to simulate observed features of the subtropical jet quite well, at least for the northern hemisphere winter (e.g., Kasahara et al., 1973). With increased spatial resolution, however, the simulated jet became excessively strong. Studies initially investigated whether underestimated surface friction drag contributed mostly to this wind bias (Swinbank, 1985). If friction drag is, say, underestimated, surface drag due to grid-scale mountains can take over what should have been represented by friction drag and in turn be overestimated in a model in order to maintain the global angular momentum balance. Studies soon concluded that underestimated friction drag was not the main cause of the bias, mainly because friction drag is not easily enhanced under the stable atmospheric conditions of winter for which

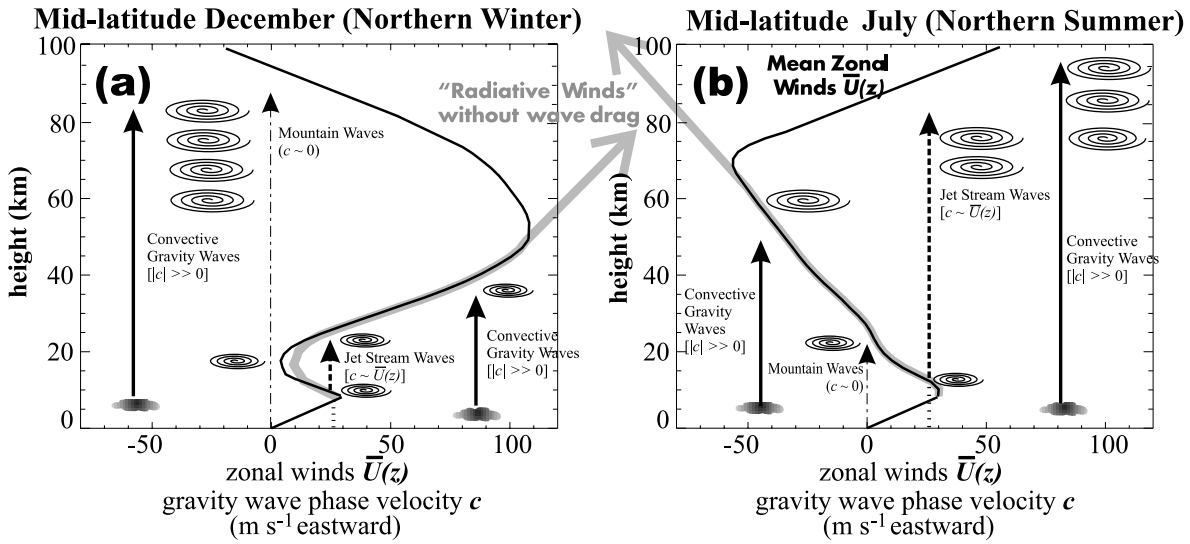

Fig. 1 Typical mid-latitude zonal winds $\bar{U}(z)$ during northern (a) winter and (b) summer. Black curve shows observed winds, grey curve shows model "radiative" winds that result without a wave drag parametrization. Sources of gravity waves with various phase speeds c are also depicted, with the source and wave breaking symbols similar to those defined in Fig. 10. On these plots, waves ascend vertically upwards since c remains constant, until they break or reach a critical level $c = \bar{U}(z_C)$. (Based on a presentation first used by Lindzen, 1981)

the bias was most dominant. Moreover, global increases in surface friction drag can have deleterious effects elsewhere: e.g., excessively weak southern hemispheric circumpolar flow (Boer and Lazare, 1988). (For a discussion on various drag processes that arise at the surface, see Appendix Aa.)

If the atmosphere were in radiative equilibrium, there would exist a polar night jet in the middle atmosphere that is much stronger and extends higher than is observed (see Fig. 1; see also Fig. 6 of Hamilton, 1996). On the other hand, "Rayleigh friction" (e.g., Boville, 1986) and "Newtonian cooling" (Dickinson, 1973), which exponentially damp winds and temperatures, respectively, to some reference state as a function of time and are often used to suppress spurious reflection of waves from model tops, were found to be quite effective in reducing the magnitude of the polar night jet in models (Leovy, 1964; Schoeberl and Strobel, 1978; Holton and Wehrbein, 1980). The success here is qualified: an important drawback of Rayleigh damping is that it always drags the winds back toward zero (or climatology), whereas observed winds go to zero then generally change direction (see Fig. 1). Moreover, this kind of ad-hoc damping usually requires a thick vertical model domain and may produce excessive damping accompanied by unrealistic changes and reductions in atmospheric variability (e.g., Shepherd et al., 1996; Lawrence, 1997a; Kim et al., 1998). Nonetheless, the ability of such ad-hoc damping over a thick stratospheric domain to alleviate the problem of excessively strong stratospheric jets suggested that some kind of drag mechanism was missing from the models.

Later studies eventually concluded that the wind bias was mainly due to the lack of an explicit simulation of "drag" generated by breaking subgrid-scale gravity waves (Houghton, 1978; Lindzen, 1981; Matsuno, 1982; Holton, 1982, 1983; details are discussed in Section 3). Earlier lower top models enjoyed apparently successful simulation of the jet because the resolution was coarse enough for the underestimated meridional eddy momentum transport by planetary waves to balance approximately the underestimated vertical momentum transport, as illustrated in Fig. 2. When the horizontal resolution of these models increased, the meridional momentum transport was more accurately resolved and thus increased, and it could no longer be balanced by the still underestimated vertical momentum transport. Without a parametrization of subgrid-scale GWD, the mid-latitude westerly (easterly) winds in winter (summer) became excessively strong due to unresolved momentum transport to the ground that should balance the resolved meridional momentum transport (see Section 7 of Palmer et al., 1986 and Section 5 of Boer and Lazare, 1988).

b *Enhanced Orography with Effects Resembling Gravity Wave Drag*

Although there were several pioneering theoretical and analytical studies on the treatment and effects of GWD on the large-scale background flow (e.g., Sawyer, 1959; Lindzen, 1981; Holton, 1982), the first practical attention to this subject came with the introduction of "envelope orography" (e.g., Wallace et al., 1983). Envelope orography is a type of grid-scale orography in which mountain heights are elevated proportionally to the standard deviation of the subgrid-scale orographic elevations within each grid box. Another similar type of orography is "silhouette orography" in which model orography is given by the average of the mountain peaks within each grid box (Mesinger and Janjic, 1986): Mesinger and Collins (1986) and Lott and Miller (1997b) review various model representations of grid-scale orography. By using

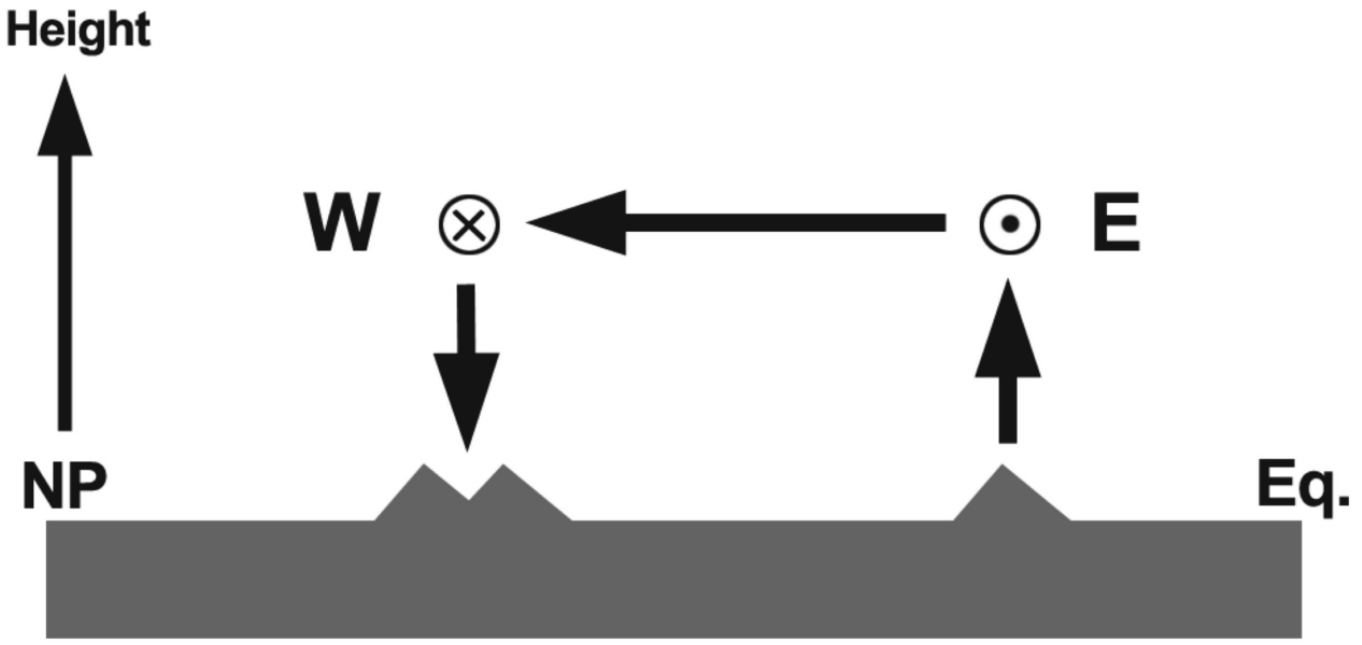

Fig. 2 Simplified schematic of the angular momentum transport between the atmosphere and the Earth's surface in atmospheric models (northern hemisphere). The angular momentum is transported vertically from westerlies to the ground over a mountainous area in middle latitudes and from the ground to easterlies in low latitudes. To balance the loss of momentum in the westerlies region and the gain in the easterlies region, meridional momentum transport arises to maintain mass continuity.

these elevated forms of orography in large-scale models, it was shown that the biases in the zonal mean wind and temperature were reduced through enhanced "mountain drag" (see Appendix Aa), i.e., enhanced generation of planetary wave activity and associated enhanced eddy flux divergences that impact mean fields (e.g., Wallace et al., 1983; Palmer and Mansfield, 1986; Tibaldi, 1986; Iwasaki and Sumi, 1986).

The improvements gained by enhancing the orography came via greater generation of Rossby waves, and not from parametrized effects of subgrid-scale gravity waves (even though information on the subgrid-scale orography is used to create the grid-scale orography). While this is of course true, enhanced orography can be viewed in a different context in terms of the spectrum of near-surface gravity waves associated with subgrid-scale orography (Kim, 1996). Enhancing orography is, in a sense, equivalent to considering stagnant flow formed over mountainous terrain, which is relatively deep/shallow over valleys/ridges (Fig. 3). This stagnant flow effectively acts as a barrier or "envelope" to the grid-scale flow. The streamlines of the terrain and the elevated surfaces due to stagnant flow resemble those of "external gravity waves" (see Appendix Ac1; Fig. 11) that are evanescent, i.e., decay in the vertical.

Envelope orography has been investigated in relation to its impact on synoptic-scale blocking (e.g., Mullen, 1994). Some recent models use explicit parametrizations of lift forces due to blocking near the surface complementing the work by GWD (Lott, 1999). Caution is, however, needed to distinguish between the drag-decreasing effect of upstream flow-blocking and the drag-enhancing effect of downstream low-level wave-breaking (Kim and Arakawa, 1995; Kim et al. 1998; see also Fig. 4). For example, Smith et al. (2002) recently showed how a low-level stagnant layer reduced the upward generation of (internal) mountain waves (see Section 7e2 for further discussion).

One of the drawbacks of enhanced orography is that these stagnant flow effects are parametrized in an invariant way, whereas in reality they are time (i.e., flow) dependent (Lott and Miller, 1997b). Further, envelope orography may interfere with data assimilation by necessitating rejection of low-level atmospheric data, and may also generate excessive precipitation in models (Lott and Miller, 1997a). There has been some debate on the relationship between and the mechanisms behind enhanced orography and GWD (e.g., Section 1 of Kim, 1996). With successive increases in horizontal resolutions, however, newer models have tended to use more realistic "mean" grid-scale orography instead of enhanced orography. It seems that the earlier beneficial impact of enhanced orography was partially due to inadequate horizontal resolution.

3 Evolution of gravity wave drag parametrization

Studies subsequent to those discussed in the previous section soon evolved into explicit consideration of the breaking of vertically propagating "internal" gravity waves (for an introduction to wave breaking and GWD, see Appendix Ad). First parametrizations were for gravity waves generated by flow over subgrid-scale orography (also called mountain waves), followed by parametrizations of horizontally propagating, but vertically "trapped" lee waves (see Appendix Ab1 and Ac for

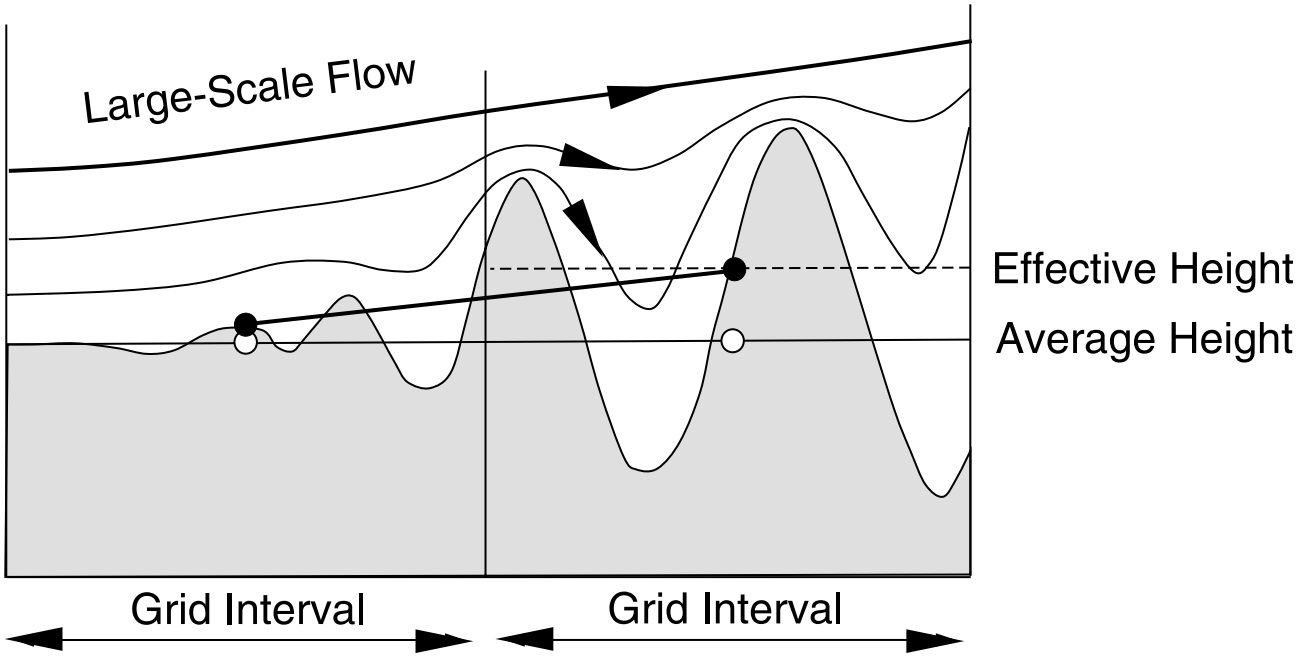

Fig. 3 Schematic figure showing the enhancement of large-scale orography due to the formation of stagnant flow over subgrid-scale orography. Large-scale flow encounters the effective height of the orography instead of the average height since it does not flow into stagnant regions at the base of valley regions. Envelope orography is an example of such enhanced orography. The streamline patterns resemble those of external gravity waves (i.e., that are vertically evanescent). (Taken from lecture notes of Prof. Akio Arakawa.)

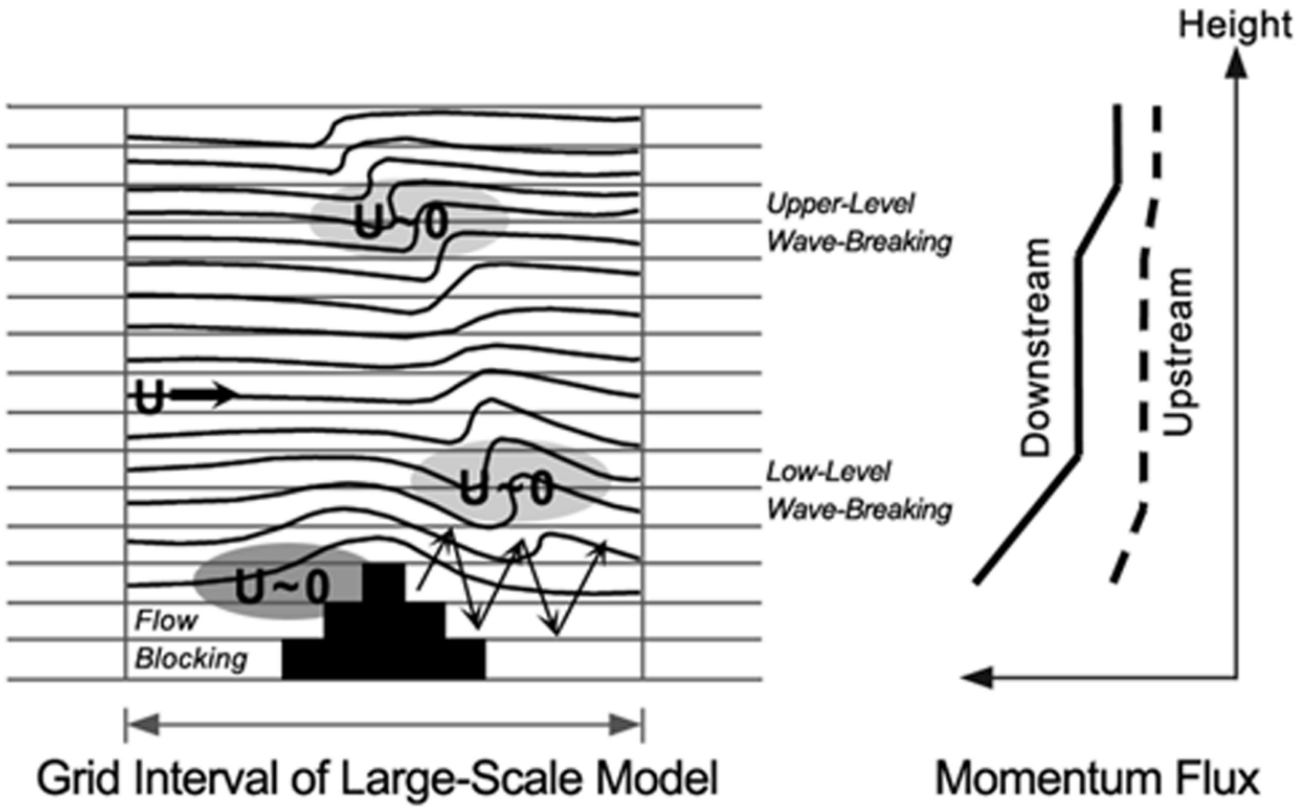

Fig. 4 (Left) Schematic figure showing low-level wave-breaking and stagnation points generated in a model by resonant amplification of mountain waves between the surface and a wave-induced critical layer near the peak of the mountains downstream. Contours and shades represent isentropes and decreased wind regions respectively. Also shown are a region of upper-level wave breaking due to the breakdown of vertically propagating mountain waves, and a region of flow-blocking in the upstream. (Right) A typical profile of horizontally averaged vertical momentum flux corresponding to the upstream and downstream regions of the schematic figure on the left. (Schematically drawn based on Kim and Arakawa, 1995)

background on these topics). With the tops of the models now extending upward, a new need has emerged to parametrize drag at upper levels due to dissipation of "non-stationary" gravity waves (see Appendices Ab2 and Ac); issues that are discussed specifically in Section 4. In tropical regions, gravity waves and tropical planetary waves (e.g., Kelvin waves) generated by deep convection are considered the major source of non-stationary wave drag that drives atmospheric variability in the stratosphere and above. Since orography and convection are currently the two most parametrized gravity wave sources, we discuss the evolution of parametrized GWD from both of these sources in the remainder of this section.

a *Orographic Gravity Wave Drag Parametrization*

In the presence of favourable background winds and static stability, gravity waves are generated by flow over mountainous terrain. The literature on "mountain waves" is extensive and comprehensive reviews of the relevant theory are available (e.g., Smith, 1979, 2001; Baines, 1995; Wurtele et al., 1996). Modelling of mountain waves goes back many years and mathematical theories have evolved that clarify many aspects of wave generation and evolution. This work greatly aided rapid development of parametrization schemes.

The first generation GWD parametrization schemes for large-scale models with relatively low model tops were developed for mountain waves (e.g., Boer et al., 1984; Palmer et al., 1986; McFarlane, 1987). The first formulations were single-wave parametrizations based on two-dimensional (2D) linear single-wave nonrotating stationary hydrostatic gravity-wave theory, utilizing (except for Boer et al. 1984) the "saturation hypothesis" (Lindzen, 1981): see Appendix Ad and Section 4b for further details. One of the main tasks of these schemes was to separate the stratospheric polar night jet from the tropospheric subtropical jet by reducing the overall magnitude of the jets and creating stronger easterly wind shear in the upper troposphere. A typical impact of these schemes is very large mid-latitude lower stratospheric drag that has a direct impact on the stratospheric jet and an indirect impact on the surface westerlies through the secondary circulation induced by the stratospheric drag (Fig. 5). This indirect impact was effective in warming/cooling the polar/tropical stratosphere (i.e., reducing cold-pole problems) and decreasing the surface westerlies associated with increased zonal asymmetry in surface pressure fields (i.e., reducing the westerly bias).

At about the same time, within the mesoscale modelling community there were active discussions on the mechanisms responsible for the so-called "severe downslope windstorms" found downstream of major mountains: e.g., Boulder windstorms downstream of the Rockies (Klemp and Lilly, 1978; Peltier and Clark, 1979; Durran and Klemp, 1987). An illustration of flow over a relatively high, isolated mountain based on a 2D mesoscale model simulation of this situation is shown in Fig. 4. "Wave resonance" occurs through formation of a self-induced mountain wave critical level associated with mountain wave breaking (see Appendices Ac3 and Ad4) that vertically traps and then amplifies wave energy. Although there has been some debate about underlying physical mechanisms (based on linear hydrostatic, non-linear non-hydrostatic or internal hydraulic theories), it is generally agreed that the GWD associated with downslope windstorms can be very large (e.g., Peltier and Clark, 1979; Bacmeister and Pierrehumbert, 1988). While these events are intermittent**,** the estimated drag each event produces is often larger than that produced by stratospheric mountain wave breaking. Similar resonance breaking and drag may also be important in the boundary layer (Nappo and Chimonas, 1992). Thus this process is important for the large-scale atmospheric momentum budget.

Subsequent development of orographic GWD parametrization was motivated by findings from these mountain wave simulations and observations, as well as the need, in models, for increased low-level drag (see Section 7d). Some schemes began to represent these effects through a simple lower tropospheric enhancement in GWD (e.g., Pierrehumbert, 1986). The effects of "linearly trapped" non-hydrostatic lee waves downstream of mountains were parametrized in an ad-hoc manner by Iwasaki et al. (1989), resulting in improved forecasts. The effects of "non-linearly trapped" lee waves in the lower troposphere due to low-level wave-breaking were systematically parametrized to generate selective enhancements (only in downstream regions with strong non-linearity) of low-level drag (Kim and Arakawa, 1995) and implemented as a parametrization in both a climate simulation model (Kim, 1996) and a weather forecast model (Alpert et al., 1996), with improvements in each case. This selective enhancement distinguished between the low-level wave-breaking region downstream and the flow-blocking region upstream that are associated with stronger and weaker vertical divergence of horizontal momentum flux, respectively (Fig. 4). The latest mountain wave parametrization schemes have devoted much effort to developing and improving these and other lower-level drag and orographic specifications (e.g., Kim and Arakawa, 1995; Lott and Miller, 1997a; Gregory et al., 1998; Scinocca and McFarlane, 2000), which led to improvements in the global models' overall forecast skill and simulation of mean sea level pressures (e.g., Milton and Wilson, 1996; Kim, 1996).

Various versions of first-generation orographic GWD parametrization schemes are now routinely implemented in large-scale models for both climate simulations and weather forecasts (e.g., Boer et al., 1984; Palmer et al., 1986; McFarlane, 1987; McFarlane et al., 1987; Helfand et al., 1987; Rind et al., 1988; Miller et al., 1989; Iwasaki et al., 1989; Broccoli and Manabe, 1992; Kim, 1996; Milton and Wilson, 1996; Chun et al., 1996; Zhou et al., 1996; Lott and Miller, 1997a; Kiehl et al., 1998; Gregory et al., 1998; Lott, 1999; Scinocca and McFarlane, 2000). Intercomparisons of various parametrization schemes in models are available in the literature (e.g., Boer et al., 1992; Gates, 1992; Kim and Arakawa, 1995; Pawson et al., 2000). Orographic GWD parametrization is in a state of continual development. A range of issues for its future development is set out in Section 7.

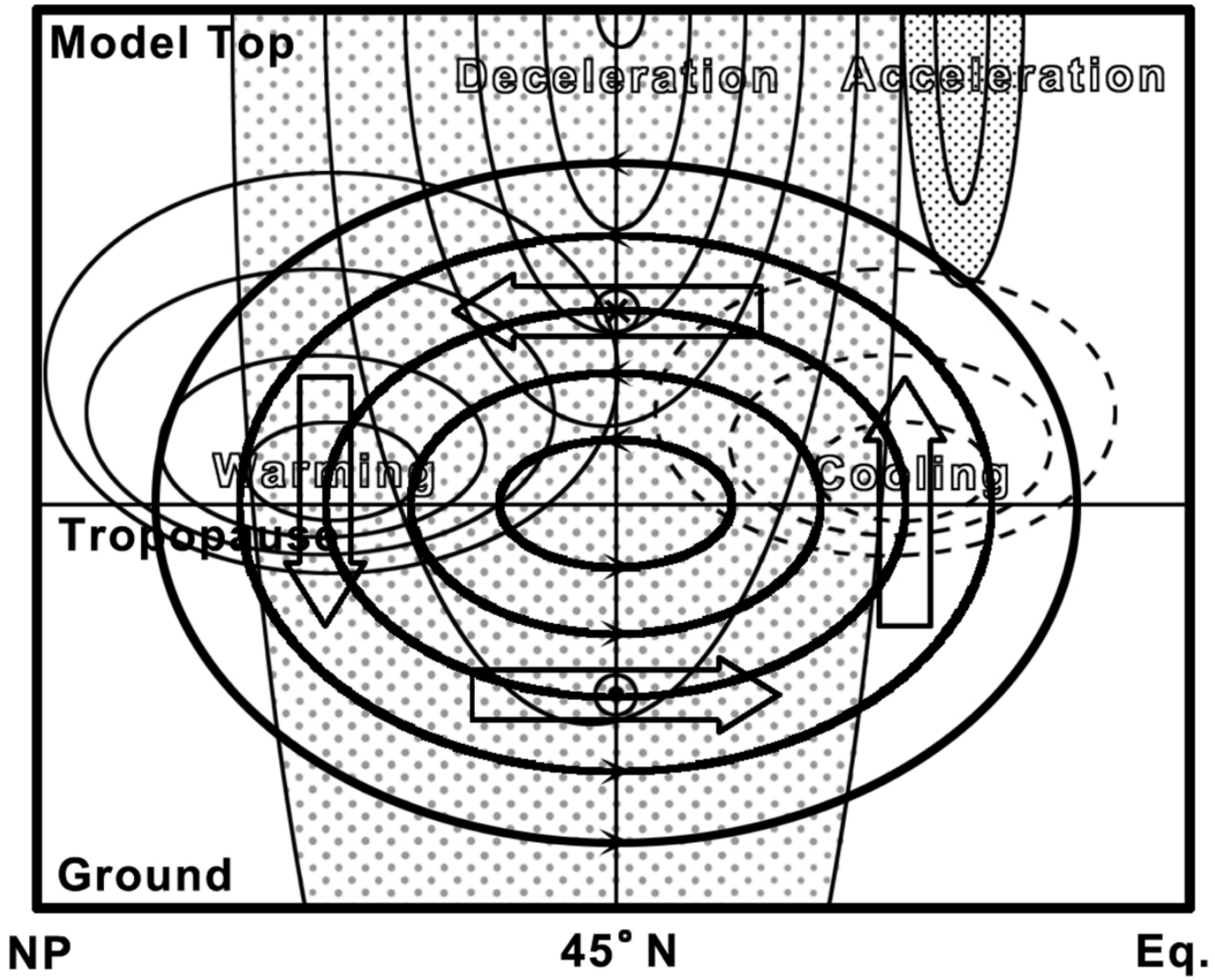

Fig. 5 An impact of a stratospheric momentum sink (with its maximum at 45°N and limits in higher and lower latitudes) on the zonally averaged large-scale circulation for the northern winter. The stratospheric drag in the mid-latitude is deflected to the North Pole due to Coriolis force, down to the troposphere, to the middle latitudes, and back to the stratosphere in the low latitudes, while inducing adiabatic warming/cooling in the high/low latitudes and deceleration of the winds throughout the atmosphere in middle latitudes. (Schematically constructed based on Palmer et al., 1986)

b *Convective Gravity Wave Drag Parametrization*

While more attention has been paid to the parametrization of orographic gravity waves to alleviate the wind and temperature biases in the mid-latitude northern winter hemisphere, significant interest has recently emerged in the parametrization of gravity waves generated by convective systems. The importance of convectively-generated tropical waves in driving the equatorial stratospheric semi-annual oscillation (SAO) and quasi-biennial oscillation (QBO) has been appreciated for many years, but the relative importance of the planetary-scale, intermediate-scale and small-scale (subgrid-scale) waves to the equatorial momentum budget has been debated for many years (e.g., Lindzen and Holton, 1968; Holton and Lindzen, 1972; Hitchman and Leovy, 1988; Boville and Randel, 1992; Bergman and Salby, 1994; Dunkerton, 1997; Garcia, 2000). Global models can be used to test this to some extent, since planetary-scale waves can be explicitly simulated while GWD, due to smaller-scale waves, can be separately parametrized.

Simulations of the QBO and/or SAO in three-dimensional (3D) global models have been attempted in various ways, using, for example; a mechanistic model that either specifies large arbitrary wave amplitudes (e.g., Takahashi and Boville, 1992) or parametrizes GWD (e.g., Lawrence, 2001); a simplified high-resolution GCM (Horinouchi and Yoden, 1998); a full GCM with either a GWD parametrization (e.g., Jackson and Gray, 1994; Scaife et al., 2000), increased vertical resolution (Hamilton et al., 1999, 2001), or an additional stratospheric dry convective adjustment process (Takahashi, 1996). This recent work with full GCMs suggests that higher fre-

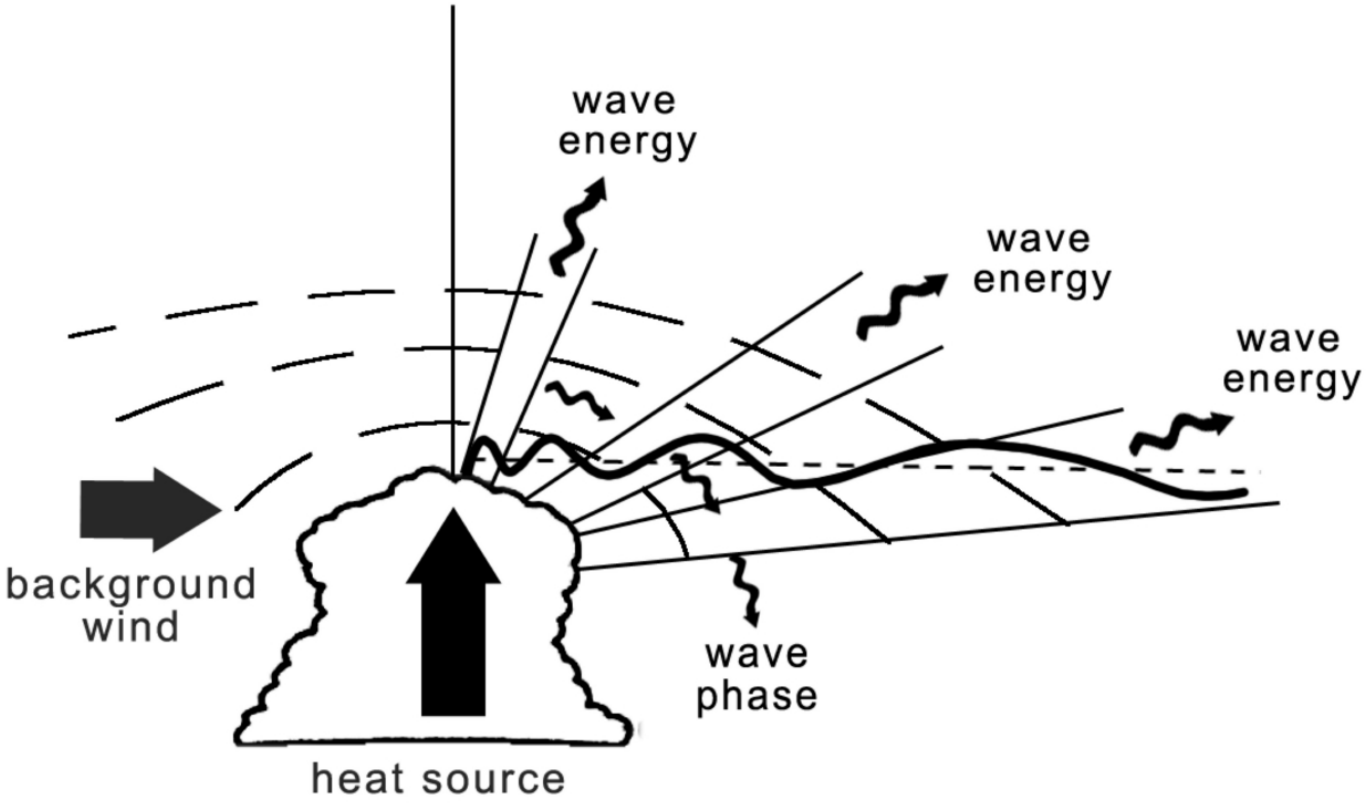

Fig. 6 Gravity waves generated by penetrative convection in the presence of background wind. (Based on Hooke, 1986; by permission of the American Meteorological Society). Similar wave features are seen in the latest numerical model simulations (e.g., Holton and Alexander, 1999).

quency tropical gravity waves generated by convection may need to be represented better in large-scale models to improve simulations of these features (see Section 6a). Thus, parametrizations of convectively-generated GWD can be considered a means of alleviating these deficiencies, allowing better simulations of important tropical circulation features such as the QBO in the lower stratosphere and the SAO in the upper stratosphere and mesosphere.

Compared with orographic gravity waves, it has proven more difficult to model the way in which gravity waves are generated by various convective sources; the simplest situation is depicted in Fig. 6. There are currently three proposed generation mechanisms in the literature. The first considers convective clouds in terms of their "diabatic" or "thermal" forcing. In this situation, thermal forcing terms within the convective clouds radiate gravity waves into the stably stratified atmosphere above the clouds (Salby and Garcia, 1987; Bergman and Salby, 1994; Garcia, 2000). It has been argued that the vertical wavelengths of convectively generated gravity waves are approximately twice the heating depth and thus intrinsic phase speeds of these waves are determined mainly by the vertical depth of the heating region (Bergman and Salby, 1994; Alexander et al., 1995; Garcia, 2000). In contrast, Holton et al. (2002) showed that the vertical wavelength in their study depends on a non-dimensional parameter related to the frequency, horizontal and vertical scales of the forcing. Detailed mesoscale model simulations by Song et al. (unpublished manuscript, 2003) suggest a dependence on the basic-state wind relative to the rearward propagating convective cells. A series of analytical studies of thermally-induced internal gravity waves related to the thermal forcing mechanism are available in the literature (e.g., Smith and Lin, 1982; Lin and Smith, 1986; Lin, 1987; Bretherton, 1988; Chun, 1995; Chun and Baik, 1998; Baik et al., 1999a,b).

The second mechanism assumes that convective heating in clouds produces "obstacles" to the flow in the form of vertical bulges of isentropic layers above the convective region. Gravity waves are generated by the relative flow over these convective obstacles, a process analogous to orographic gravity wave generation (Clark et al., 1986). This mechanism has been identified in observations of waves above the convective boundary layer (Kuettner et al., 1987). It has also been applied to time-dependent clouds as a "transient mountain" mechanism (Pfister et al., 1993). It is noted in passing that when a stationary convective source is considered there is no major difference between the thermal forcing and obstacle mechanisms in that the gravity waves are generated only when there is a non-zero background wind relative to the forcing (Fovell et al., 1992; Chun and Baik, 1998). When a transient source is considered, however, gravity waves can be generated even for zero storm-relative wind, and thus the two mechanisms are distinguishable in this case.

The third mechanism is the so-called "mechanical oscillator" (Clark et al., 1986; Fovell et al., 1992; Lane et al., 2001).

Here, oscillatory motions within a convective system impinge on the tropopause and generate gravity waves in stable regions above the clouds under zero background wind relative to the convective system. As noted by Fritts and Alexander (2003), this mechanism is very similar to a diabatic/thermal forcing mechanism in which the period of the thermal forcing term is fixed. It is also similar to an "oscillatory obstacle" forcing process (e.g., Prusa et al., 1996).

Even though these three mechanisms are frequently discussed and investigated, a fundamental question exists as to whether these mechanisms are really distinguishable or are just different ways of looking at the same mechanism. This issue has not been answered clearly yet. Lane et al. (2001) calculated source terms of the linear gravity waves induced by a mesoscale convective system, and showed that the magnitudes of non-linear momentum and heat advection terms (representing mechanical oscillator forcing) are much larger than the diabatic heating term. From this result, they concluded that the mechanical oscillator mechanism dominates the thermal forcing mechanism. However, recent 2D numerical modelling by Song et al. (unpublished manuscript, 2003) reveals that the amplitudes of convectively forced gravity waves in the stratosphere are largely determined by the wave propagation conditions defined within the horizontal wavenumber-frequency domain for given basic-state wind and stability profiles, rather than by the magnitude of wave forcing terms. Song et al. (unpublished manuscript, 2003) performed quasi-linear simulations forced separately by non-linear advection and diabatic sources in the troposphere, and showed that although the magnitude of the non-linear advection source is much larger than that of the diabatic source, similar to the result of Lane et al. (2001), the gravity waves radiated into the stratosphere were comparable to each other in both their amplitude and spectral characteristics. They went on to show that vertical propagation conditions restricted the effectiveness of some wave sources, such that a large portion of the non-linear advection forcing could not produce gravity waves in the stratosphere.

More detailed reviews of convective wave generation are given in Section 3 of Garcia (2000) and in Sections 3.1.2 and 7.1 of Fritts and Alexander (2003). Detailed 2D and 3D mesoscale modelling has provided new insights into gravity waves generated by realistic convective systems (Hauf and Clark, 1989*;* Alexander et al., 1995; Piani et al., 2000; Lane et al., 2001). From these studies it has emerged that the waves radiated from convection seem to be interpretable using linear gravity wave theory (e.g., Alexander, 1996; Pandya and Alexander, 1999; Lane et al., 2001), which greatly simplifies their parametrization.

There have been several attempts to parametrize GWD induced by subgrid-scale cumulus convection in large-scale models using different theoretical models for determining cloud-top wave stresses. Lindzen (1984) assumed that gravity wave momentum flux is proportional to the square of vertically integrated convective mass flux, and this parametrization was tested in the global model simulations of Rind et al. (1988). A later parametrization by Kershaw (1995) assumed that the wave energy above the convective region is proportional to the convective kinetic energy in the cloud region. Bosseut et al. (1998) used a scheme in a climate model where wave momentum fluxes were proportional to the precipitation flux from the convective scheme, with beneficial impacts. Chun and Baik (1998) derived an analytical expression for the gravity wave momentum flux forced by specified stationary diabatic forcing representing the latent heating by cumulus convection for uniform background wind and buoyancy frequency. This formulation of the cloud-top wave stress has been found to be analogous to that of surface mountain drag (Pierrehumbert, 1986) if the non-dimensional mountain height is replaced by the "non-linearity factor" of thermally induced internal gravity waves (Lin and Chun, 1991). The cloud-top wave stress was shown to be inversely proportional to the basic-state wind speed and the cube of the buoyancy frequency for a given diabatic heating rate. The formulation by Chun and Baik (1998) has been implemented in an atmospheric GCM (Chun et al., 2001) and also in a global spectral forecast model (Kim and Hogan, unpublished manuscript, 2003). This parametrization has also been updated by including basic-state wind shear in the convective region and stability differences between the convective region and the regions above it (Chun and Baik, 2002).

In addition to its impact in the tropics, the parametrization of convective GWD may offer the additional benefit of alleviating model climate biases in the southern hemisphere (Chun et al., 2001) where orographic GWD has much more limited impact due to fewer mountains. Furthermore, in the extratropical summer middle atmosphere, orographic gravity waves cannot penetrate far vertically due to critical levels (see Fig. 1), and thus the reversal of the summer stratopause jets must be driven by non-orographic GWD (e.g., Jackson, 1993). This issue is expanded upon in the next section.

4 Treatment of the middle atmosphere in gravity wave drag parametrization

Most earlier and many current NWP models do not include a middle atmosphere (heights ~20–90 km). Possible reasons for this are numerous: it adds substantially to the computational burden; the existence of the middle atmosphere can be considered unnecessary for "short-" and "medium-range" forecasting; and there may be insufficient data to assimilate in the middle atmosphere. An extension toward "long-range" forecasts, however, requires the inclusion of the middle atmosphere, which affects the lower atmosphere through the "downward control" induced by upper-level drag (Haynes et al., 1991) and other dynamical coupling effects (e.g., Ambaum and Hoskins, 2002). Indeed it has been argued that, for periods greater than one week, it is necessary to know the initial state of the entire global atmosphere from the stratosphere to the surface, as well as the state of the upper layers of the oceans (Holton, 1992, based on Smagorinsky, 1967). An emerging body of work is the verification of the importance of the middle atmosphere for long-range forecasting of winter weather in the northern hemisphere (Baldwin and

Dunkerton, 2001; Thompson et al., 2002). Global NWP models are also including a middle atmosphere to improve the forward modelling of satellite radiances in the operational data assimilation procedures that provide initial atmospheric states for the forecast model.

Thus, there is a trend to extend the vertical domains of 3D large-scale models (Pawson et al., 2000). As these upper boundaries of NWP and climate models are extended into the middle and upper atmosphere, GWD parametrization becomes more important and more challenging. Since the winds are generally stronger at high altitudes, the model time steps must be decreased for numerical stability thereby limiting the increase of spatial resolution to maintain computational efficiency. The stratosphere and mesosphere are impacted much more profoundly by GWD than the troposphere (e.g., Hamilton, 1996; Shepherd, 2000). Since unsaturated gravity wave momentum flux densities, $\rho\overline{u'w'}$, are conserved in the absence of dissipation (see Appendix Ad1 for background), the exponential decrease of atmospheric densities ρ with height means that gravity wave velocity fluctuations [e.g., $u'(x,z,t)$] tend to grow exponentially in amplitude with height (Lindzen, 1981). Thus, waves with miniscule amplitudes in the lower atmosphere can attain large breaking amplitudes at upper levels. Basic climatological wind patterns throughout the global mesosphere (z~50–90 km) and the entire equatorial middle atmosphere (z~15–90 km) cannot be reproduced without parametrizing GWD at these altitudes (McLandress, 1998; Holton and Alexander, 2000).

In this section, a general overview of the current status of GWD parametrization for the middle atmosphere is provided. More exhaustive reviews can be found elsewhere: an introduction to some of the single-wave and spectral parametrizations for the middle atmosphere is given in Section 5 of McLandress (1998); a collection of articles on gravity wave parametrization issues and their performance in middle atmospheric models is provided in the volume edited by Hamilton (1997a); Fritts and Alexander (2003) provide a thorough overview of single-wave and spectral gravity wave theories and their transition to parametrization schemes. A historical perspective is provided by Hamilton (1999).

a *Critical Level Filtering of Gravity Waves*

Gravity waves generally dissipate totally and are absorbed into the flow as they approach their critical level z_C where their intrinsic horizontal phase speed and vertical wavelength vanish (as discussed in Appendices Ac3 and Ad4). This "critical level filtering" of gravity waves is important in middle atmospheric GWD parametrization.

In a 2D configuration, a hydrostatic irrotational gravity wave of ground-based horizontal phase speed c has a critical level z_C where the condition $c = \overline{U}(z_C)$ is met, where $\overline{U}(z)$ is the background wind profile. Since wave phase speeds c are constant in GWD parametrizations, one can easily inspect wind profiles $\overline{U}(z)$ to see which waves will encounter critical levels at what heights. Figure 1 does this graphically for a typical mid-latitude location during winter and summer.

During northern winter (Fig. 1a), stationary orographic gravity waves ($c = 0$) typically do not encounter critical levels and thus can propagate through the middle atmosphere. If we assume that convection, on average, tends to generate waves with large eastward and westward phase speeds (Section 3b), then the waves with westward phase speeds ($c < 0$) also reach the mesosphere. However, the eastward phase speed waves ($c > 0$) encounter critical levels due to the strong eastward stratospheric jet. Similarly, any gravity waves launched from the tropospheric jet stream (see Section 7h), which here are assumed to have phase speeds similar to those of local jet stream wind speeds, also are absorbed at critical levels in the stratosphere. This leaves a preponderance of stationary and westward phase speed waves in the mesosphere, where $c - \overline{U}(z) < 0$, and thus wave breaking in this region will drag winds strongly to the west (as discussed in Appendix Ad3). Note the importance of critical level filtering: without the removal of eastward phase speed waves, this westward drag would be largely cancelled by a compensating eastward drag from $c > 0$ waves. Instead, these waves dissipate lower down at stratospheric critical levels, and should accelerate winds there slightly: recent work suggests that this lower stratospheric non-stationary GWD may be significant for stratospheric climate (Alexander and Rosenlof, 1996). Note too that in the lower stratosphere, orographic intrinsic phase speeds become small and thus orographic gravity waves tend to saturate there as well (see Appendix Ad), producing some additional westward orographic GWD (Lindzen, 1985; Palmer et al., 1986; McFarlane, 1987).

In northern summer (Fig. 1b) the situation reverses. Now a strong westward stratospheric jet absorbs mountain waves and westward phase speed gravity waves, whereas the jet-stream waves and eastward phase-speed waves from convection reach the mesosphere. This immediately highlights the importance of non-stationary GWD parametrizations to the summer extratropical middle atmosphere (e.g., Jackson, 1993). A qualitatively similar situation in the equatorial middle atmosphere makes non-stationary waves from deep tropical convection important all year around (see also Sections 3b and 6a).

b *Single-Wave Gravity Wave Drag Parametrization*

Rayleigh friction was used in the first generation of global 3D models with middle atmospheres (Section 2a), followed by single-wave Lindzen-type GWD parametrization schemes (Section 3a). The latter parametrizations are natural vertical extensions of the first generation lower atmospheric schemes and can usually provide the orographic component of the middle atmosphere GWD in models (see e.g., McFarlane et al., 1997; Manzini and McFarlane, 1998; Pawson et al., 1998; Scaife et al., 2000; Jackson et al., 2001).

In generalized Lindzen schemes, a collection of individual waves with assigned phase speeds c are propagated vertically from below under a hydrostatic saturation model (Appendix Ad2), assuming no interactions among the waves. These schemes must be carefully tuned by varying wave parameters such as amplitudes, phase speeds and launch height at the

source until acceptable results are obtained. Lindzen schemes tend to produce large rapid onset of drag with height, which may degrade some model simulations (see e.g., Norton and Thuburn, 1999) and may necessitate further tuning of parameters or inclusion of some kind of smoothing (e.g., Holton, 1982; McLandress and McFarlane, 1993; Hamilton, 1997b). A common solution is to invoke an "intermittency" factor and/or varying saturation thresholds that help scale down and vertically redistribute the drag, while the factor and thresholds can also be tuned (Holton, 1982; Hamilton, 1997b; Norton and Thuburn, 1999; Alexander and Dunkerton, 1999). Despite the problems of sensitivity and arbitrary tuning, these schemes can reproduce the basic circulation features of the middle atmosphere and, until recently, were the standard way of parametrizing GWD at these altitudes in 3D models (see e.g., Rind et al., 1988; Jackson and Gray, 1994; Hamilton, 1997b; Norton and Thuburn, 1999).

c *Spectral Gravity Wave Drag Parametrization*

As waves propagate higher into the atmosphere, their wave amplitudes grow and propagation paths start to intersect (Fig. 10). Increased amplitudes mean greater potential for both instabilities (saturation) and interactions among the waves. Consistent with this idea, improved observations during the 1980s revealed broad frequency and wavenumber power spectral densities of gravity wave-induced wind and temperature perturbations in the middle atmosphere (see reviews by Fritts, 1989; Gardner, 1996; Section 4 of Fritts and Alexander, 2003). It was found that these spectra had quite reproducible shapes (VanZandt, 1982; Smith et al., 1987). In the case of the vertical wavenumber spectrum, spectral densities at high wavenumbers were almost constant with height and location, again suggestive of some kind of saturation mechanism acting on the wave field. This spurred development of a range of competing theories to explain how these intriguingly reproducible spectra are formed and maintained. Almost all invoke some kind of "spectral saturation" model (see Appendix Ad2). Recent reviews of this area are available in the literature (Gardner, 1996; Section 6.3 of Fritts and Alexander, 2003).

The recent profusion of new spectral GWD parametrizations has been motivated in part by this ongoing debate. The uncertainties surrounding it have led to two separate approaches to formulating spectral GWD schemes. One class of spectral parametrizations retains close connections to observed spectral shapes, but tries to simplify the spectral saturation issue by making basic assumptions about it when formulating drag algorithms (Fritts and VanZandt, 1993; Fritts and Lu, 1993a, 1993b; Warner and McIntyre, 1996, 1999, 2001). The approach is to build single-wave propagation physics into a spectrum of component waves constrained in amplitude by observed wave spectra. These schemes then generate GWD by saturating individual waves that reach amplitudes in excess of limits imposed by observed spectral shapes thereby preserving both basic single-wave physics and observed spectral distributions of wave energy.

The second class of parametrizations takes the opposite view: they stress their own specific spectral theory of wave saturation processes in generating a GWD parametrization (Hines, 1997a, 1997b; Medvedev and Klaassen, 1995, 2000). This approach tries to invoke wave-wave interactions to provide a more physical basis for removing arbitrary intermittency factors and artificial smoothing of drag profiles, etc. The different non-linear wave physics in these parametrizations spawns different nomenclature: "critical-level filtering" and "wave breaking" are replaced by model-dependent concepts such as "wave obliteration", "non-linear wave-diffusive damping", and "Doppler spreading".

Another "spectral" GWD parametrization has recently been added to the mix (Alexander and Dunkerton, 1999). While advertised as spectral, it really differs from the aforementioned spectral schemes in that it makes no attempt to utilize or model the observed shapes of gravity wave power spectral densities. In fact, it might better be described as a "continuous single-wave" parametrization that improves upon the "discrete single-wave" formulation of the Lindzen-like schemes discussed in Section 4a. The latter schemes choose a collection of discrete phase speeds c and propagate them successively through the atmosphere (Jackson, 1993; Hamilton, 1997b; Norton and Thuburn, 1999). The Alexander-Dunkerton parametrization uses a Lindzen-like approach to model wave propagation and saturation, but extends it by incorporating continuous phase-speed distribution functions, modifying an approach originally used for the QBO by Lindzen and Holton (1968). This leads to differences in the GWD calculation: waves dissipate totally at their saturation altitude, rather than partially as in the Lindzen (1981) model.

These spectral parametrizations also offer some attractive practical advantages in models. The GWD profiles they produce tend to be smoother than those typically generated by Lindzen-like models (Alexander and Dunkerton, 1999), which reduces the possibility of model instabilities. The observational constraint of spectral shapes should also mean that they demand less arbitrary tuning than Lindzen-like parametrizations. Nonetheless, they all require source specifications as a lower boundary condition which, given the current uncertainties about non-stationary gravity wave sources, in practice implies arbitrary parameter choices and/or extensive tuning.

Despite this range of spectral parametrization approaches, they all respond in the same general manner as single waves in Fig. 1: a spectrum of wave momentum flux density is distributed at source levels among a continuous distribution of wave phase speeds c, and is propagated vertically into the atmosphere. Certain portions are filtered out by the background winds, and surviving portions of the spectrum saturate at various heights to generate a directional force that either accelerates or decelerates the background flow. Nonetheless, important differences emerge among the GWD profiles predicted by various schemes (e.g., Lawrence, 1997a; McLandress, 1997; Osprey, 2001; Charron et al., 2002).

Given current uncertainties in non-stationary wave sources, to date spectral GWD parametrizations have been used in 3D models mostly to parametrize global middle atmospheric GWD from indistinct non-orographic sources (e.g., Mengel et al., 1995; Manzini and McFarlane, 1998; Scaife et al., 2000; Scinocca, 2002). They appear to be promising tools: they variously generate equatorial QBOs and SAOs (Mengel et al., 1995; Scaife et al., 2000; Medvedev and Klaassen, 2001) and realistic extratropical wind, temperature and eddy diffusion climatologies (McFarlane et al., 1997; Manzini and McFarlane, 1998; Medvedev et al., 1998; Akmaev, 2001; Scinocca, 2002).

5 Evaluation of gravity wave drag parametrization

a *Online Evaluation*

Any GWD scheme needs to be tested within a climate or NWP model to assess its worth. Accurate objective evaluations of a given scheme in a large-scale model are, however, nontrivial.

The first problem is that it is impossible to find a "perfect" model in which only the subgrid-scale GWD processes are not represented. Therefore, it is important that the simulated atmosphere without any GWD parametrization is well understood in its own right. When a GWD scheme is added, it may accentuate certain model errors or act to mask errors in other parametrizations or ad-hoc drag terms (e.g., Klinker and Sardeshmukh, 1992; Milton and Wilson, 1996; Kim et al., 1998). For instance, Rayleigh friction, Newtonian cooling and other arbitrary diffusion or dissipation processes are often used in models to tune and/or stabilize the model. While all this interacting damping can seem beneficial in terms of the simulated monthly zonal-mean fields, it can often suppress realistic dynamical variability within the model (Shepherd et al., 1996; Lawrence, 1997b; Pawson et al., 1998). This problem is further exacerbated by the fact that most, if not all, GWD schemes contain parameters that are not well constrained and must, in practice, be varied or "tuned" until the simulated climate looks reasonable. Such tuning makes it difficult to assess any given GWD scheme objectively. In some cases, tuning GWD is erroneously regarded as a final means to fix all the remaining biases in the simulated atmosphere, and such an approach can lead to problems. For example, if the model's ozone heating parametrization is misrepresented in such a way as to induce an excessively strong stratospheric jet, tuning a GWD scheme can mask the problem, an effect that clearly does not improve the model (Kim et al., 1998).

Even neglecting such problems, there are other issues to consider when assessing model simulations performed with, or without, GWD. Observational assessments of GWD parametrization schemes can be performed; e.g., by a network of medium frequency (MF) radar observations comparing measured winds and waves with those generated by a middle atmospheric model with parametrized GWD (Manson et al., 2002). With climate models, however, simulations are usually performed for months or years, and monthly and zonal-mean averages are composed from model output and compared with observed climatology as a basic performance indicator for a GWD scheme. NWP models can also be assessed in "climate mode" without invoking periodic data assimilation cycles: however, short- and medium-range forecast integrations are usually performed using various initialization and data assimilation procedures which makes the GWD scheme's net impact harder to evaluate. Assessments based on "skill scores" of standard metrics such as the root-mean-square (RMS) error and anomaly correlation of the geopotential heights can be useful. In this case the performance of a GWD scheme is highly dependent on its harmony with the initialization and assimilation schemes as well as its physical adequacy. Another useful approach has been to diagnose the large-scale momentum balance of the simulated atmosphere at various time steps by outputting all the modelled and parametrized terms in the momentum balance equation (Bell et al., 1991; Klinker and Sardeshmukh, 1992; Milton and Wilson, 1996). "Single column" versions of the model, which are often used to test convection and radiation parametrizations (e.g., Wu and Moncrieff, 2001), can also be used to test GWD column parametrizations.

b *Offline Evaluation*

1 AGAINST OBSERVATIONS

In addition to testing and/or tuning GWD schemes within large-scale models, it is useful to test the schemes "offline" against actual observations of waves and GWD. Due to the relative ease of making low-level atmospheric measurements over land, orographic GWD schemes are amenable to these observational assessments. Near-surface mountain (pressure) drag predictions (see Appendix Aa) have been evaluated using data from microbarograph chains (e.g., Smith, 1978; Vosper and Mobbs, 1997; Miranda et al., 1999). More rigorous tests of GWD predictions have been made using data from multi-instrument field campaigns over major mountain ranges (e.g., Bougeault et al., 1993, 2001; Beau and Bougeault, 1998).

Since convective GWD parametrizations are more recent, currently observations help most in developing rather than evaluating these schemes. Clear correlations between convective activity and enhanced gravity wave energy have been observed, particularly in the tropics (e.g., Tsuda et al., 1994, 2000; Karoly et al., 1996; Alexander et al., 2000; McLandress et al., 2000; Preusse et al., 2001). Wave momentum fluxes and GWD have been estimated from observations of waves near convection in various ways (e.g., Sato, 1993; Vincent and Alexander, 2000; Alexander et al., 2000).

While spectral models of gravity wave variances were originally motivated (and constrained) by observations, their GWD predictions are harder to evaluate observationally. Eckermann (1995) has shown that observed gravity wave spectra, rather than being "universal" as was originally assumed (VanZandt, 1982), vary in response to background winds in a manner consistent with some spectral GWD parametrizations. Other observed spectral sensitivities (e.g., Nastrom et al., 1997; Whiteway, 1999) seem to be at odds with standard model predictions.

2 AGAINST MESOSCALE MODEL SIMULATIONS

While measurements should ideally be used for validation, this can prove difficult in practice. Although wave perturbation profiles can be measured fairly easily, gravity wave momentum flux, $\rho\overline{u'w'}$, the key wave quantity for GWD calculations (see Appendices Aa and Ad) is notoriously difficult to measure directly (e.g., Worthington and Thomas, 1996). Further, when measured it proves to be an intrinsically "noisy" quantity (Kudeki and Franke, 1998), and thus its vertical divergence — the GWD — can be still noisier and thus uncertain (e.g., Chang et al., 1997).

Since high-resolution mesoscale models can simulate regional wave breaking episodes explicitly, GWD can be calculated from a mesoscale model's output and compared with the prediction of a simpler GWD scheme. Some of the earliest GWD parametrizations were compared with available analytic solutions based mainly on 2D linear single stationary waves over an isolated idealized mountain (e.g., Wurtele et al., 1987), and then against progressively more complex mesoscale model simulations of orographic flows (Kim and Arakawa, 1995; Broad, 1996; Hereil and Stein, 1999) and convective systems (e.g., Kershaw, 1995).

Operational 3D mesoscale models can "hindcast" particular wave events in great detail (e.g., Powers, 1997; Doyle and Shapiro, 2000), and so can provide a useful link between imperfect data and GWD schemes. For validation, a detailed 3D mesoscale model simulation of a measured wave event can be performed, and its results can be compared with available data. If those comparisons are acceptable, this "validated" mesoscale model output can be used to compute the GWD, which can then be compared to that predicted by the GWD parametrization (Broad, 1996, 2000). Recent high-resolution global models have resolved gravity wave motions whose spectral shapes agree with both observations and forms implemented in spectral GWD schemes (Koshyk et al., 1999). The next section discusses resolved gravity waves in large-scale models more fully.

6 Resolved gravity waves versus parametrized gravity wave drag

Since GWD parametrizations are designed to act primarily on synoptic-scale flows, they derive and use equations that assume that GWD acts on a large-scale quasi-stationary atmosphere largely devoid of any resolved gravity waves. It is well known that, while unbalanced initialization fields generate spurious gravity waves in global models, balanced initialization procedures largely eliminate these problems. Thus, these simplifying premises are appropriate when using these parametrizations in low-to-medium resolution global models.

Currently, however, global models are being run at sufficiently fine spatial resolutions that "real" gravity waves are being generated explicitly by sources within the models. Spectral analysis of high-resolution model output in the upper troposphere and lower stratosphere based on spherical harmonic expansions reveals a transition in behaviour at total spherical harmonic wavenumbers $n \approx 80$, from rotationally dominated flow at scales $n < 80$ to shallower spectra at $n > 80$ where divergent gravity wave motions are as energetic as, or more energetic than, vortical motion (Koshyk et al., 1999; Koshyk and Hamilton, 2001). This breakpoint wavenumber decreases with altitude as these gravity waves increase in amplitude with height. Since current state-of-the-art spectral NWP models run anywhere in the range ~T200–T500 (i.e., triangular spectral truncation at a total wavenumber ~200–500, implying horizontal resolutions of Δx ~0.25°–0.6°, i.e., ~40–100 km), it is clear that these models are generating significant amounts of gravity wave activity and that these waves likely dominate small-scale model variability at upper levels. Thus it is very important to study these waves, particularly the way in which they contribute to GWD and interact with any subgrid-scale GWD parametrizations.

a *Tropical Gravity Waves Generated by Convection*

Since $f \to 0$ in the tropics, long-period gravity waves with long zonal wavelengths can exist there (see Appendix Ac), as well as other tropical modes such as Kelvin waves and mixed Rossby-gravity waves. Deep tropical convection generates a rich spectrum of such waves in global models run at quite moderate resolutions. For example, Ricciardulli and Garcia (2000) compared spectra of the vertical component of the Eliasson-Palm (E-P) flux (essentially $\rho\overline{u'w'}$ for gravity waves; Appendix Ad1) of tropical waves generated by various convective adjustment parametrizations in the Community Climate Model (CCM3) model (T42L18, Δx~2.8°) with those calculated from observed proxies for deep convective activity derived from high-resolution global cloud imagery (GCI). Nissen et al. (2000) conducted similar experiments with a T21 GCM (Δx~5.6°), while Amodei et al. (2001) compared tropical wave properties from a variety of large-scale models (Δx~2.5°–5.5°). Mesoscale activity in models appears to be enhanced generally in the tropics relative to the extratropics (Koshyk and Hamilton, 2001) in agreement with observations (e.g., Alexander et al., 2002).

Ricciardulli and Garcia (2000) found large discrepancies between wave fields inferred from observed GCI convection and those generated by some convective schemes in models: the latter significantly underestimated wave momentum fluxes, particularly gravity wave fluxes, as shown in Fig. 7. They noted that convection schemes in models have been developed and tested mostly for their ability to generate realistic time-mean distributions of tropical convection, and suggested attention also be paid to their ability to reproduce temporal variability in convection. This assumes that the algorithms used by Ricciardulli and Garcia (2000) to convert observed GCI data into latent heating rates yield accurate radiated wave fields. In assessing and reviewing various GCM studies, Amodei et al. (2001) noted that simple moist convective adjustment seemed to generate greater and more realistic tropical wave fields than some of the more sophisticated schemes currently used in models. These findings, while interesting, are also preliminary and more work is needed to

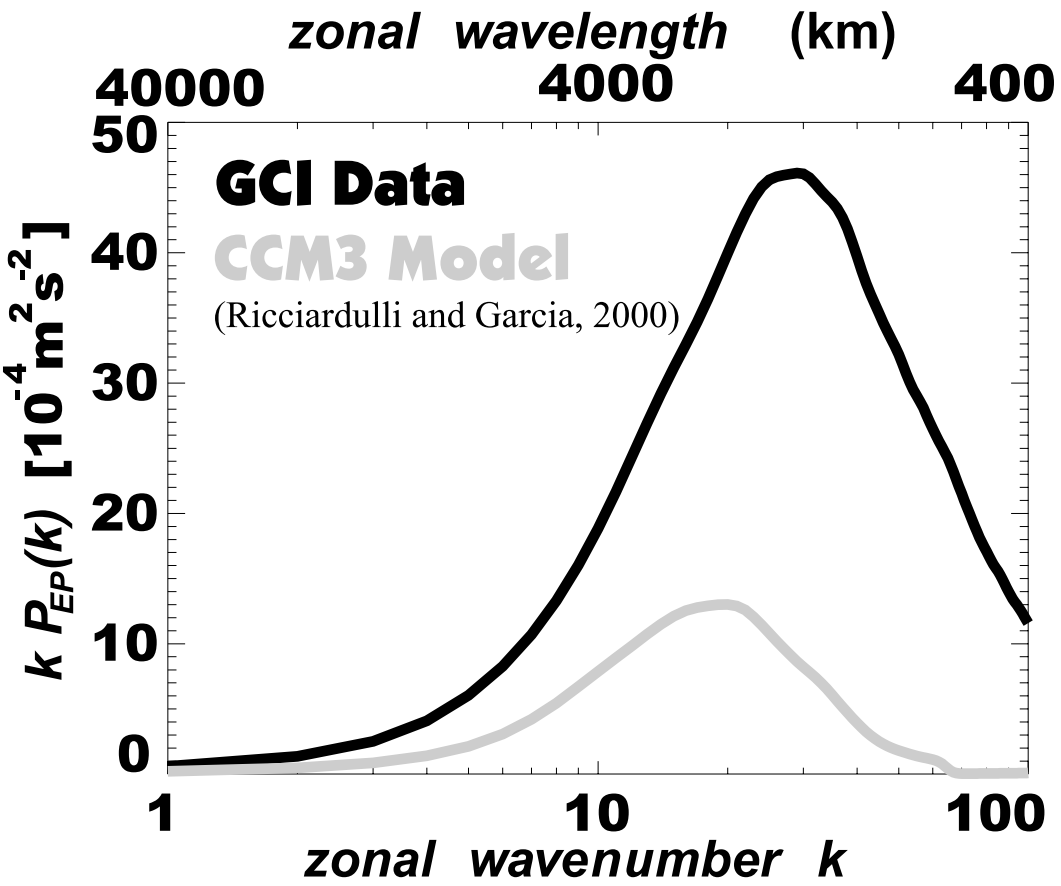

Fig. 7 Zonal wavenumber spectra $P_{EP}(k)$ of vertical component of EP-flux for all equatorial gravity waves with periods > 6 hours generated by deep tropical convection between 15°S–15°N, derived by adding relevant component curves in Figs 13b and 14b of Ricciardulli and Garcia (2000) and plotting in "energy content" or "area preserving" form $kP_{EP}(k)$. The black curve is derived from convective heating specified by 3-hourly global cloud imagery (GCI) data. The grey curve is output from the CCM3 global model using the convective heating parametrization of Hack (1994). Curves are averaged and smoothed in wavenumber space: see Ricciardulli and Garcia (2000) for full details.

understand and evaluate tropical convection and waves in models, particularly with regard to their roles in the simulation of tropical circulation features like the QBO and SAO.

b *Sensitivity to Vertical and Horizontal Resolutions*

Increasing the spatial resolution of a model should obviously help it resolve more gravity waves, their dissipation and GWD. However, Lindzen and Fox-Rabinovitz (1989) argued for consistency in choices of the ratio of horizontal to vertical resolution in models, and claimed that excess horizontal resolution due to inadequately low vertical resolution might increase model "noise". The precise dependencies of models to changes in vertical and horizontal resolution are not clear (e.g., Lander and Hoskins, 1997; Davies and Brown, 2001) and so modellers have explored these sensitivities experimentally (e.g., Hamilton et al., 1999).

Resolved tropical wave fields prove most sensitive to increases in model vertical resolution, Δz (e.g., Nissen et al., 2000). The consequent improvements in explicitly simulated tropical wave fields and wave drag are now cited as reasons for the elusiveness, until recently, of simulating a QBO in a GCM without parametrized GWD (see Section 3b). While models show some sensitivity to increased horizontal resolution, Δx, this is more of a secondary effect and may be an indirect manifestation of other more pertinent influences, such as horizontal diffusivity (e.g., Hamilton et al., 2001).

Almost the opposite dependencies arise in the extratropics. Since $f \neq 0$, extratropical gravity waves typically have shorter periods and, according to the dispersion relation (e.g., Gill, 1982; see Eq. (2) in Appendix A), shorter horizontal wavelengths than in the tropics. Thus models must be run at higher horizontal resolutions before explicitly-resolved gravity waves appear prominently in the extratropics. As shown in Fig. 8, improved horizontal resolution yields larger and more variable extratropical gravity wave momentum fluxes. At $\Delta x \sim 1°$, a fairly rich spectrum of extratropical gravity waves emerges in most models (e.g., Hayashi et al., 1989; Sato et al., 1999). However, these wave fields show much less sensitivity to increases in vertical resolution (e.g., O'Sullivan and Dunkerton, 1995). Such dependencies are reflected in the resolved GWD: simulations of the extratropical middle atmosphere without fully parametrized GWD improve noticeably when horizontal resolution is increased (i.e., Δx is reduced), but show much less sensitivity to increased vertical

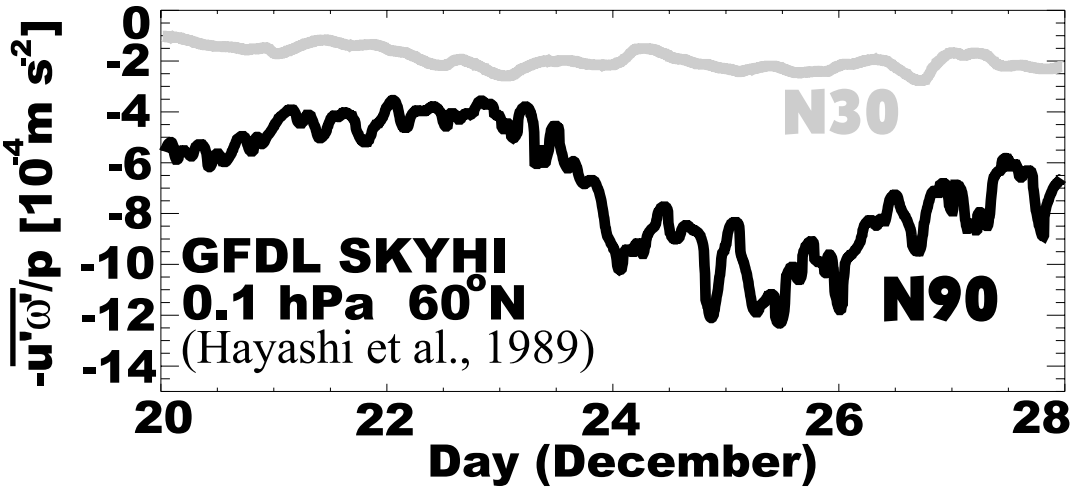

Fig. 8 Time series of the momentum flux term divided by pressure, $-\overline{u'\omega'}/p$, at ~60°N and 0.1 hPa (~65 km) for wavenumbers $k \geq 5$ in GFDL SKYHI simulations for 20–28 December. Here ω' is the vertical pressure velocity perturbation. The black curve shows the results from N90 resolution model (Δx~1° – 1.2°), the grey curve results from N30 resolution model (Δx~3° – 3.6°). (Adapted from Fig. 5 of Hayashi et al., 1989; with permission from Birkhauser Publishing Inc.)

resolution (Boville, 1991, 1995; Hamilton et al., 1995, 1999; Jones et al., 1997).

c *An End to GWD Parametrization?*

Unlike climate-chemistry models, which still run at fairly moderate resolutions, some global NWP models now equal or even exceed the resolution of the modelling studies discussed in the previous subsection. Since such models are now simulating some GWD, it suggests that as resolutions improve, GWD parametrization might soon become unnecessary in high-resolution models. However, several factors raised in the following text suggest that the spatial resolutions necessary to achieve this are still much shorter than the highest resolutions attained to date by global models, indicating that GWD parametrization will remain important for both global NWP and climate models for some time to come.

1 RESOLVING THE WAVE OSCILLATIONS

Gravity wave energy spectra vary with zonal wavenumber k roughly as $k^{-5/3}$ and thus the bulk of the energy variance can be contained at larger resolved scales (Hamilton, 1996; Koshyk et al., 1999). On the other hand, as pointed out by Hamilton (1996), spectra of wave momentum flux, the most relevant quantity for GWD calculations, decrease much more gradually with increasing k. Figure 9 plots a cospectrum of zonal and vertical (pressure) velocity perturbations from a Geophysical Fluid Dynamics Laboratory (GFDL) SKYHI N90L40 (Δx~1°–1.2°) simulation at ~45ºN during summer at a height of ~0.03 hPa (Hamilton, 1996). The spectrum is plotted in "energy content" form, so that the area beneath it is proportional to the total $\overline{u'\omega'}$ flux (a close proxy for momentum flux $\rho\overline{u'w'}$), where ω' is the vertical pressure velocity perturbation. Beyond $k \approx 30$ we see that the curve (and hence the flux contribution) increases gradually but monotonically up to the smallest resolvable scales in the model. While these spectral shapes vary considerably (note that $\overline{u'\omega'}$ is signed and thus its cospectrum can be positive or negative), Fig. 9 nonetheless highlights the importance of the smallest resolved wave scales to the total wave momentum flux. Observations and models suggest that the final break in these spectra, at which the horizontal spectrum of gravity wave oscillations would be fully resolved, occurs at scales O(1–10 km) (e.g., Bacmeister et al., 1996; Broad, 2000). This implies ~10–100-fold increases in horizontal resolution beyond even these state-of-the-art simulations that already stretch current computing capabilities.

2 RESOLVING THE SATURATION PROCESS

The previous arguments relate to resolving the wave oscillations themselves. Wave saturation and GWD, however, involve "subwavelength-scale" instabilities. While the exact details are uncertain (see Section 7a and Appendix Ad), saturation generally involves formation of unstable turbulent layers that are significantly shorter fractions of the wavelengths of the dissipating waves (see, e.g., Lindzen, 1988; McIntyre, 1989; Hines, 1991, 1992). Thus, resolving GWD in models would seem to require resolving these unstable portions of a wave field, then invoking the model's turbulent diffusion parametrization to mix them and thereby explicitly saturate the waves (e.g., Liu et al., 1999). Observations suggest these layers have vertical widths ≤50–200 m in the troposphere and lower stratosphere, increasing perhaps to ≤500–1000 m in the upper stratosphere and lower mesosphere (Sato and Woodman, 1982; Cot and Barat, 1986; Yamamoto et al., 1987; Fritts and Werne, 2000), with theory implying horizontal widths ~10–100 times longer (e.g., Lindzen, 1988). Such resolution in global 3D models is well beyond current computing capabilities: further, it probably also requires new generations of non-hydrostatic global models (e.g., Daley, 1988; Smolarkiewicz et al., 2001).

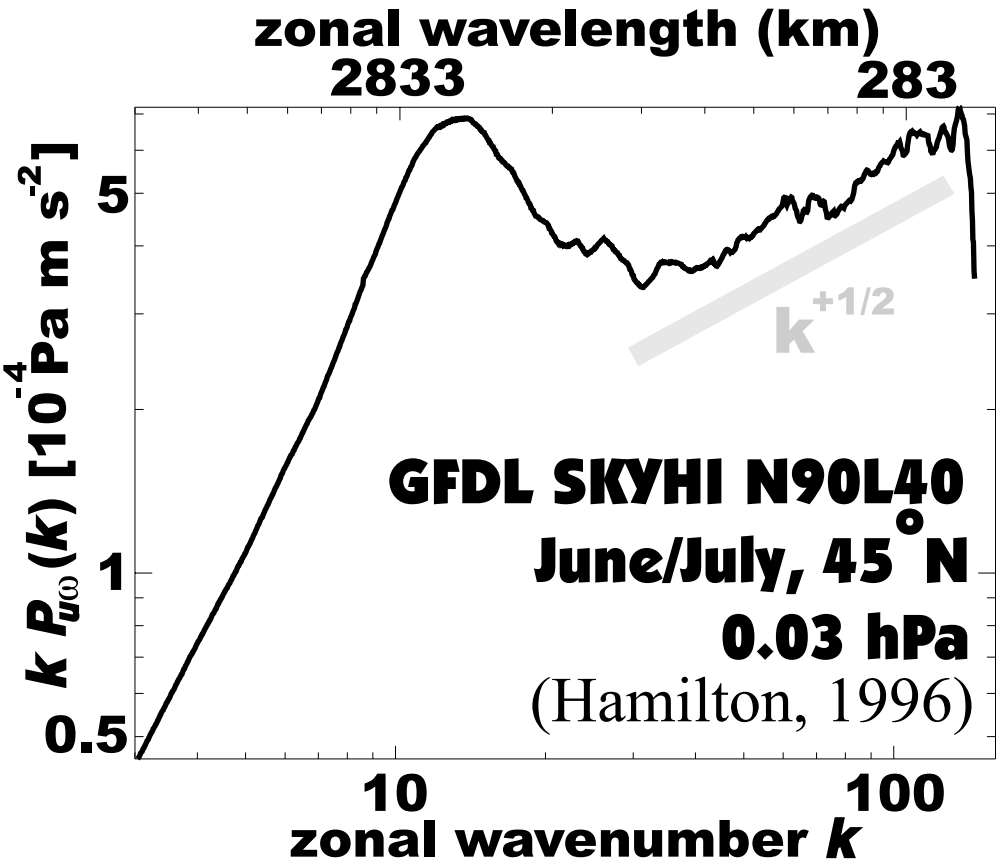

Fig. 9 Zonal wavenumber cospectrum $P_{u\omega}(k)$ of perturbations of zonal velocity u' and vertical pressure velocity ω' due to gravity waves explicitly resolved at 0.03 hPa (~73 km) and ~45°N in a GFDL SKYHI N90L40 (Δx~1° – 1.2°) model run for June/July. The result is taken from Fig. 18 of Hamilton (1996), with permission from Elsevier Science and replotted in "energy content" form $kP_{u\omega}(k)$ appropriate in log-log space. The spectrum is an average of many individual spectra and is smoothed in wavenumber space. The grey curve shows the $k^{+1/2}$ power law.

Given this, it is natural to ask how realistic-looking GWD can have been explicitly simulated within some current high-resolution global middle atmosphere models (see, e.g., Jones et al., 1997; Hamilton et al., 1999). Rather than being saturated by small-scale turbulent instabilities within the wave, it seems likely that waves within these models are refracted to shorter wavelengths and then removed or "quenched" by large-scale (i.e., wavelength-scale and above) turbulent and numerical diffusion schemes within the model (see, e.g., Fig. 6 of Marks and Eckermann, 1995). This has interesting similarities to the total breakdown assumption used in some GWD schemes, which also seem to produce reasonable estimates of GWD (e.g., Alexander and Dunkerton, 1999). Thus, while the precise saturation mechanisms may be wrong, such "quenched GWD" simulated in models may be entirely adequate for current global modelling purposes, which might then require the comparatively more moderate increases in resolution implied in the previous sub-subsection simply to resolve the waves themselves.

7 Further issues in gravity wave drag parametrization

The discussion in the previous sections has made clear that GWD parametrization for NWP and climate models is an important ongoing endeavour that is by no means solved. As evident from Section 6c, even optimistic projections of spatial resolution increases in models do not offer any imminent prospect of eliminating the need to parametrize GWD.

Thus, further developments are essential. This section raises a series of issues (many interrelated) for GWD parametrization that we believe deserve further study.

a *Wave Saturation*

As has been discussed (Sections 4b, 4c and 6c; Appendix Ad), wave instabilities that lead to saturation and GWD are still poorly understood, and so their specification in GWD schemes remains fairly basic.

While most single-wave schemes still use a saturation model similar to that of Lindzen (1981), a number of issues associated with this have been explored and extensions proposed (see e.g., the review of Dunkerton, 1989). GWD and vertical mixing of heat and momentum prove acutely sensitive to uncertainties in the degree of wave supersaturation and turbulence localization (Fritts and Dunkerton, 1985; Lindzen, 1988; McIntyre, 1989; Kim and Mahrt, 1992; Liu, 2000). It has also been shown that inertia gravity waves break at smaller amplitudes through dynamical rather than convective

instabilities (e.g., Lelong and Dunkerton, 1998). Mechanisms of saturation and GWD due to the "resonance breaking" of trapped mountain waves also remain somewhat uncertain (e.g., Georgelin and Lott, 2001). The uncertainties in spectral saturation theories are even larger (Gardner, 1996; Fritts and Alexander, 2003). As discussed in Section 4c, some spectral schemes assume that these saturation details are relatively unimportant for GWD calculations, while others assume that they are critical. All these issues merit further study.

Numerical studies suggest that much different dynamics govern breakdown/saturation of gravity waves in 3D than in 2D. Fritts and Werne (2000) review some of this recent work, but note that it is perhaps too early, at present, to assess the general impact for GWD and mixing (see also Fritts and Alexander, 2003). 3D effects are discussed more generally in the following subsection.

b *Three Dimensionality*

Noticeable differences in many gravity wave properties emerge on progressing from 2D to 3D models. Isolated 3D sources radiate characteristic 3D gravity wave patterns, such as "ship waves" from circular mountains (Smith, 1980; Sharman and Wurtele, 1983; Shutts, 1998) and circular/conical gravity wave patterns from convection (Piani et al., 2000; Lane et al., 2001). This implies directional GWD and critical level effects that are beginning to receive attention in parametrizations (e.g., Bacmeister, 1993; Shutts, 1995; Broad, 1995; Hines, 1997a; Gregory et al., 1998; Scinocca and McFarlane, 2000). Such 3D waves radiate into progressively greater horizontal volumes, an effect that taxes the validity of the column parametrization approach (discussed in the next subsection), particularly at upper levels. Moreover, this geometrical spreading of wave action leads to conservative wave amplitude evolution, saturation and GWD that can differ markedly from standard 2D theory (Shutts, 1998; Vosper and Mobbs, 1998; Broad, 1999; Broutman et al., 2001). 3D spreading tends to reduce wave momentum fluxes and GWD at upper levels compared to 2D predictions (e.g., Shutts, 1998). Both lateral spreading of, and reductions in, upper-level GWD seem to be needed in many models (see Section 7d).

Important changes can also occur at or near the source. Modelling flow over 3D mountains yields surface pressure drag and radiated wave momentum fluxes that again are smaller than for 2D ridges (e.g., Clark and Farley, 1984; Nappo and Chimonas, 1992). Low-level mountain wave breaking also varies in form and location on transitioning from 2D to 3D obstacles (e.g., Smith, 1989; Bauer et al., 2000), as does resonance breaking (Miranda and Valente, 1997). 3D surface flow can be blocked upstream, or else pass around the mountain where it can generate vortices downstream, producing drag in either case and often reducing wave amplitudes aloft (e.g., Peng et al., 1995; Schär and Durran, 1997; Bauer et al., 2000; Epifanio and Durran, 2001; Smith, 2001). These and other 3D effects have been partially implemented in some subgrid-scale orographic GWD schemes through additional orographic statistics (Kim and Arakawa, 1995) and are beginning to be fully parametrized in newer GWD schemes (e.g., Lott and Miller, 1997a; Gregory et al., 1998; Lott, 1999; Scinocca and McFarlane, 2000) and surface roughness schemes (e.g., Wood et al., 2001).

c *Column Parametrization*

Global models prefer parametrizations that operate in vertical columns above each horizontal grid box, since they run quickly and efficiently on parallel architectures. Thus, all existing parametrizations of GWD, both single-wave (see Sections 3a, 3b and 4b) and spectral (see Section 4c), are formulated as column algorithms. Stationary 2D orographic gravity waves propagate almost vertically, and thus orographic GWD parametrizations translate fairly naturally into "column parametrizations". Conversely, non-stationary waves from non-orographic (and orographic) sources propagate obliquely from their source into adjacent horizontal grid boxes (see Fig. 10), as do 3D and non-hydrostatic orographic waves. In reality this should yield a lateral spreading of GWD that has been pointed out from time to time (e.g., Kim and Arakawa, 1995; see also previous subsection). Nonetheless, any parametrization that attempted to model this lateral wave spreading directly would probably add drastically to the computational burden. Simpler ways of parametrizing this may be worth exploring since horizontally localized GWD sometimes seems to generate model errors (e.g., Klinker and Sardeshmukh, 1992).

d *Low-Level versus Upper-Level Gravity Wave Drag Parametrization*

As discussed in Section 4b, single-wave GWD schemes in the middle atmosphere tend to produce somewhat excessive drag rather suddenly, and GWD profiles can be scaled down and/or smoothed out in various ways. Orographic GWD schemes in global models often produce excessive "upper-level" (stratospheric) GWD and insufficient "low-level" (lower tropospheric) GWD (Klinker and Sardeshmukh, 1992; Kim, 1996; Milton and Wilson, 1996; Kim et al., 1998; Gregory et al., 1998).

A beneficial impact has been reported through an overall ad-hoc decrease of the ratio of upper-level to lower-level orographic GWD in models (e.g., Miller et al., 1989; Iwasaki et al., 1989), or through a selective and systematic decrease of this ratio (e.g., Kim, 1996; Milton and Wilson, 1996). Finding an optimal ratio, however, can be complicated: moreover, the ratio may not be the only problem.

Recent work has focused on parametrizing additional sources of low-level GWD (Section 3a) and surface friction drag (see Section 7e2), which act to redistribute low-level drag in models (Kim and Hogan, unpublished manuscript, 2003). Further, for orographic waves, addition of enhanced surface friction drag (Section 7e2), three-dimensionality (Section 7b) and stagnant flow regimes in valleys (e.g., Smith, 2001) all seem to reduce wave amplitudes and breaking at upper levels. Such work perhaps represents a new and more methodical approach to rectifying this recurrent problem.

e *Coupling among Drag Parametrizations*

1 SINGLE-WAVE AND SPECTRAL GRAVITY WAVE DRAG SCHEMES

An emerging trend in models with middle atmospheres is to use spectral schemes to parametrize collectively non-orographic GWD, with orographic GWD parametrized separately as a single-wave scheme (e.g., Fomichev et al., 2002). As parametrizations of non-orographic sources such as convection improve, it may be natural to implement them as single-wave schemes also (see Section 3b). Observationally at least, this approach seems reasonable: the gravity-wave field in the middle atmosphere shows "ambient" wave spectra at most locations (e.g., Fritts, 1989; Eckermann, 1995), punctuated by intermittent bursts of wave energy from individual wave events from sources such as orography (e.g., Eckermann and Preusse, 1999) and convection (e.g., Dewan et al., 1998). The larger issue, then, is how best to combine these GWD schemes in a model.

The simplest way is to run them non-interactively and sum the separate GWD contributions from each. In contrast to the horizontally localized column GWD from the single-wave schemes activated by spotty sources in the lower atmosphere (see Section 7c), the GWD from the spectral scheme is generally applied in every model grid box globally and thus has a smoother overall structure. In such implementations, the spectral scheme is most likely to be used as a final global tuning mechanism for the model's middle atmosphere, accounting for unparametrized sources of GWD in much the same way that Rayleigh friction is currently used to stabilize many models (e.g., Jackson et al., 2001): unlike Rayleigh friction, however, well-tuned spectral schemes should not lead to unrealistic reductions in model variability (e.g., Lawrence, 1997a). Most model tests to date have implemented spectral and single-wave schemes non-interactively (e.g., McFarlane et al., 1997; Manzini and McFarlane, 1998; Scaife et al., 2000; Osprey, 2001; Akmaev, 2001; Scinocca, 2002; Fomichev et al., 2002), with the spectral GWD scheme initialized and tuned using a highly simplified source (e.g., zonally uniform source-level spectrum).

While this is a sensible way to start, most spectral schemes advocate "interactive implementations" in which individual wave source information is coupled within the spectral scheme itself (e.g., Hines, 1997b; Alexander and Dunkerton, 1999; Medvedev and Klaassen, 2000). Osprey (2001) has tested both interactive and non-interactive implementations of orographic and spectral GWD schemes in offline single-column tests and within a 3D stratosphere-mesosphere model. Differences in each implementation were not huge, though sensitivity to the strength of the source was apparent. More studies along these lines are needed to clarify the dependencies.

The distinction between the single-wave and spectral schemes reflects, to some extent, differing needs in various models and different theoretical approaches to the parametrization problem. Most schemes have been implemented successfully, to some extent, in models and there has, to date, been little effort to couple several schemes systematically within a global model. Some single-wave GWD schemes, which were developed originally for lower atmospheric models, have also been extended to act as multiple-wave (multiple single-wave) schemes to cover the middle and upper atmospheres (e.g., Jackson, 1993; Norton and Thuburn, 1999). Whether more explicit coupling among different schemes is useful or even desirable remains to be seen: for example, the lack of success in coupling lower-level and upper-level radiation parametrizations in models may augur poorly for similar efforts with GWD schemes.

2 OROGRAPHIC GRAVITY WAVE DRAG SCHEME AND ENHANCED SURFACE FRICTION DRAG

The surface friction drag induced by flows over/around complex orography has been actively studied: see, for example, recent reviews by Belcher and Hunt (1998) and Wood (2000). Like boundary layers over flat terrain, studies suggest near-surface flow over hilly terrain can also be represented as a "form drag" with enhanced effective roughness lengths due to both vegetative and subgrid-scale orographic effects (Wood and Mason, 1993). In addition to drag on the large-scale flow, surface friction can significantly affect orographic GWD: studies suggest it reduces mountain wave amplitudes and breaking aloft (Section 7d) and is critical for the realistic formation of downslope windstorms and rotor flows (e.g., Richard et al., 1989; Ólafsson and Bougeault, 1997; Leutbecher and Volkert, 2000; Doyle et al., 2000; Doyle and Durran, 2002). This suggests a need to couple surface friction and orographic GWD parametrizations in models, an issue that is beginning to receive attention (Wood et al., 2001).

Inclusion of both a parametrization of an enhanced surface friction drag and an orographic GWD parametrization in large-scale models can yield beneficial impacts (Mason, 1986; Milton and Wilson, 1996; Gregory et al., 1998; Hogan et al., 1999). In particular, Gregory et al. (1998) showed that insertion of a surface friction scheme reduced parametrized orographic gravity wave fluxes by half, possibly due to direct frictional retardation of surface flow forcing of waves. Such work may help further alleviate the excess of upper-level to lower-level orographic GWD ratio noted in Section 7d. These improvements follow from running the schemes non-interactively. Whether more explicit coupling is needed to simulate other effects of surface friction on orographic GWD remains to be seen.

Enhanced friction drag (i.e., form drag), however, should be inserted into models with caution. As discussed in Section 2a, introduction of a new drag mechanism will modify the balance among the models' various drag mechanisms. For example, an increase in surface friction drag may compensate for the underestimation of other drag terms, such as GWD or mountain drag (see Kim and Hogan, unpublished manuscript, 2003), leading to an apparent (i.e., illusory) improvement of the model simulation. Boer and Lazare (1988) reported a paradoxical increase in net surface drag (mountain drag + friction drag) when a GWD parametrization was removed from their model, but this may be due to the omission of GWD from their budget calculations (Kim and Hogan, unpublished manuscript, 2003).

f *Interactions among Gravity Wave Drag and Convection/Cloud Parametrizations*

As noted by Shepherd (2000), subgrid-scale GWD schemes control the accuracy of global middle atmosphere simulations in much the same way that subgrid-scale parametrizations of clouds/convection (and radiation/land surface processes) impact simulations of the global weather and climate of the troposphere. It is not surprising, then, that as global models extend their boundaries to encompass both the troposphere and middle atmosphere, a number of potentially important interactions among GWD schemes and convection/cloud schemes are coming to light. We consider a few here.

1 SOURCE TERMS FOR CONVECTIVE GRAVITY WAVE DRAG PARAMETRIZATION

As discussed in Section 3b, output from convective parametrizations is beginning to be used to initialize convective GWD parametrizations. Various parameters have been used to specify this wave source term to date: convective mass flux, precipitation, latent heating, and so on. Since convectively generated gravity waves are generally non-stationary, formulating the radiated gravity wave stress at the cloud tops is nontrivial. Steady-state formulations of cloud-top wave stress induced by stationary diabatic forcing by Chun and Baik (1998) are based on a reference frame moving with the convection, generating waves that are stationary relative to the diabatic forcing. However, recent cloud-resolving numerical modelling studies (e.g., Alexander et al., 1995; Piani et al., 2000; Lane et al., 2001) show more momentum flux contributed by waves propagating westward relative to the convective system. These non-stationary gravity waves need to be included in convective GWD parametrizations.

The study of explicitly resolved gravity waves generated by tropical convection may aid this undertaking. Such studies in global models (discussed in Section 6a) raised a more general question about whether convective adjustment and cloud parametrization schemes in models are sufficiently accurate at present to permit reliable specifications of the convective wave source term in global models. This is particularly critical to assess, since, if unreliable, the large amounts of resolved wave activity generated by these schemes in the tropics could negatively impact climate and forecast skill as model resolutions increase.

2 SUBGRID-SCALE GRAVITY WAVE FEEDBACKS ON CLOUD FIELDS

Fractional cloud cover and precipitation within a model grid box are often calculated in convective schemes with the aid of probability distributions of water saturation due to subgrid-scale variability. While it has generally been assumed that this variability stems from convective eddies and turbulence, it is clear that gravity waves and other sources of subgrid-scale variability at mesoscale resolutions also contribute (Balaji and Redelsperger, 1996).

The general banding of cloud cover by gravity waves is well established from observations (e.g., Erickson and Whitney, 1973; Worthington, 2001), while modelling has shown how typical gravity wave temperature variability affects microphysics of high cirrus (Jensen and Toon, 1994) and polar stratospheric clouds (e.g., Bacmeister et al., 1999; Dörnbrack et al., 2001). Gravity waves associated with convective weather feed back to modify or organize severe convection and precipitation (e.g., Koch and Siedlarz, 1999).

Flows over subgrid-scale orography also affect precipitation. Smith (1979) cites three essentially independent mechanisms for producing orographic rain: large-scale upslope rain due to condensation caused by orographic ascent or orographically-triggered convection; rainfall enhancement by low-level clouds over small hills through washout of upper-level cloud droplets; local downslope rain from cumulonimbus forming in thermals as mountain slopes are heated by the sun. Some studies suggest orographic rain enhancements are significantly impacted by mountain wave dynamics (Richard et al., 1987; Reinking et al., 2000; Brady and Waldstreicher, 2001).

Recent work has focused on the way in which gravity waves and other sources of unresolved mesoscale variability can significantly influence output of cloud/convection parametrizations in large-scale models (Balaji and Redelsperger, 1996; Cusack et al., 1999; Nilsson et al., 2000). In models it is conceivable that GWD schemes could be used to feed subgrid-scale gravity wave fluctuations directly into cloud parametrizations (e.g., Bacmeister et al., 1999).

3 DIABATIC CLOUD/MOISTURE EFFECTS ON OROGRAPHIC GRAVITY WAVE DRAG

Diabatic effects within clouds, such as latent heat release or cloud-top infra-red cooling, can modify the tropospheric environment in ways that significantly impact the trapping and amplitude evolution of mountain waves and the GWD they produce (e.g., Durran and Klemp, 1982a, 1982b; Weissbluth and Cotton, 1989; Doyle and Shapiro, 2000; Doyle and Smith, 2003). Surgi (1989) included a moisture-modified Brunt-Väisälä frequency tuned arbitrarily to various cloud types in an orographic GWD scheme that was tested in a global model. Since then, these effects have received little attention in parametrizations. Again, the issue of whether convective schemes in models are good enough at present (Section 6a) may dictate the feasibility, or otherwise, of pursuing developments along these lines.

g *Interactions between Resolved Gravity Waves and Parametrized Gravity Wave Drag in High-Resolution Models*

As discussed in Section 6, increases in resolution are allowing models to resolve the "outer scales" of the gravity wave spectrum and to capture some GWD. This implies that any changes in grid-box resolution in next-generation models will be accompanied by changes in resolved GWD that will necessitate retuning of the parametrized subgrid-scale GWD. Beyond such practical concerns, this raises some deeper and perhaps thornier issues for subgrid-scale GWD parametrization.

1 TEMPORAL VARIABILITY OF GRAVITY WAVES

At each model time step, column parametrizations of GWD ingest a vertical profile of model winds and temperatures within a given grid box and propagate gravity waves through this vertical column as if the atmosphere were static. Of course these winds and temperatures vary over time, but if wave propagation times are sufficiently fast this complication can usually be ignored.

As models' spatial resolutions improve, however, model time steps Δt decrease unless a more efficient transport algorithm such as a semi-Lagrangian scheme is used, and thus there is greater potential for significant temporal atmospheric variability to be resolved. Furthermore, as the tops of models are extended into the middle atmosphere and beyond, the total time required for any given gravity wave to propagate vertically through the column from its tropospheric source, t_{PROP}, increases considerably. Decreases in Δt and increases in t_{PROP} both conspire to make the neglect of temporal variability in modelling gravity wave propagation in GWD parametrizations potentially less tenable. In situations where time dependence of the background atmosphere has been shown to be important, the modifications it makes to GWD profiles can be quite large (see, e.g., Eckermann and Marks, 1996).

Increased temporal variability in models also leads to greater time variations in applied subgrid-scale GWD. Steady GWD drives the atmosphere to a new steady dynamical state, whereas temporally unsteady GWD produces vacillating mean flows. In particular, if steady GWD in some region suddenly increases or abates, the flow there becomes unbalanced and will try to relax to a new balanced state through reradiation of secondary gravity waves (e.g., Vadas and Fritts, 2001). It could be argued that spectral models parametrize the net effects of all waves, including reradiated secondary waves, and as such might also be less affected by the "transit time" issue for single waves discussed here. As model resolutions improve, temporal intermittency in GWD applied by subgrid-scale parametrizations could cause these models to radiate an explicitly resolved spectrum of secondary gravity waves spontaneously much of the time. Their existence and any potential effects on model accuracy are unclear at present.

2 WAVE-WAVE INTERACTIONS

Much of the increased spatio-temporal variability in high-resolution models is produced by explicitly resolved long wavelength gravity waves, particularly above the tropopause (Koshyk and Hamilton, 2001; Section 7). These resolved waves produce oscillations or "wiggles" on the background wind and temperature profiles passed to GWD parametrizations. In models where resolved waves are energetic, these oscillations can significantly modulate the predicted subgrid-scale GWD, and thus the GWD scheme implicitly simulates some form of wave-wave interaction between the resolved gravity waves and the subgrid-scale (parametrized) gravity waves.

Such situations were never envisaged in the formulation of most GWD parametrizations, and thus these effects require scrutiny. Detailed modelling of the modulations of short gravity waves propagating through longer gravity waves indicate that the interactions are much more complicated than single-wave GWD parametrizations would predict: for instance, the time dependence of the long wave field usually cannot be neglected when modelling the propagation and amplitudes of short waves (Eckermann and Marks, 1996; Walterscheid, 2000). Indeed, a whole class of potentially relevant wave-wave interactions may occur, none of which is included in single-wave GWD schemes. While some spectral models are formulated to encapsulate the net spectral effects of certain wave-wave interactions, the GWD parametrizations they spawn are again formulated under the premise that they act on, and respond to, only a large-scale atmosphere devoid of resolved gravity waves (e.g., Hines, 1997a, 1997b; Medvedev and Klaassen, 2000).

In short, existing GWD parametrizations are not designed for models containing energetic resolved gravity waves. As more pressing parametrization problems are tackled and solved, this wave-wave interaction issue may become progressively more important, particularly as model resolutions improve and upper boundaries are extended. One near-term solution could follow from modifying Lander and Hoskins' (1997) suggestion to use only the "believable scales" of a model as input for parametrizations. Current GWD parametrizations in high-resolution models could remain "believable" if they used vertical profiles of model winds and temperatures that have been "averaged" or "filtered" so as to eliminate resolved gravity wave oscillations. Studies of resolved wave-wave interactions within models could also be very helpful in understanding and ultimately parametrizing these effects.

h *The Jet Stream (as an Example of Other Gravity Wave Sources)*

Gravity wave sources besides convection and topography exist, which have proven difficult to understand and parametrize. Section 3 of Fritts and Alexander (2003) provides a good review of a variety of sources that merit attention. In this subsection, we discuss waves from the "jet stream", since their potential relevance to GWD in the summer middle atmosphere, for instance, has been established (e.g., Bühler and McIntyre, 1999; Scinocca and Ford, 2000; see also Fig. 1). In the lower atmosphere, they may also exert an important "emission drag" on the jet itself (Sutherland and Peltier, 1995).

While observational associations go back many years (e.g., Hooke and Hardy, 1975), modelling jet-stream gravity waves has proven difficult. Uccellini and Koch (1987) tackled the problem from an observational meteorological perspective. They noticed that energetic "mesoscale waves" reported over the continental U.S.A. arose in conjunction with diffluent "exit" regions of the jet at ~300 hPa. They argued that geostrophic adjustment of these regions radiates long-wavelength inertia gravity waves. In their theory, these waves become trapped in the troposphere due to a critical layer made

reflective (or "overreflective") by unstable vertical shear. Subsequent observations and modelling have supported the general scenario, while substantially developing the overall picture, and with details varying on a case-by-case basis (e.g., Koch and Dorian, 1988; Powers, 1997; Koch and Siedlarz, 1999; Zhang et al., 2001). Their potential GWD contribution is unclear. In the absence of ducting by an unstable critical layer, these waves should propagate into the middle atmosphere, as has been verified by observation (Guest et al., 2000; Pavelin et al., 2001) and 3D modelling studies (Luo and Fritts, 1993; O'Sullivan and Dunkerton, 1995). Breaking of these waves higher up (e.g., Pavelin et al., 2001) produces GWD.

However, other types of instabilities can also radiate waves from the jet: for example, the unstable shear layers that duct waves in the Uccelini and Koch (1987) model can also radiate waves via dynamical (Kelvin-Helmholtz) instabilities in certain circumstances (e.g., Sutherland and Peltier, 1995; Bühler et al., 1999; Scinocca and Ford, 2000). Still other models associate jet-level wave generation with other dynamics, such as "inertial instability" (Ciesielski et al., 1989) or "Lighthill radiation" (Ford, 1994; Medvedev and Gavrilov, 1995; Reeder and Griffiths, 1996; Ford et al., 2000).

These generation mechanisms are all interrelated to varying extents, focusing on some diagnosed form of dynamical imbalance or instability that develops in the jet and then triggers radiation of gravity waves to restore balance. A unified theory of such dynamics has been sought but remains elusive: for example, the formal existence or otherwise of a "slow (or quasi-slow) manifold" that would unambiguously separate "balanced" motion from "unbalanced" motions such as gravity waves (e.g., McIntyre and Norton, 2000; Ford et al., 2000). A variety of measures have been proposed for diagnosing balance to various levels of approximation for potential use in identifying when and where waves might originate due to jet imbalances (e.g., Knox, 1997; Olsson and Cotton, 1997; Zhang et al., 2000). Koch and O'Handley (1997) showed that some of these measures, when calculated from NWP model output, showed promise in forecasting mesoscale wave occurrences in the troposphere. Other quantities (e.g., Rossby radii of deformation, duct depth) seem to specify observed parameters of these waves reasonably well (Uccellini and Koch, 1987; Koch and O'Handley, 1997). Such terms could be calculated within global models as source terms for a subgrid-scale parametrization of "jet-exit" GWD.

One difficulty, however, may be that, similar to wave-induced instabilities (see Section 6c2), these source regions of flow instability may often be of subgrid scales themselves (see e.g., Sutherland and Peltier, 1995; Section 5b of Scinocca and Ford, 2000), making this source of GWD hard to parametrize. If so, the only recourse may be higher model resolutions. O'Sullivan and Dunkerton (1995) used a simplified global spectral model to simulate gravity wave radiation explicitly from exit regions of evolving mid-latitude baroclinic disturbances. Appreciable wave radiation occurred at T106 with $\Delta z \sim 700$ m in the stratosphere. Comparable or better resolution is used in many NWP models, which suggests (see Section 6) that these jet-stream source regions and some of the large-scale gravity waves they radiate may already be appearing explicitly in some higher resolution global models.

8 Conclusions

Expanding scientific knowledge and advancing computing technologies have encouraged converging trends in development of global atmospheric models. For example, the distinctions between global NWP models and GCMs are now becoming less obvious: NWP models are gradually increasing the temporal range of their numerical integrations, while GCMs are gradually increasing their spatial resolutions. Further, middle atmosphere modellers have come to appreciate the importance of a realistic troposphere (e.g., Hamilton, 1996; Garcia, 2000), while tropospheric modellers and forecasters are incorporating middle atmospheres to improve both climate and forecast skill (e.g., Pawson et al., 2000; Thompson et al., 2002). As spatial model resolutions increase the need for non-hydrostatic model formulations has arisen (see Fig. 11; see also Smolarkiewicz et al., 2001), which removes a major distinction between global and regional NWP models (e.g., UK Met Office Unified Model; Cullen et al., 1997).

There will still be important differences of course: for example, the tops of NWP models are expected to be extended to include the middle atmosphere, but perhaps not as high as those of GCMs which include the upper atmosphere. NWP models will always tend to have higher resolutions and shorter integration time steps than GCMs, with GCMs including more diverse physics and chemistry packages and NWP models focusing more on data assimilation.

Nonetheless, these evolving similarities mean that differing perspectives on GWD parametrization that have emerged among various segments of the global modelling communities (e.g., troposphere versus middle atmosphere modellers; Sections 3 and 4) now need to be combined and reconciled for wider future modelling use. This paper has attempted to summarize some of these perspectives and some of the issues that arise in combining them more generally. Emerging issues have also been discussed and/or anticipated, such as explicitly resolved gravity waves and coupling among parametrizations (Sections 6 and 7). We also speculated on the model resolutions ultimately required to eliminate the need for GWD parametrization (Section 6).

The science of GWD parametrization is only about 20 years old, yet it has progressed and evolved significantly during that time. Thus, beyond the general issues and trends cited above, it is difficult, and probably futile, to speculate on exactly how things might develop in the next 5–10 years as next-generation global models come online. It is certainly safer to assert that many of the current uncertainties in GWD parametrization specifically, and atmospheric dynamics generally, may be solved in no small measure by the insights provided by these next-generation modelling tools. Such breakthroughs imply much improved understanding and forecasting of our atmosphere as a whole, and in particular the role of gravity wave processes within it.

Acknowledgments

The authors acknowledge the support of Dr. John Montgomery, Director of Research at the Naval Research Laboratory. YJK was supported by the Office of Naval Research under ONR Program Element 0602435N. SDE acknowledges partial support for this work through the Office of Naval Research, NASA's Office of Earth Sciences' Atmospheric Chemistry Modeling and Analysis Program (ACMAP) and NASA's Office of Space Sciences' Geospace Sciences Program. HYC was supported by the Climate Environment System Research Center sponsored by the SRC Program of the Korea Science and Engineering Foundation. The authors appreciate the three anonymous reviewers who provided a thorough review of the manuscript along with valuable comments that led to improvement of the manuscript. The authors also thank Drs. Tim Hogan, Larry Coy, Jim Doyle, Alex Medvedev, Gary Klaassen and Joan Alexander for constructive comments; Mr. Jung-Suk Goh for improving some figures; Prof. Akio Arakawa for providing Fig. 3; and Dr. Lucrezia Ricciardulli for providing data to generate Fig. 7.

Appendix A: Basic theories and nomenclature relevant to gravity wave drag parametrization

We will briefly summarize some basic concepts and dynamical theories that are needed to understand the parametrization of GWD in large-scale atmospheric models. Figure 10 provides an idealized picture of the type of gravity wave generation, propagation and dissipation processes in the atmosphere that parametrizations seek to approximate. Parametrizations focus on the drag effects produced by gravity wave dissipation that are important for NWP and climate models. This represents the end stage of the wave's life cycle, but to describe it accurately, parametrizations must also describe the earlier "birth" and "evolution" stages that lead up to it. This basic three-stage "life cycle" paradigm for a gravity wave underpins the construction of most GWD parametrization schemes (see, e.g., Section 7 of Fritts and Alexander, 2003), and will be used here to introduce common terminology and concepts encountered in the field.

a *Surface Drag*

We begin by briefly discussing drag processes operating at the surface. Even for stably stratified flow over a symmetric frictionless surface obstacle, a pressure difference can occur between the surface flow upstream and downstream of an obstacle. For a 2D ridge, this yields a "drag" force $\tau = \int p_{surf}(x)\frac{dh(x)}{dx}\,dx$ where $p_{surf}(x)$ is the surface pressure as a function of horizontal distance x in response to variations in elevation due to the ridge height $h(x)$, and the integral is across the full x extent of the obstacle. This drag force, referred to as "mountain drag" or sometimes "pressure drag" (e.g., Smith, 1978), represents a transfer of angular momentum from the atmosphere to the solid Earth, which acts to decelerate the zonal flow at the surface.

For higher mountain elevations $h(x)$ the flow sometimes cannot pass over the mountain, and thus the flow becomes blocked upstream for 2D ridges or flows around the mountain peak for 3D obstacles, leading to drag and altered atmospheric responses (e.g., lee vortices).

There must be an equal and opposite exchange of momentum from the solid Earth back to the atmosphere. This atmospheric response manifests itself in different forms depending on the wind speed and horizontal and vertical scales of the orographic feature (e.g., Smith, 1978). At planetary topographic scales, for example, the response can be in the form of radiated planetary Rossby waves, a process that is resolved in most GCMs and NWP models. At very short topographic scales the atmospheric response is turbulent, often parametrized in terms of an effective surface roughness that acts like a frictional force on the flow within the planetary boundary layer ("form drag"). These processes are discussed in more detail in Sections 7b, 7d and 7e2 (see also recent reviews by Belcher and Hunt (1998), Wood (2000) and Smith (2001)). At horizontal topographic scales, ~10–100 km, where buoyancy forces tend to dominate, the atmospheric response is often a radiated field of gravity waves (mountain waves) with a vertical flux of horizontal momentum density $\rho\overline{u'w'}$ that balances the surface mountain drag τ produced by these particular topographic features, where ρ is the atmospheric density, u' and w' are, respectively, the horizontal and vertical velocity perturbations of the wave, and the overbar denotes averaging over a full wave cycle (wave momentum flux is discussed further in Section d1 of this Appendix). Since 10–100-km scale topography is not fully resolved in GCMs or NWP models, this subgrid-scale surface mountain drag and the radiated mountain waves must be parametrized.

b *Wave Generation*

1 OROGRAPHIC VERSUS NON-OROGRAPHIC GRAVITY WAVES

As we have just noted, one very important source of gravity waves for drag parametrization at all levels is flow over topography ("orographic" forcing), and drag due to mountain waves has been widely parametrized (details discussed in Section 3a). In fact, gravity waves are generated by a variety of other sources that are located mostly in the troposphere, however, waves from sources other than mountains are less well understood, and currently are often ignored or parametrized collectively. For this reason, GWD parametrizations are often classified as either "orographic" or "non-orographic". Sources of non-orographic gravity waves include convection (Sections 3b, 6a), jet streams (Section 7h) and fronts, among others. See Section 3.1 of Fritts and Alexander (2003) for a detailed review of atmospheric processes that generate gravity waves.

2 SINGLE GRAVITY WAVES VERSUS WAVE SPECTRA

Parametrizations tend to fall into "single-wave" schemes, which deal with individual waves, and "spectral" schemes, which collectively parametrize the effects of a broad spectrum of gravity waves. Based on an earlier understanding that

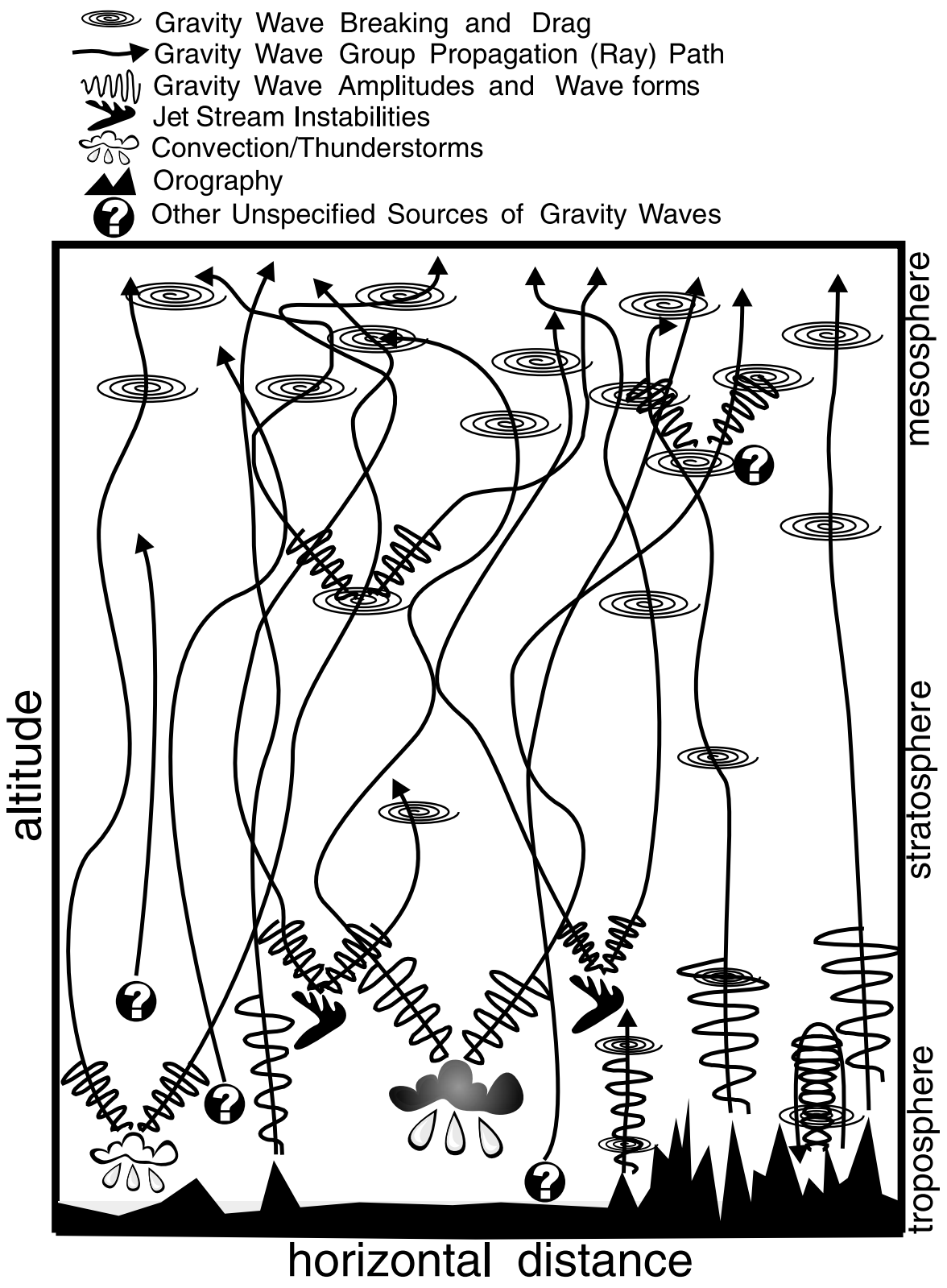

Fig. 10 Schematic of various gravity wave production, propagation and dissipation processes that parametrizations seek to capture, along with associated processes (see symbol key at top). Surface orography, convection and jet streams are shown as sources of waves, with stationary mountain waves launched quasi-vertically and non-stationary waves launched obliquely into the atmosphere. Wave breaking is depicted along wave propagation paths in various regions of the atmosphere. Wave breaking is more prevalent higher in the atmosphere, where wave propagation paths cross and thus waves interact more, yielding broader wave spectra, and some breaking reradiates secondary waves. Other waves break lower down, nearer their source or reflect vertically and break via trapping/resonance effects (see mountain wave, lower-right). The figure depicts a basic paradigm of the troposphere as a source region, the stratosphere as a propagation region and the upper stratosphere and mesosphere as a strong breaking region.

gravity wave sources mostly radiate coherent wave packets (Fig. 10), most near-source parametrizations have been single-wave schemes (though not always – see, e.g., Gregory et al., 1998). As gravity waves propagate away from their tropospheric source regions, their propagation paths start to meander further and intersect with those of other waves (Fig. 10), so that a broader distribution of wavelengths and frequencies is encountered higher up and total wave variance is less identifiable with low-level sources. For these historical and scientific reasons, spectral GWD schemes tend to be applied in the middle atmosphere, whereas in the lower atmosphere single-wave schemes tend to dominate GWD parametrizations. However, these distinctions are oversimplified and somewhat arbitrary: for example, broad gravity wave spectra are often observed in the troposphere, while coherent single-wave patterns from identifiable sources sometimes extend well into the middle atmosphere (e.g., Dewan et al., 1998). Also, the single-wave schemes are not restricted to treating just one wave, instead, it is common to apply single-wave schemes iteratively to a set of waves, summing the single-wave contributions from each to yield the total drag (e.g., Norton and Thuburn, 1999). These and other issues are discussed in greater detail in Sections 3 and 4.

3 STATIONARY VERSUS NON-STATIONARY GRAVITY WAVES

Source parametrizations are important because they set the properties of the waves (e.g., wavelength, amplitude) that control subsequent wave evolution and the form and intensity of the wave-induced drag. A particularly important parameter for GWD calculations is the wave's ground-based horizontal phase speed, c, which is set at the source and typically assumed to remain constant thereafter. As discussed in the next two subsections, its value determines where waves tend to break and the strength of the GWD. Parametrizations commonly differentiate between "stationary" ($c = 0$) and "non-stationary" ($c \neq 0$) gravity waves, mainly because this classification in parametrizations is currently synonymous with orographic and non-orographic waves, respectively. While this correspondence is a useful guide for parametrization, in reality sources other than mountains can generate stationary waves (discussed in Sections 3b and 7h), while orography can generate both stationary and non-stationary gravity waves (e.g., Nance and Durran, 1997, 1998).

c *Wave Propagation and Evolution*

1 INTERNAL VERSUS EXTERNAL GRAVITY WAVES

The linearized 2D equation governing vertical velocities due to gravity waves (neglecting the Coriolis force, curvature of the horizontal wind $\bar{U}(z)$ and density effects) can be written as

$$\frac{\partial^2 \tilde{w}}{\partial z^2} + \left(\ell^2 - k^2\right)\tilde{w} = 0. \qquad (1)$$

Here, $\tilde{w}(k,z,t)$ is the Fourier-transformed vertical velocity $w(x,z,t)$ at height z, and $\ell^2(z) \approx N^2(z)/[c - \bar{U}(z)]^2$, where $N(z)$ is the Brunt-Väisälä frequency, and $k = 2\pi/\lambda_x$ is the horizontal wavenumber. For stationary mountain waves ($c = 0$), $\ell^2(z)$ is known as the Scorer parameter (e.g., Durran, 1990). For an assumed form of solution $\tilde{w}(k,z,t) = W(k) \exp[i(\int m(z)dz - kct)]$, Eq. (1) yields the local gravity wave dispersion relation

$$m^2(z) = \ell^2(z) - k^2 = k^2[N^2/\hat{\omega}^2(z) - 1], \qquad (2)$$

which relates k to the vertical wavenumber m and intrinsic frequency $\hat{\omega} = k(c - \bar{U})$. The form of the gravity wave depends on the sign of $m^2(z) = \ell^2(z) - k^2$, which is determined mostly by flow conditions and the source of the gravity wave. The wave is propagating or "internal", if $m^2 = \ell^2 - k^2 > 0$, i.e., m is real. When $m^2 = \ell^2 - k^2 < 0$ the solution is "external", in that m becomes imaginary, the wave is not propagating, and $\tilde{w}(k,z,t)$ decays with height as $\exp[-\int|m(z)|dz]$. When a free propagating wave ($m^2 > 0$) propagates to a height z_t where $m^2(z_t) \to 0$, its vertical wavelength locally becomes infinitely long and wave energy is reflected downwards, with wave solutions becoming external above this "turning point" z_t. In the current approximation Eq. (2), turning points occur where $\ell^2 = k^2$ or equivalently where $\hat{\omega} = N^2$.

For stationary mountain waves, turning points can often lead to the trapping of wave energy between the surface and the turning point. Figure 11 shows examples of these regimes, plotted as a function of zonal wavelength λ_x and height z under typical mid-latitude winter conditions for $\bar{U}(z)$ and $N(z)$. The internal mountain waves to the right of this figure propagate obliquely away from their surface topography. The waves with longer horizontal wavelengths λ_x propagate into the stratosphere, whereas the shorter scale waves encounter turning points z_t, denoted by the thick $\ell^2 = k^2$ line. These waves reflect vertically and become "trapped" between the surface and z_t and can be channelled downstream within their duct layer. The magnitude of this trapping can be measured by the vertical decrease of the Scorer parameter, $\ell^2(z)$.

2 HYDROSTATIC VERSUS NON-HYDROSTATIC GRAVITY WAVES

Gravity waves with $\ell^2/k^2 >> 1$ are termed "hydrostatic", since simplified hydrostatic equations adequately describe their propagation and evolution (e.g., Lindzen, 1981). For example, the dispersion relation Eq. (2) simplifies to $m^2 \approx \ell^2 = N^2/(c - \bar{U})^2$ for hydrostatic waves. Many parametrization schemes are based on a hydrostatic framework. Conversely, internal gravity waves for which $\ell^2/k^2 \sim O(1)$ are termed "non-hydrostatic". From this limit and the dispersion relation Eq. (2), we note that reflected and ducted waves are non-hydrostatic, and that free-propagating non-hydrostatic waves tend to have relatively shorter horizontal wavelengths λ_x, longer vertical wavelengths λ_z, faster intrinsic phase speeds $|\hat{c}$ $(= c - \bar{U})|$, higher intrinsic frequencies $\hat{\omega}$ compared to hydrostatic waves (see Fig. 11). Non-hydrostatic waves are important in the parametrization of low-level "trapped" mountain waves and "fast" gravity waves generated by convection (see Section 3).

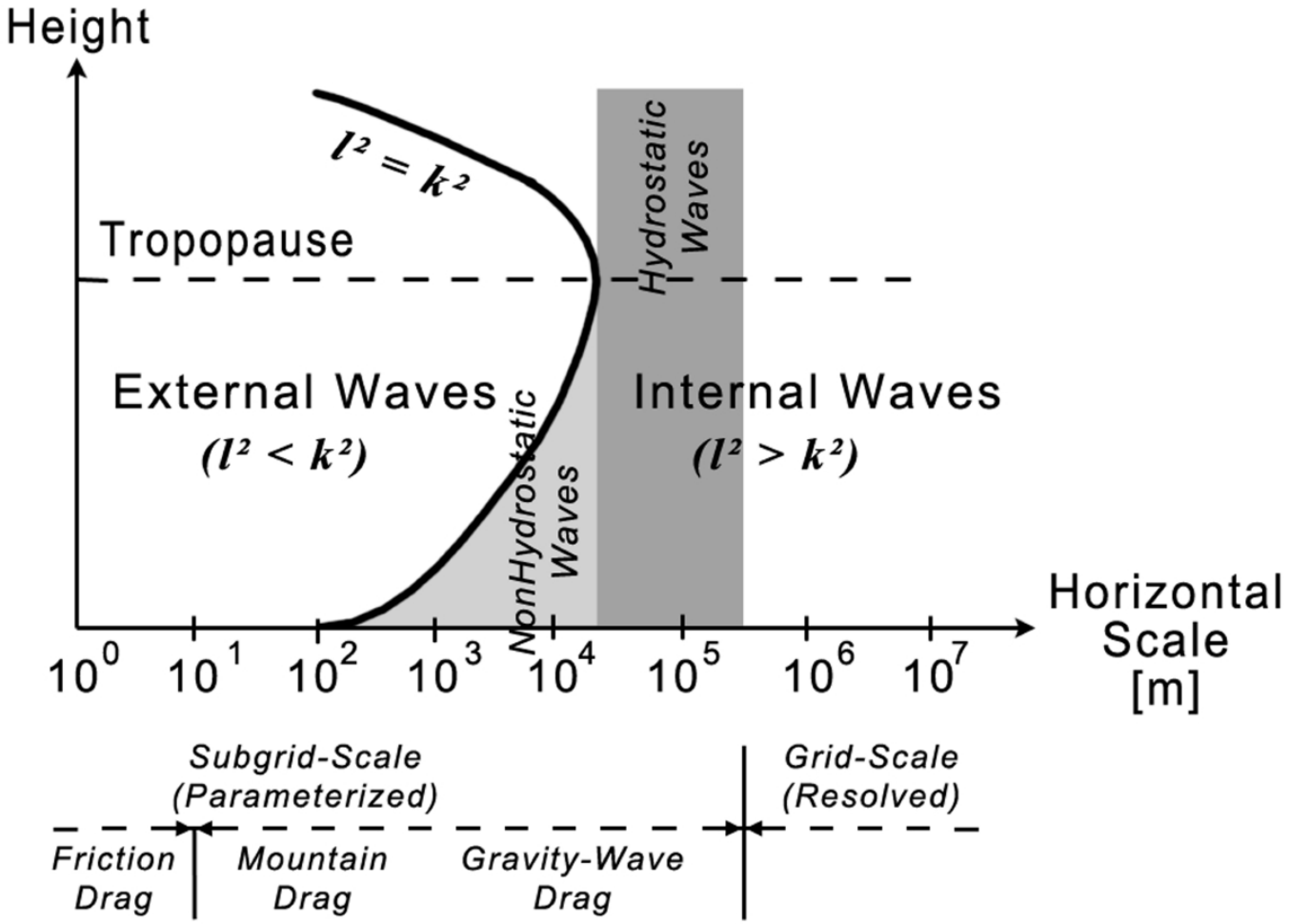

Fig. 11 Spectrum of the vertical propagation of orographic gravity waves as a function of height and horizontal scale, under typical mid-latitude northern hemisphere winter conditions. ℓ^2 denotes the Scorer parameter, which depends on static stability, wind speed and curvature, and $k = 2\pi/\lambda_x$ denotes the zonal wavenumber. (Based on Iwasaki et al. (1989; with permission from the Meteorological Society of Japan) and Kim (1996; with permission from the American Meteorological Society))

Inclusion of the Coriolis parameter (inertial frequency) f in Eq. (1) leads to a dispersion relation in which the $N^2/\hat{\omega}^2 - 1$ factor in Eq. (2) becomes $(N^2 - \hat{\omega}^2)/(\hat{\omega}^2 - f^2)$. Thus, f imposes a low-frequency limit for gravity waves, so that allowable frequencies for internal gravity waves are $|f| < |\hat{\omega}| < N$. Gravity waves with frequencies near $|f|$ are termed "inertia gravity waves", since the Coriolis force modifies their propagation and polarization characteristics compared to gravity waves for which $|\hat{\omega}| >> |f|$.

3 THE CRITICAL LEVEL z_C

An important physical process that needs to be considered in GWD parametrizations is the "critical level", an altitude where the wind speed component along the wave's horizontal wave vector equals its phase speed c: in 2D and ignoring rotation the criterion is $c = \bar{U}(z_C)$, where z_C is the critical level (Lindzen, 1981). Since $\hat{c} = c - \bar{U}(z)$ in this case, this corresponds to vanishing intrinsic phase speed $|\hat{c}|$ and vertical wavelength λ_z from Eq. (2). With rotation added, the equivalent criterion is $|\hat{\omega}| - |f|$ and $|\hat{c}|$ becomes very small rather than vanishing completely. In most circumstances gravity waves dissipate strongly as they approach critical levels and are totally dissipated at or just below the critical level. This process is important as a wave filtering mechanism for the middle atmosphere (see Section 4a). However, strong wave dissipation and/or mean wind shear near a critical level can induce strong non-linearity that can sometimes turn these regions into efficient resonant reflectors that vertically trap wave energy (e.g., Peltier and Clark, 1979). Such effects are important in parametrizing GWD due to low-level mountain waves (Section 3a) and tropospheric gravity waves associated with the jet stream (Section 7h). The effects of non-linear wave trapping can be represented by the vertical derivative of the Scorer parameter, similar to the linear trapping case (Section c1 of this Appendix). The Scorer parameter has been used explicitly in some parametrization schemes to represent the effects of linear and/or non-linear wave trapping (Kim and Mahrt, 1992; Kim and Arakawa, 1995; Gregory et al., 1998).

d *Wave Dissipation and Gravity Wave Drag*

1 MOMENTUM FLUX / E-P FLUX DIVERGENCE

Steady 2D gravity waves conserve their vertical flux of horizontal wave momentum flux density in the absence of dissipation. For gravity waves propagating east-west, this is given by $\rho\overline{u'w'}$ where u' and w' are, respectively, the zonal and vertical velocity perturbations of the wave. Eliassen and Palm (1961) first derived this for orographic gravity waves, a result that has since been expanded into a generalized Eliassen-Palm (E-P) theorem for atmospheric waves of various types (e.g., Andrews et al., 1987). In general an E-P-flux vector governs wave activity, with $\rho\overline{u'w'}$ being associated with its vertical component, the most relevant component for gravity waves. Drag on the mean flow caused by wave dissipation is referred to as GWD and is given by the divergence of the wave's E-P flux. For irrotational gravity waves, this is given by $\frac{1}{\rho}\frac{\partial}{\partial z}\left(\rho\overline{u'w'}\right)$, which is zero prior to saturation since $\rho\overline{u'w'}$ is constant. Parametrizations compute GWD by evaluating the vertical gradients of momentum flux that are produced by saturated waves: "saturation" is discussed further in the following sub-subsection.

Thus gravity wave momentum flux must be specified accurately at its source. For mountain waves, this is achieved (as discussed in Section a of this Appendix) by calculating the surface pressure drag across the subgrid-scale mountains and apportioning it to a total vertical flux of horizontal momentum of radiated waves. The momentum flux generally takes the form $\kappa\rho_0 N_0 |\overline{U}_0| h'^2$, where the subscript "0" denotes the surface or near-surface level, κ is a dimensionless coefficient that varies with definitions, topographic shape and so on (e.g., Baines, 1995) and h' is an elevation proportional to the standard deviation of subgrid-scale orographic height. A variety of similar-looking expressions, which vary in details (e.g., the treatment of low-level blocking and wave-breaking) have been derived in parametrizations for various large-scale models: Kim and Arakawa (1995) show a table summarizing most of the earlier schemes.

2 SATURATION

While various atmospheric processes can damp waves, parametrizations focus mostly on dissipation due to wave-induced instabilities that develop when wave amplitudes become sufficiently large. This is a complex non-linear process that is not fully understood (see, the review by Fritts and Werne, 2000), but is characterized macroscopically by limiting "saturation" amplitudes for the waves, beyond which instabilities develop and gravity-wave dissipation and drag occur (Fritts, 1984, 1989; Fritts and Alexander, 2003).

GWD parametrizations utilize these ideas: many schemes classify waves into a "saturated" regime, where dissipation processes limit the wave amplitudes and produce drag, and an "unsaturated" regime within which waves do not dissipate. The wide variety of parametrizations that have emerged also reflect many of the current uncertainties in gravity wave saturation theories, which continue to be debated. In single-wave parametrizations, saturation is usually associated with "wave breaking" (e.g., Lindzen, 1981; Palmer et al., 1986; McFarlane, 1987), a process somewhat analogous to surface ocean waves breaking on a shore. Rather than breaking down totally, however, it is assumed that waves "saturate" by dissipating only enough wave energy into turbulent layers to return the wave to marginal stability (Fritts, 1984, 1989; Dunkerton, 1989; Palmer et al., 1986; McFarlane, 1987).

For spectral parametrizations, saturation is also a key concept. However, its connotation varies due to a wide variety of proposed physical mechanisms underlying dissipation of and interactions among a spectrum of waves (see Section 4c). These differences lead to quite different algorithms for parametrizing GWD. For example, in some schemes the onset of wave-induced instabilities marks total dissipation and removal of certain waves (e.g., Hines, 1997a; Alexander and Dunkerton, 1999). In others, waves dissipate their amplitudes much more gradually with altitude (Weinstock, 1990; Medvedev and Klaassen, 2000; Warner and McIntyre, 2001).

3 RELATIONSHIP TO INTRINSIC PHASE SPEED

Quantitatively, the wave's intrinsic phase speed $\hat{c}$ (given in 2D by $\hat{c} = c - \overline{U}(z)$; see Section c of this Appendix) is an important quantity in specifying saturation amplitudes and GWD in parametrizations. "Convective" saturation sets in when waves attain an amplitude that causes potential temperature surfaces to "overturn": $\partial/\partial z(\overline{\theta} + \theta') < 0$, where $\overline{\theta}$ is the mean potential temperature and θ' is the gravity-wave potential temperature perturbation. For a 2D hydrostatic irrotational gravity wave, this occurs when the peak horizontal velocity amplitude of the wave, u'_{PEAK}, exceeds $|\hat{c}|$, and so the saturation amplitude equals the intrinsic phase speed: $(u'_{PEAK})_{SAT} = |\hat{c}|$ (Fritts, 1984). In more complex saturation schemes, wave saturation amplitudes are often directly proportional to $|\hat{c}|$ also (e.g., Medvedev and Klaassen, 2000). Thus, saturation becomes more likely in regions where $|\hat{c}|$ is small, since waves saturate at smaller wave amplitudes and so become unstable more easily. The strength of the ensuing GWD is also sensitively dependent on $\hat{c}$: for example, in some schemes the GWD is proportional to $|\hat{c}|^3$ (Lindzen, 1981; Medvedev and Klaassen, 1995; McLandress, 1998; Alexander and Dunkerton, 1999). For single-wave saturation, this arises because $(u'_{PEAK})_{SAT} = |\hat{c}|$ implies $(w'_{PEAK})_{SAT} = \pm k\,|\hat{c}|^2/N$ from basic polarization relations for gravity waves (see, Eq. (36) of Fritts and Alexander, 2003), and thus $(\overline{u'w'})_{SAT} \propto |\hat{c}^3|$ (Lindzen, 1981).

The sign of $\hat{c}$ is also important. In essence, wave saturation tends to "drag" the wind towards the ground-based phase speed c of the dissipating wave (Lindzen, 1981), so that if $\hat{c} < 0$ [$c < \overline{U}(z)$] the GWD is negative (westward) whereas if $\hat{c} > 0$ [$c > \overline{U}(z)$] the GWD is directed eastward. This explains the origin of the term "gravity wave drag": the first GWD parametrizations were for stationary orographic waves ($c = 0$), dissipation of which always drags the flow towards this zero phase speed and thus always decelerates winds.

Throughout this paper we use the familiar term "gravity wave drag", with the understanding that this "drag" has a broader definition that allows both acceleration and deceleration (including reversal) of atmospheric winds due to dissipation of both stationary and non-stationary gravity waves.

4 RELATIONSHIP TO CRITICAL LEVELS

Since $|\hat{c}| \rightarrow 0$ on approaching a critical level, the previous arguments show that saturation becomes essentially inevitable near 2D critical levels, since $(u'_{PEAK})_{SAT} \rightarrow |\hat{c}| \rightarrow 0$ as well. This 2D saturation condition $(u'_{PEAK})_{SAT} = |\hat{c}|$ can be re-expressed as $c - [\overline{U}(z) + u'(x,z,t)] = 0$, where $u'(x,z,t)$ is the horizontal velocity oscillation of the gravity wave. By analogy (from Section c of this Appendix) with the regular critical-level criterion $c - \overline{U}(z) = 0$, we see that convective saturation can be viewed as the onset of a "wave-induced critical level" caused by the large velocity amplitudes $u'(x,z,t)$ of the wave itself. This concept is revisited in the parametrization of low-level orographic GWD (Section 3a). Since $c = 0$ for orographic waves, the condition is that the total flow velocity $\overline{U}(z) + u'(x,z,t)$ vanishes. Because of this, overturning regions for low-level mountain waves in downstream regions (see Fig. 4) are often associated with so-called "stagnation points" in low-level orographic flow in upstream regions (Smith, 2001).

For multi-wave fields, this condition can be generalized still further to $c - [\overline{U}(z) + U'(x,z,t) + u'(x,z,t)] = 0$ where $U'(x,z,t)$ denotes the horizontal velocity oscillations of all the other gravity waves in the spectrum. This formulation is key to the spectral GWD parametrization of Hines (1997a, 1997b), in which gravity waves are saturated and eventually removed ("obliterated") by the "Doppler-spreading" effects of $U'(x,z,t)$ fields due to these other waves in the spectrum acting on wave intrinsic frequencies and vertical wavenumbers (see Section 4).

Appendix B: Abbreviations and symbols

TABLE 1. Acronyms/abbreviations

Abbreviation	Term
2D	two dimensions/two-dimensional
3D	three dimensions/three-dimensional
CCM	Community Climate Model
E-P	Eliassen-Palm
GCI	global cloud imagery
GCM	general circulation model
GFDL	Geophysical Fluid Dynamics Laboratory
GWD	gravity wave drag
MF radar	medium frequency radar
NWP	numerical weather prediction
QBO	quasi-biennial oscillation
SAO	semiannual oscillation

TABLE 2. Mathematical symbols

Symbol	Meaning
c	ground-based zonal/horizontal phase speed
$\hat{c}$	intrinsic zonal/horizontal phase speed
f	Coriolis parameter
Fr_d	(inverse) Froude number
h	subgrid-scale orographic height
h_d	vertical displacement height
κ	tuning coefficient
k	zonal/horizontal wavenumber
ℓ^2	Scorer parameter
λ_x	zonal/horizontal wavelength
λ_z	vertical wavelength
m	vertical wavenumber
N	Brunt-Väisälä frequency
n	total spherical harmonical wavenumber
p	atmospheric pressure
$P_X(k)$	zonal/horizontal wavenumber spectrum of quantity X
ρ	atmospheric density
Ri	Richardson number
Ri_m	minimum (wave-modified) Richardson number
τ	vertical flux of zonal/horizontal momentum
t	time
t_{PROP}	gravity wave propagation time
Δt	model time step
U	zonal/horizontal wind magnitude
$\overline{U}$	background zonal/horizontal wind profile
U'	zonal/horizontal velocity perturbation of a field of waves
u'	zonal/horizontal velocity perturbation of a wave
u'_{PEAK}	peak zonal/horizontal velocity amplitude of a wave
$(u'_{PEAK})_{SAT}$	saturated peak zonal/horizontal velocity amplitude of a wave
$\hat{\omega}$	intrinsic wave frequency
ω'	vertical pressure velocity perturbation
w'	vertical velocity perturbation
$\tilde{w}$	Fourier-transformed vertical velocity
x	zonal/horizontal displacement
Δx	zonal/horizontal model grid size
z	altitude
z_C	critical level
Δz	vertical model grid size

References

AKMAEV, R. 2001. Simulation of large-scale dynamics in the mesosphere and lower thermosphere with the Doppler-spread parameterization of gravity waves. I, Implementation and zonal mean climatologies. *J. Geophys. Res.* **106**: 1193–1204.

ALEXANDER, M.J. 1996. A simulated spectrum of convectively generated gravity waves: Propagation from the tropopause to the mesopause and effects on the middle atmosphere. *J. Geophys. Res.* **101**: 1571–1588.

———; J.R. HOLTON and D. DURRAN. 1995. The gravity wave response above deep convection in a squall line simulation. *J. Atmos. Sci.* **52**: 2212–2226.

——— and K.H. ROSENLOF. 1996. Nonstationary gravity wave forcing of the stratospheric zonal mean wind. *J. Geophys. Res.* **101**: 23465–23474.

——— and T.J. DUNKERTON. 1999. A spectral parameterization of mean-flow forcing due to breaking gravity waves. *J. Atmos. Sci.* **56**: 4167–4182.

———; J.H. BERES and L. PFISTER. 2000. Tropical stratospheric gravity wave activity and relationships to clouds. *J. Geophys. Res*. **105**: 22299–22309.

———; T. TSUDA and R.A. VINCENT. 2002. Latitudinal variations observed in gravity waves with short vertical wavelengths. *J. Atmos. Sci*. **59**: 1394-1404.

ALPERT, J.; S.-Y. HONG and Y.-J. KIM. 1996. Sensitivity of cyclogenesis to lower tropospheric enhancement of gravity wave drag using the environmental modeling center medium range model. *In*: Preprints. 11th Conference on NWP. 19-23 August 1996, Norfolk, Virginia. Am. Meteorol. Soc. pp. 322–323.

AMBAUM, M.H.P. and B.J. HOSKINS. 2002. The NAO troposphere–stratosphere connection. *J. Clim*. **15**: 1969–1978.

AMODEI, M.; S. PAWSON, A.A. SCAIFE, U. LANGEMATZ, W. LAHOZ, D.M. LI and P. SIMON. 2001. The SAO and Kelvin waves in the EuroGRIPS GCMs and the UK Met. Office analyses. *Ann. Geophysicae*, **19**: 99–114.

ANDREWS, D.G. 1987. The influence of atmospheric waves on the general circulation of the middle atmosphere. *Phil. Trans. R. Soc. Lond. Ser. A* **323**: 693–705.

———; J.R. HOLTON and C.B. LEOVY. *Middle atmosphere dynamics*. Academic Press, San Diego, Calif., 489 pp.

BACMEISTER, J.T. 1993. Mountain-wave drag in the stratosphere and mesosphere inferred from observed winds and a simple mountain-wave parameterization scheme. *J. Atmos. Sci*. **50**: 377–399.

——— and R.T. PIERREHUMBERT. 1988. On high-drag states of nonlinear flow across an obstacle. *J. Atmos. Sci*. **45**: 63–80.

———; S.D. ECKERMANN, P.A. NEWMAN, L. LAIT, K.R. CHAN, M. LOEWENSTEIN, M.H. PROFFITT and B.L. GARY. 1996. Stratospheric horizontal wavenumber spectra of winds, potential temperature, and atmospheric tracers observed by high-altitude aircraft. *J. Geophys. Res*. **101**: 9441-9470.

———; ———, A. TSIAS, K.S. CARSLAW and T. PETER. 1999. Mesoscale temperature fluctuations induced by a spectrum of gravity waves: A comparison of parameterizations and their impact on stratospheric microphysics. *J. Atmos. Sci*. **56**: 1913–1924.

BAIK, J.-J.; H.-S. HWANG and H.-Y. CHUN. 1999a. Transient critical level effect for internal gravity waves in a stably stratified flow with thermal forcing. *Phys. Fluids*, **11**: 238–240.

———; ——— and ———. 1999b. Transient, linear dynamics of a stably stratified shear flow with thermal forcing and a critical level. *J. Atmos. Sci*. **56**: 483–499.

BAINES, P.G. 1995. *Topographic effects in stratified flows*. Cambridge Univ. Press, 482 pp.

BALAJI, V. and J.L. REDELSPERGER. 1996. Sub-grid scale effects in mesoscale deep convection: initiation, organization and turbulence. *Atmos. Res*. **40**: 339–381.

BALDWIN, M.P. and T.J. DUNKERTON. 2001. Stratospheric harbingers of anomalous weather regimes. *Science*, **294**: 581–584.

BAUER, M.H.; G.J. MAYR, I. VERGEINER and H. PICHLER. 2000. Strongly nonlinear flow over and around a three-dimensional mountain as a function of the horizontal aspect ratio. *J. Atmos. Sci.* **57**: 3971–3991.

BEAU, I. and P. BOUGEAULT. 1998. Assessment of a gravity wave drag parameterization with PYREX data. *Q. J. R. Meteorol. Soc*. **124**: 1443–1464.

BELCHER, S.E. and J.C.R. HUNT. 1998. Turbulent flow over hills and waves. *Ann. Rev. Fluid Mech*. **30**: 507–538.

BELL, M.J.; R. HIDE and G. SAKELLARIDES. 1991. Atmospheric angular momentum forecasts as novel tests of global numerical weather prediction models. *Phil. Trans. R. Soc. Lond., Ser. A*, **334**: 55–92.

BERGMAN, J.W. and M.L. SALBY. 1994. Equatorial wave activity derived from fluctuations in observed convection. *J. Atmos. Sci.* **51**: 3791–3806.

BOER, G.J.; N.A. MCFARLANE, R. LAPRISE, J.D. HENDERSON and J.-P. BLANCHET. 1984. The Canadian Climate Centre spectral atmospheric general circulation model. ATMOSPHERE-OCEAN, **22**: 397–429.

———. and M. LAZARE. 1988. Some results concerning the effect of horizontal resolution and gravity-wave drag on simulated climate. *J. Clim*. **1**: 789–806.

———; K. ARPE, M. BLACKBURN, M. DÉQUÉ, W.L. GATES, T.L. HART, H. LETREUT, E. ROECKNER, D.A. SHEININ, I. SIMMONDS, R.N.B. SMITH, T. TOKIOKA, R.T. WETHERALD and D. WILLIAMSON. 1992. Some results from an intercomparison of the climates simulated by 14 atmospheric general circulation models. *J. Geophys. Res*. **97**: 12771–12786.

BOSSEUT, C.; M. DÉQUÉ and D. CARIOLLE. 1998. Impact of a simple parameterization of convective gravity-wave drag in a stratosphere-troposphere general circulation model and its sensitivity to vertical resolution. *Ann. Geophysicae*, **16**: 238–239.

BOUGEAULT, P.; A. JANSA, J.J. ATTIE, I. BEAU, B. BENECH, R. BENOIT, P. BESSEMOULIN, J.I. CACCIA, J. CAMPINS, B. CARISSIMO, J.I. CHAMPEAUX, M. CROCHET, A. DRUILHET, P. DURAND, A. ELKHALFI, P. FLAMANT, A. GENOVES, M. GEORGELIN, K.P. HOINKA, V. KLAUS, E. KOFFI, V. KOTRONI, C. MAZAUDIER, J. PELON, M. PETITDIDIER, Y. POINTIN, D. PUECH, E. RICHARD, T. SATOMURA, J. STEIN and D. TANNHAUSER. 1993. The atmospheric momentum budget over a major mountain range: first results of the PYREX field campaign. *Ann. Geophysicae*, **11**: 395–418.

———; P. BINDER, A BUZZI, R. DIRKS, R. HOUZE, J. KUETTNER, R.B. SMITH, R. STEINACKER and H. VOLKERT. 2001. The MAP special observing period. *Bull. Am. Meteorol. Soc*. **82**: 433–462.

BOVILLE, B. 1986. Wave-mean flow interactions in a general circulation model of the troposphere and stratosphere. *J. Atmos. Sci.* **43**: 1711–1725.

———. 1991. Sensitivity of simulated climate to model resolution. *J. Clim*. **4**: 469–485.

———. 1995. Middle atmosphere version of CCM2 (MACCM2) - annual cycle and interannual variability. *J. Geophys. Res*. **100**: 9017–9039.

——— and W.J. RANDEL. 1992. Equatorial waves in a stratospheric GCM: effects of vertical resolution. *J. Atmos. Sci.* **49**: 785–801.

BRADY, R.H. and J.S. WALDSTREICHER. 2001. Observations of mountain wave-induced precipitation shadows over northeast Pennsylvania. *Weather Forecast.* **16**: 281–300.

BRETHERTON, C.S. 1988. Group velocity and the linear response of stratified fluids to internal heat or mass sources. *J. Atmos. Sci.* **45**: 81–93.

BROAD, A.S. 1995. Linear theory of momentum fluxes in 3-D flows with turning of the mean wind with height. *Q. J. R. Meteorol. Soc*. **121**: 1891–1902.

———. 1996. High-resolution numerical-model integrations to validate gravity-wave-drag parameterization schemes: A case study. *Q. J. R. Meteorol. Soc.* **122**: 1625–1653.

———. 1999. Do orographic gravity waves break in flows with uniform wind direction turning with height? *Q. J. R. Meteorol. Soc*. **125**: 1695–1714.

——— 2000. Gravity wave momentum fluxes and surface pressure drags due to the Pyrénées: variation with numerical model horizontal resolution. *Meteorol. Atmos. Phys*. **72**: 1–11.

BROCCOLI, A.J. and S. MANABE. 1992. The effects of orography on midlatitude northern hemisphere dry climates. *J. Clim*. **5**: 1181–1201.

BROUTMAN, D.; J,W, ROTTMAN and S.D. ECKERMANN. 2001. A hybrid method for analyzing wave propagation from a localized source, with application to mountain waves. *Q. J. R. Meteorol. Soc*. **127**: 129–146.

BÜHLER, O. and M.E. MCINTYRE. 1999. On shear-generated gravity waves that reach the mesosphere, II, wave propagation. *J. Atmos. Sci*. **56**: 3764–3773.

———; ——— and J.F. SCINOCCA. 1999. On shear-generated gravity waves that reach the mesosphere, I, wave generation. *J. Atmos. Sci*. **56**: 3749–3763.

CHANG, J.L.; S.K. AVERY, A.C. RIDDLE, S.E. PALO and K.S. GAGE. 1997. First results of tropospheric gravity wave momentum flux measurements over Christmas Island. *Radio Sci*. **32**: 727–748.

CHARRON, M.; E. MANZINI and C.D. WARNER. 2002. Intercomparison of gravity wave parameterizations: Hines Doppler-spread and Warner and McIntyre ultra-simple schemes, *J. Meteorol. Soc. Jpn.* **80**: 335–345.

CHUN, H.-Y. 1995. Enhanced response of a stably stratified two-layer atmosphere to low-level heating. *J. Meteorol. Soc. Jpn.* **73**: 685–696.

———; J.-H. JUNG, J.-W. KIM and J.-H. OH. 1996. Effects of mountain-induced gravity wave drag on atmospheric general circulation. *J. Korean Meteorol. Soc*. **32**: 581–592.

——— and J.-J. BAIK. 1998. Momentum flux by thermally induced internal gravity waves and its approximation for large-scale models. *J. Atmos. Sci*. **55**: 3299–3310.

———; M.-D. SONG, J.-W. KIM and J.-J. BAIK. 2001. Effects of gravity wave drag induced by cumulus convection on the atmospheric general circulation. *J. Atmos. Sci*. **58**: 302–319.

——— and J.-J. BAIK. 2002. An updated parameterization of convectively forced gravity wave drag for use in large-scale models. *J. Atmos. Sci*. **59**: 1006–1017.

CIESIELSKI, P.E.; D.E. STEVENS, R.H. JOHNSON and K.R. DEAN. 1989. Observational evidence for asymmetric inertial instability. *J. Atmos. Sci*. **46**: 817–831.

CLARK, T.L. and R.D. FARLEY. 1984. Severe downslope windstorm calculations in two and three spatial dimensions using anelastic interactive grid nesting: a possible mechanism for gustiness. *J. Atmos. Sci*. **41**: 329–350.

———; T. HAUF and J.P. KUETTNER. 1986. Convectively forced internal gravity waves: Results from two-dimensional numerical experiments. *Q. J. R. Meteorol. Soc.* **112**: 899–925.

COT, C. and J. BARAT. 1986. Wave-turbulence interaction in the stratosphere: a case study. *J. Geophys. Res*. **91**: 2749–2756.

CULLEN, M.J.P.; DAVIES, M.H. MAWSON, J.A. JAMES and S.C. COULTER. 1997. An overview of numerical methods for the next generation UK NWP and climate model. In: *Numerical Methods in Atmospheric Modelling. The André Robert memorial volume*. C. Lin, R. Laprise and H. Ritchie, (Eds), Canadian Meteorological and Oceanographic Society, Ottawa, Canada. pp. 425–444.

CUSACK, S.; J.M. EDWARDS and R. KERSHAW. 1999. Estimating the subgrid variance of saturation, and its parameterization for use in a GCM cloud scheme. *Q. J. R. Meteorol. Soc.* **125**: 3057–3076.

DALEY, R. 1988. The normal modes of the spherical non-hydrostatic equations with applications to the filtering of acoustic modes. *Tellus*, **40A**: 96–106.

DAVIES, L.A. and A.R. BROWN. 2001. Assessment of which scales of orography can be credibly resolved in a numerical model. *Q. J. R. Meteorol. Soc*. **127**: 1225–1237.

DEWAN, E.M.; R.H. PICARD, R.R. O'NEIL, H.A. GARDINER, J. GIBSON, J.D. MILL, E. RICHARDS, M. KENDRA and W.O. GALLERY. 1998. MSX satellite observations of thunderstorm-generated gravity waves in mid-wave infrared images of the upper stratosphere. *Geophys. Res. Lett.* **25**: 939–942.

DICKINSON, R.E. 1973. Method of parameterization for infrared cooling between the altitudes of 30 and 70 kilometers. *J. Geophys. Res*. **78**: 4451–4457.

DOYLE, J.D. and M.A. SHAPIRO. 2000. A multi-scale simulation of an extreme downslope wind-storm over Norway. *Meteorol. Atmos. Phys*. **74**: 83–101.

———; D.R. DURRAN, C. CHEN, B.A. COLLE, M. GEORGELIN, V. GRUBISIC, W.R. HSU, C.Y. HUANG, D. LANDAU, Y. L. LIN, G.S. POULOS, W.Y. SUN, D.B. WEBER, M.G. WURTELE and M. XUE. 2000. An intercomparison of model-predicted wave breaking for the 11 January 1972 Boulder Windstorm. *Mon. Weather Rev*. **128**: 901–914.

——— and ———. 2002. The dynamics of mountain wave-induced rotors. *J. Atmos. Sci*. **59**: 186–201.

——— and R.B. SMITH. 2003. Mountain waves over the Hohe Tauern: Influence of upstream diabatic effects. *Q. J. R. Meteorol. Soc.* **129**: 799.

DÖRNBRACK, A.; M. LEUTBECHER, J. REICHARDT, A. BEHRENDT, K.-P. MÜLLER and G. BAUMGARTEN. 2001. Relevance of mountain waves for the formation of polar stratospheric clouds over Scandinavia: Mesoscale dynamics and observations for January 1997. *J. Geophys. Res*. **106**: 1569–1581.

DUNKERTON, T.J. 1989. Theory of internal gravity wave saturation. *Pure Appl. Geophys*. **130**: 373–397.

———. 1997. The role of gravity waves in the quasi-biennial oscillation. *J. Geophys. Res.* **102**: 26,053–26,076.

DURRAN, D.R. 1990. Mountain waves and downslope winds. *In*: Atmospheric Processes over Complex Terrain. W. Blumen, (Ed), *Meteorol. Monogr. Am. Meteorol. Soc*. **23 (45)**: 59–81.

——— and J.B. KLEMP. 1982a. On the effects of moisture on the Brunt-Väisälä frequency. *J. Atmos. Sci.* **39**: 2152–2158.

——— and ———. 1982b. The effects of moisture on trapped mountain lee waves. *J. Atmos. Sci.* **39**: 2490–2506.

——— and ———. 1987. Another look at downslope winds. Part II: Nonlinear amplification beneath wave-overturning layers. *J. Atmos. Sci.* **44**: 3402–3412.

ECKERMANN, S.D. 1995. Effect of background winds on vertical wavenumber spectra of atmospheric gravity waves. *J. Geophys. Res*. **100**: 14097–14112.

——— and C.J. MARKS. 1996. An idealized ray model of gravity wave-tidal interactions. *J. Geophys. Res*. **101**: 21195–21212.

——— and P. PREUSSE. 1999. Global measurements of stratospheric mountain waves from space. *Science*, **286**: 1534–1537.

ELIASSEN, A. and E. PALM. 1961. On the transfer of energy in stationary mountain waves. *Geofys. Publ*. **22(3)**: 1–23.

EPIFANIO, C.C. and D.R. DURRAN. 2001. Three-dimensional effects in high-drag-state flows over long ridges. *J. Atmos. Sci*. **58**: 1051–1065.

ERICKSON, C.O. and L.F. WHITNEY. 1973. Gravity-waves following severe thunderstorms. *Mon. Weather Rev*. **101**: 708–711.

FELS, S.B. 1987. Response of the middle atmosphere to changing O_3 and CO_2 – A speculative tutorial. In: *Transport processes in the middle atmosphere*. G. Visconti and R. R. Garcia (Eds), R. Reidel Publishing. pp. 371–386.

FOMICHEV, V.I.; W.E. WARD, S.R. BEAGLEY, C. MCLANDRESS, J.C. MCCONNELL, N.A. MCFARLANE and T.G. SHEPHERD. 2002. Extended Canadian middle atmosphere model: zonal-mean climatology and physical parameterizations. *J. Geophys. Res*. **107**: 10.1029/2001JD000479.

FORD, R. 1994. Gravity-wave radiation from vortex trains in rotating shallow-water. *J. Fluid Mech*. **281**: 81–118.

———; M.E. MCINTYRE and W.A. NORTON. 2000. Balance and the slow quasi-manifold: some explicit results. *J. Atmos. Sci*. **57**: 1236–1254.

FOVELL, R.; D. DURRAN and J.R. HOLTON. 1992. Numerical simulations of convectively generated stratospheric gravity waves. *J. Atmos. Sci*. **49**: 1427–1442.

FRITTS, D.C. 1984. Gravity wave saturation in the middle atmosphere: A review of theory and observations. *Rev. Geophys*. **22**: 275–308.

———. 1989. A review of gravity wave saturation processes, effects, and variability in the middle atmosphere. *Pure Appl. Geophys*. **130**: 343–372.

——— and T.J. DUNKERTON. 1985. Fluxes of heat and constituents due to convectively unstable gravity-waves. *J. Atmos. Sci.* **42**: 549–556.

——— and W. LU. 1993a. Spectral estimates of gravity wave energy and momentum fluxes. Part II. Parameterization of wave forcing and variability. *J. Atmos. Sci.* **50**: 3695–3713.

——— and ———. 1993b. Spectral estimates of gravity wave energy and momentum fluxes. Part III. Gravity wave-tidal interactions. *J. Atmos. Sci.* **50**: 3714–3727.

——— and T.E. VANZANDT. 1993. Spectral estimates of gravity wave energy and momentum fluxes. Part I. Energy dissipation, acceleration, and constraints. *J. Atmos. Sci.* **50**: 3685–3694.

——— and J.A. WERNE. 2000. Turbulence dynamics and mixing due to gravity waves in the lower and middle atmosphere. *In*: Atmospheric Science Across the Stratopause. D. E. Siskind, S. D. Eckermann and M. E. Summers, (Eds), AGU Geophysical Monograph Series, Vol. 123, pp. 143–159.

——— and M.J. ALEXANDER. 2003. Gravity wave dynamics and effects in the middle atmosphere. *Rev. Geophys*. in press.

GARCIA, R.R. 2000. The role of equatorial waves in the semiannual oscillation of the middle atmosphere. *In*: Atmospheric Science Across the Stratopause. D. E. Siskind, S. D. Eckermann and M. E. Summers (Eds), AGU Geophysical Monograph Series. Vol. 123, pp. 161–176.

GARDNER, C.S. 1996. Testing theories of atmospheric gravity wave saturation and dissipation. *J. Atmos. Terr. Phys*. **58**: 1575–1589.

GATES, W.L. 1992. AMIP: The atmospheric model intercomparison project. *Bull. Am. Meteorol. Soc*. **73**: 1962–1970.

GEORGELIN, M. and F. LOTT. 2001. On the transfer of momentum by trapped lee waves: case of the IOP3 of PYREX. *J. Atmos. Sci*. **58**: 3563–3580.

GILL, A.E. 1982. *Atmosphere-ocean dynamics*. Academic Press, New York, 488 pp.

GOSSARD, E.E. and W.H. HOOKE. 1975. *Waves in the atmosphere*. Elsevier, New York, 456 pp.

GREGORY, D.; G.J. SHUTTS and J.R. MITCHELL. 1998. A new gravity-wave-drag scheme incorporating anisotropic orography and low-level wave breaking: impact upon the climate of the UK Meteorological Office Unified Model. *Q. J. R. Meteorol. Soc*. **124**: 463–493.

GUEST, F.M.; M.J. REEDER, C.J. MARKS and D.J. KAROLY. 2000. Inertia-gravity waves observed in the lower stratosphere over Macquarie Island. *J. Atmos. Sci*. **57**: 737–752.

HACK, J.J. 1994. Parameterization of moist convection in the National Center for Atmospheric Research Community Climate Model (CCM2). *J. Geophys. Res*. **99**: 5551–5568.

HAMILTON, K. 1996. Comprehensive meteorological modeling of the middle atmosphere: A tutorial review. *J. Atmos. Terr. Phys*. **58**: 1591–1627.

———. 1997a. Preface. *In*: Proc. NATO Advanced Research Workshop "Gravity wave processes and their parameterization in global climate models". NATO ASI Series. Vol. I-50. K. Hamilton (Ed.), Springer-Verlag. 404 pp.

———. 1997b. The role of parameterized drag in a troposphere-stratosphere-mesosphere general circulation model. *In*: Proc. NATO Advanced Research Workshop "Gravity wave processes and their parameterization in global climate models". NATO ASI Series. Vol. I-50. K. Hamilton (Ed.), Springer-Verlag. pp 337–350.

———. 1998. Dynamics of the tropical middle atmosphere: A tutorial review. ATMOSPHERE-OCEAN, **36**: 319–354.

———. 1999. Dynamical coupling of the lower and middle atmosphere: historical background to current research. *J. Atmos. Sol.-Terr. Phys*. **61**: 73–84.

———; R.J. WILSON, J.D. MAHLAMN and L.J. UMSCHEID. 1995. Climatology of the SKYHI troposphere-stratosphere-mesosphere general-circulation model. *J. Atmos. Sci*. **52**: 5–43.

———; ——— and R.S. HEMLER. 1999. Middle atmosphere simulated with high vertical and horizontal resolution versions of a GCM: Improvements in the cold pole bias and generation of a QBO-like oscillation in the tropics. *J. Atmos. Sci*. **56**: 3829–3846.

———; ——— and ———. 2001. Spontaneous stratospheric QBO-like oscillations simulated by the GFDL SKYHI general circulation model. *J. Atmos. Sci*. **58**: 3271–3292.

HAUF, T. and T.L. CLARK. 1989. Three-dimensional numerical experiments on convectively forced internal gravity waves. *Q. J. R. Meteorol. Soc*. **115**: 309–333.

HAYASHI, Y.; D.G. GOLDER, J.D. MAHLMAN and S. MIYAHARA. 1989. The effect of horizontal resolution on gravity-waves simulated by the GFDL SKYHI general-circulation model. *Pure Appl. Geophys*. **130**: 421–443.

HAYNES, P.H.; C.J. MARKS, M.E. MCINTYRE, T.G. SHEPHERD and K.P. SHINE. 1991. On the "downward control" of extratropical diabatic circulations by eddy-induced mean zonal forces. *J. Atmos. Sci*. **48**: 651–678.

HELFAND, H.M.; J.C. JUSEM, J. PFAENDTNER, J. TENENBAUM and E. KALNAY. 1987. The effects of a gravity-wave drag parameterization scheme on GLA fourth order GCM forecast. *J. Meteorol. Soc. Jpn.* Special volume for the WMO/IUGG NWP symposium, Tokyo, Japan, pp. 729–742.

HEREIL, P. and J. STEIN. 1999. Momentum budgets over idealized orography with a non-hydrostatic anelastic model, II, three-dimensional flows. *Q. J. R. Meteorol. Soc*. **125**: 2053–2073.

HINES, C.O. 1991. The saturation of gravity-waves in the middle atmosphere, 3, formation of the turbopause and of turbulent layers beneath it. *J. Atmos. Sci*. **48**: 1380–1385.

———. 1992. Mesospheric VHF echoing layers: an interpretation in terms of wave scavenging. *J. Atmos. Terr. Phys*. **54**: 1043–1049.

———. 1997a. Doppler-spread parameterization of gravity wave momentum deposition in the middle atmosphere. 1, Basic formulation. *J. Atmos. Sol.-Terr. Phys*. **59**: 371–386.

———. 1997b. Doppler-spread parameterization of gravity wave momentum deposition in the middle atmosphere. 2, Broad and quasi-monochromatic spectra and implementation. *J. Atmos. Sol.-Terr. Phys*. **59**: 387–400.

HITCHMAN, M.H. and C.B. LEOVY. 1988. Estimation of the Kelvin wave contribution to the semiannual oscillation. *J. Atmos. Sci*. **45**: 1462–1475.

HOGAN, T.F.; T.E. ROSMOND and R.L. PAULEY. 1999. The Navy Operational Global Atmospheric Prediction System: Recent changes and testing of gravity wave and cumulus parameterizations. *In*: Preprints. 13th Conference on NWP. 13–17 Sept. 1999, Denver, Colorado, Am. Meteorol. Soc. pp. 60–65.

HOLTON, J.R. 1982. The role of gravity wave-induced drag and diffusion in the momentum budget of the mesosphere. *J. Atmos. Sci*. **39**: 791–799.

———. 1983. The influence of gravity wave breaking on the general circulation of the middle atmosphere. *J. Atmos. Sci*. **40**: 2497–2507.

———. 1992. *An introduction to dynamic meteorology*. Third Ed., Academic Press, 511 pp.

——— and R.S. LINDZEN. 1972. An updated theory for the quasi-biennial oscillation of the tropical stratosphere. *J. Atmos. Sci*. **29**: 1076–1080.

——— and W.M. WEHRBEIN. 1980. A numerical model of the zonal mean circulation of the middle atmosphere. *Pure Appl. Geophys*. **118**: 284–306.

——— and M.J. ALEXANDER. 1999. Gravity waves in the mesosphere generated by tropospheric convection. *Tellus*, **51A-B**: 45–58.

——— and ———. 2000. The role of waves in the transport circulation of the middle atmosphere. *In*: Atmospheric Science Across the Stratopause. D. E. Siskind, S. D. Eckermann and M. E. Summers (Eds), AGU Geophysical Monograph Series. **123**: 21–35.

———; J.H. BERES and X.L. ZHOU. 2002. On the vertical scale of gravity waves excited by localized thermal forcing. *J. Atmos. Sci*. **58**: 2019-2023.

HOOKE, W.H. 1986. Gravity Waves. *In*: Mesoscale meteorology and forecasting. P. S. Ray, (Ed.), Am. Meteorol. Soc. pp. 272–288.

——— and K.R. HARDY. 1975. Further study of atmospheric gravity-waves over eastern seaboard on 18 March 1969. *J. Appl. Meteorol*. **14**: 31–38.

HORINOUCHI, T. and S. YODEN. 1998. Wave-mean flow interaction associated with a QBO-like oscillation simulated in a simplified GCM. *J. Atmos. Sci.* **55**: 502–526.

HOUGHTON, J.T. 1978. The stratosphere and mesosphere. *Q. J. R. Meteorol. Soc*. **104**: 1–29.

IWASAKI, T. and A. SUMI. 1986. Impact of envelope orography on JMA's hemispheric NWP forecasts for winter circulation. *J. Meteorol. Soc. Jpn.* **64**: 245–258.

———; S. YAMADA and K. TADA. 1989. A parameterization scheme of orographic gravity-wave drag with two different vertical partitionings. Part I: Impacts on medium-range forecasts. *J. Meteorol. Soc. Jpn.* **67**: 11–27.

JACKSON, D.R. 1993. Sensitivity of the extended UGAMP general-circulation model to the specification of gravity-wave phase speeds. *Q. J. R. Meteorol. Soc.* **119**: 457–468.

——— and L.J. GRAY. 1994. Simulation of the semiannual oscillation of the equatorial middle atmosphere using the extended UGAMP general-circulation model. *Q. J. R. Meteorol. Soc.* **120**: 1559–1588.

———; J. AUSTIN and N. BUTCHART. 2001. An updated climatology of the troposphere–stratosphere configuration of the Met Office's unified model. *J. Atmos. Sci.* **58**: 2000–2008.

JENSEN, E.J. and O.B. TOON. 1994. Ice nucleation in the upper troposphere - sensitivity to aerosol number density, temperature, and cooling rate. *Geophys. Res. Lett*. **21**: 2019–2022.

JONES, P.W.; K. HAMILTON and R.J. WILSON. 1997. A very high resolution general circulation model simulation of the global circulation in austral winter. *J. Atmos. Sci*. **54**: 1107–1116.

KAROLY, D.J.; G.L. ROFF and M.J. REEDER. 1996. Gravity wave activity associated with tropical convection detected in TOGA COARE sounding data. *Geophys. Res. Lett*. **23**: 261–264.

KASAHARA, A.; T. SASAMORI and W.M. WASHINGTON. 1973. Simulation experiments with a 12-layer stratospheric global circulation model. I: Dynamical effect of the earth's orography and thermal influence of continentality. *J. Atmos. Sci.* **30**: 1229–1251.

KERSHAW, R. 1995. Parameterization of momentum transport by convectively generated gravity waves. *Q. J. R. Meteorol. Soc*. **121**: 1023–1040.

KIEHL, J.T.; J.J. HACK, G.B. BONAN, B.A. BOVILLE, D.L. WILLIAMSON and P.J. RASCH. 1998. The National Center for Atmospheric Research community climate model: CCM3. *J. Clim.* **11**: 1131–1149.

KIM, J. and L. MAHRT. 1992. Momentum transport by gravity waves. *J. Atmos. Sci*. **49**: 735–748.

KIM, Y.-J. 1996. Representation of subgrid-scale orographic effects in a general circulation model: Part I. Impact on the dynamics of a simulated January climate. *J. Clim.* **9**: 2698–2717.

——— and A. ARAKAWA. 1995. Improvement of orographic gravity-wave parameterization using a mesoscale gravity-wave model. *J. Atmos. Sci.* **52**: 1875–1902.

———; J.D. FARRARA and C.R. MECHOSO. 1998. Sensitivity of AGCM simulations to modifications in the ozone distribution and refinements in selected physical parameterizations. *J. Meteorol. Soc. Jpn.* **76**: 695–709.

KLEMP, J.B. and D.K. LILLY. 1978. Numerical simulation of hydrostatic mountain waves. *J. Atmos. Sci.* **35**: 78–107.

KLINKER, E. and P.D. SARDESHMUKH. 1992. The diagnosis of mechanical dissipation in the atmosphere from large-scale balance requirements. *J. Atmos. Sci*. **49**: 608–627.

KNOX, J.A. 1997. Generalized nonlinear balance criteria and inertial instability. *J. Atmos. Sci*. **54**: 967–985.

KOCH, S.E. and P.B. DORIAN. 1988. A mesoscale gravity-wave event observed during CCOPE, 3, wave environment and probable source mechanisms. *J. Atmos. Sci*. **116**: 2570–2592.

——— and C. O'HANDLEY. 1997. Operational forecasting and detection of mesoscale gravity waves. *Weather Forecast.* **12**: 253–281.

——— and L.M. SIEDLARZ. 1999. Mesoscale gravity waves and their environment in the central United States during STORM-FEST. *Mon. Weather Rev*. **127**: 2854–2879.

KOSHYK, J.N.; B.A. BOVILLE, K. HAMILTON, E. MANZINI and K. SHIBATA. 1999. Kinetic energy spectrum of horizontal motions in middle-atmosphere models. *J. Geophys. Res*. **104**: 27177–27190.

——— and K. HAMILTON. 2001. The horizontal kinetic energy spectrum and spectral budget simulated by a high-resolution troposphere-stratosphere-mesosphere GCM. *J. Atmos. Sci*. **58**: 329–348.

KUDEKI, E. and S.J. FRANKE. 1998. Statistics of momentum flux estimation. *J. Atmos. Sol.-Terr. Phys*. **60**: 1549–1553.

KUETTNER, J.P.; P.A. HILDERBRAND and T.L. CLARK. 1987. Convection waves: Observations of gravity wave systems over convectively active boundary layers. *Q. J. R. Meteorol. Soc*. **113**: 445–467.

LANDER, J. and B.J. HOSKINS. 1997. Believable scales and parameterizations in a spectral transform model. *Mon. Weather Rev*. **125**: 292–303.

LANE, T.; M.J. REEDER and T.L. CLARK. 2001. Numerical modeling of gravity wave generation by deep tropical convection. *J. Atmos. Sci.* **58**: 1249–1274.

LAWRENCE, B.N. 1997a. The effect of parameterized gravity wave drag on simulations of the middle atmosphere during northern winter 1991/1992 – general evolution. *In*: Proc. NATO Advanced Research Workshop "Gravity wave processes and their parameterization in global climate models". NATO ASI Series. Vol. I-50. K. Hamilton, (Ed.), Springer-Verlag. pp. 291–307.

———. 1997b. Some aspects of the sensitivity of stratospheric climate simulation to model lid height. *J. Geophys. Res.* **102**: 23805–23811.

———. 2001. A gravity wave-induced quasi-biennial oscillation in a three-dimensional mechanistic model. *Q. J. R. Meteorol. Soc*. **127**: 2005–2021.

LELONG, P. and T.J. DUNKERTON. 1998. Inertia-gravity wave breaking in three dimensions, 1, convectively stable waves. *J. Atmos. Sci*. **55**: 2473–2488.

LEOVY, C. 1964. Simple models of the thermally driven mesospheric circulation. *J. Atmos. Sci*. **21**: 327–341.

LEUTBECHER, M. and H. VOLERT. 2000. The propagation of mountain waves into the stratosphere: Quantitative evaluation of three-dimensional simulations. *J. Atmos. Sci*. **57**: 3090–3108.

LIN, Y.-L. 1987. Two-dimensional response of a stably stratified shear flow to diabatic heating. *J. Atmos. Sci.* **44:** 1375–1393.

——— and R.B. SMITH. 1986. Transient dynamics of airflow near a local heat source. *J. Atmos. Sci.* **43**: 40–49.

——— and H.-Y. CHUN. 1991. Effects of diabatic cooling in a shear flow with a critical level. *J. Atmos. Sci.* **48**: 2476–2491.

LINDZEN, R.S. 1981. Turbulence and stress owing to gravity wave and tidal breakdown. *J. Geophys. Res.* **86:** 9707–9714.

———. 1984. Gravity waves in the middle atmosphere. In: *Dynamics of the Middle Atmosphere*. J. R. Holton and T. Matsuno (Eds), Terra. pp. 3–18.

———. 1985. Multiple gravity-wave breaking levels. *J. Atmos. Sci.* **42**: 301–305.

———. 1988. Supersaturation of vertically propagating internal gravity waves. *J. Atmos. Sci*. **45**: 705–711.

——— and J.R. HOLTON. 1968. A theory of the quasi-biennial oscillation. *J. Atmos. Sci*. **25**: 1095–1107.

——— and M. FOX-RABINOVITZ. 1989. Consistent vertical and horizontal resolution. *Mon. Weather Rev*. **117**: 2575–2583.

LIU, H.L. 2000. Temperature changes due to gravity wave saturation. *J. Geophys. Res*. **105**: 12,329–12,336.

———; P.B. HAYS and R.G. ROBLE. 1999. A numerical study of gravity wave breaking and impacts on turbulence and mean state. *J. Atmos. Sci*. **56**: 2152–2177.

LOTT, F. 1999. Alleviation of stationary biases in a GCM through a mountain drag parameterization scheme and a simple representation of mountain lift forces. *Mon. Weather Rev*. **127**: 788–801.

——— and M.J. MILLER. 1997a. A new subgrid-scale orographic parameterization: its formulation and testing. *Q. J. R. Meteorol. Soc.* **123**: 101–127.

——— and ———. 1997b. The representation of sub-grid scale orography in GCMs. *In:* Gravity wave processes: their parameterization in global climate models. NATO ASI Series. Vol. I-50. K. Hamilton (Ed.), Springer-Verlag. pp. 275–290.

LUO, Z.A. and D.C. FRITTS. 1993. Gravity-wave excitation by geostrophic adjustment of the jet-stream, 2, 3-dimensional forcing. *J. Atmos. Sci*. **50**: 104–115.

MANSON, A.H.; C.E. MEEK, J. KOSHYK, S. FRANKE, D.C FRITTS, D. RIGGIN, C.M. HALL, W.K. HOCKING, J. MACDOUGALL, K. IGARASHI and R.A. VINCENT. 2002. Gravity wave activity and dynamical effects in the middle atmosphere (60–90 km): observations from an MF/MLT radar network, and results from the Canadian Middle Atmosphere Model (CMAM). *J. Atmos. Sol.-Terr. Phys.* **64**: 65–90.

MANZINI, E. and N.A. MCFARLANE. 1998. The effect of varying the source spectrum of a gravity wave drag parameterization in a middle atmosphere general circulation model. *J. Geophys. Res.* **103**: 31523–31539.

MARKS, C.J. and S.D. ECKERMANN. 1995. A three-dimensional nonhydrostatic ray-tracing model for gravity waves: formulation and preliminary results for the middle atmosphere. *J. Atmos. Sci*. **52**: 1959–1984.

MASON, P.J. 1986. On the parameterization of orographic drag. *In*: Proc. Seminar/Workshop on observation, theory and modeling of orographic effects. Sept. 1986, ECMWF, Shinfield Park, Reading, UK. Vol. 1 pp. 167–194.

MATSUNO, T. 1982. A quasi one-dimensional model of the middle atmosphere circulation interacting with internal gravity waves. *J. Meteorol. Soc. Jpn.* **60**: 215–227.

MCFARLANE, N.A. 1987. The effect of orographically excited gravity-wave drag on the general circulation of the lower stratosphere and troposphere. *J. Atmos. Sci.* **44**: 1775–1800.

———; C. GIRARD and D.W. SHANTZ. 1987. Reduction of systematic errors in NWP and general circulation models by parameterized gravity-wave drag. *J. Meteor. Soc. Jpn.* Special volume for the WMO/IUGG NWP symposium. Tokyo, Japan, 713–728.

———; C. MCLANDRESS and S. BEAGLEY. 1997. Seasonal simulations with the Canadian Middle Atmosphere Model: Sensitivity to a combination of orographic and Doppler spread parameterization of gravity wave drag. *In*: Proc. NATO Advanced Research Workshop "Gravity wave processes and their parameterization in global climate models". NATO ASI Series. Vol. I-50. K. Hamilton (Ed.), Springer-Verlag. pp. 351–366.

MCINTRYE, M.E. 1989. On dynamics and transport near the polar mesopause in summer. *J. Geophys. Res.* **94**: 14,617–14,628.

———. 2001. Global effects of gravity waves in the middle atmosphere: A theoretical perspective. *Adv. Space Res.* **27(10)**: 1723–1736.

——— and W.A. NORTON. 2000. Potential vorticity inversion on a hemisphere. *J. Atmos. Sci*. **57**: 1214–1235.

MCLANDRESS, C. 1997. Sensitivity studies using the Hines and Fritts gravity wave drag parameterizations. *In*: Proc. NATO Advanced Research Workshop "Gravity wave processes and their parameterization in global climate models". NATO ASI Series. Vol. I-50. K. Hamilton (Ed.), Springer-Verlag. pp. 245–255.

———. 1998. On the importance of gravity waves in the middle atmosphere and their parameterization in general circulation models. *J. Atmos. Terr. Phys.* **60**: 1357–1383.

——— and N.A. MCFARLANE. 1993. Interactions between orographic gravity wave drag and forced stationary planetary waves in the winter northern hemisphere middle atmosphere. *J. Atmos. Sci*. **50**: 1966–1990.

———; M.J. ALEXANDER and D.L. WU. 2000. Microwave Limb Sounder observations of gravity waves in the stratosphere: a climatology and interpretation. *J. Geophys. Res*. **105**: 11947–11967.

MEDVEDEV, A.S. and N.M. GAVRILOV. 1995. The nonlinear mechanism of gravity wave generation by meteorological motions in the atmosphere. *J. Atmos. Sol.-Terr. Phys.* **57**: 1221–1231.

——— and G.P. KLAASSEN. 1995. Vertical evolution of gravity wave spectra and the parameterization of associated wave drag. *J. Geophys. Res.* **100**: 25841–25853.

———; ——— and S.R. BEAGLEY. 1998. On the role of an anisotropic gravity wave spectrum in maintaining the circulation of the middle atmosphere. *Geophys. Res. Lett.* **25**: 509–512.

——— and ———. 2000. Parameterization of gravity wave momentum deposition based on nonlinear wave interactions: Basic formulation and sensitivity tests. *J. Atmos. Sol.-Terr. Phys.* **62**: 1015–1033.

——— and ———. 2001. Realistic semiannual oscillation simulated in a middle atmosphere general circulation model. *Geophys. Res. Lett.* **28**: 733–736.

MENGEL, J.H.; H.G. MAYR, K.L. CHAN, C.O. HINES, C.A. REDDY, N.F. ARNOLD and S.F. PORTER. 1995. Equatorial oscillations in the middle atmosphere generated by small-scale gravity waves. *Geophys. Res. Lett.* **22**: 3027–3030.

MESINGER, F. and W.G. COLLINS. 1986. Review of the representation of mountains in numerical weather prediction models. *In*: Proc. Seminar/Workshop on observation, theory and modeling of orographic effects. Vol. 2. ECMWF, Shinfield Park, Reading, U. K. 15–20 Sept. 1986, Vol. 2, pp. 1–28.

——— and Z.I. JANJIC. 1986. Numerical techniques for the representation of mountains. *In*. Proc. Seminar/Workshop on observation, theory and modeling of orographic effects ECMWF, Shinfield Park, Reading, U. K. Sept. 1986, Vol. 2, pp. 29–80.

MILLER, M.J.; T.N. PALMER and R. SWINKBANK. 1989. Parameterization and influence subgrid-scale orography in general circulation and numerical weather prediction models. *Meteorol. Atmos. Phys.* **40**: 84–109.

MILTON, S.F. and C.A. WILSON. 1996. The impact of parameterized subgrid-scale orographic forcing on systematic errors in a global NWP model. *Mon. Weather Rev.* **124**: 2023–2045.

MIRANDA, P.M.A. and M.A. VALENTE. 1997. Critical level resonance in three-dimensional flow past isolated mountains. *J. Atmos. Sci*. **54**: 1574–1588.

———; J.J. FERREIRA and A.J. THORPE. 1999. Gravity-wave drag produced by Madeira. *Q. J. R. Meteorol. Soc.* **125**: 1341–1357.

MULLEN, S.L. 1994. The impact of an envelope orography on low-frequency variability and blocking in a low-resolution general circulation model. *J. Clim*. **7**: 1815–1826.

NANCE, L.B. and D.R. DURRAN. 1997. A modeling study of nonstationary trapped mountain lee waves. Part I: Mean-flow variability. *J. Atmos. Sci*. **54**: 2275–2291.

——— and ———. 1998. A modeling study of nonstationary trapped mountain lee waves. Part II: Nonlinearity. *J. Atmos. Sci*. **55**: 1429–1445.

NAPPO, C.J. and G. CHIMONAS. 1992. Wave exchange between the ground surface and a boundary-layer critical level. *J. Atmos. Sci.* **49**: 1075–1091.

NASTROM, G.D.; T.E. VANZANDT and J.M. WARNOCK. 1997. Vertical wavenumber spectra of wind and temperature from high-resolution balloon soundings over Illinois. *J. Geophys. Res*. **102**: 6685–6701.

NEWMAN, P.A.; E.R. NASH and J.E. ROSENFIELD. 2001. What controls the temperature of the Arctic stratosphere during spring? *J. Geophys. Res*. **106**: 19999–20010.

NILSSON, E.D.; L. PIRJOLA and M. KULMALA. 2000. The effect of atmospheric waves on aerosol nucleation and size distribution. *J. Geophys. Res.* **105**: 19917–19926.

NISSEN, K.M.; P. BRAESICKE and U. LANGEMATZ. 2000. QBO, SAO, and tropical waves in the Berlin TSM GCM: Sensitivity to radiation, vertical resolution, and convection. *J. Geophys. Res.* **105**: 24771–24790.

NORTON, W.A. and J. THUBURN. 1999. Sensitivity of mesospheric mean flow, planetary waves, and tides to strength of gravity wave drag. *J. Geophys. Res*. **104**: 30,897–30,912.

ÓLAFSSON, H. and P. BOUGEAULT. 1997. The effect of rotation and surface friction on orographic drag. *J. Atmos. Sci.* **54**: 193–210.

OLSSON, P.Q. and W.R. COTTON. 1997. Balanced and unbalanced circulations in a primitive equation simulation of a midlatitude MCC. II. analysis of balance. *J. Atmos. Sci*. **54**: 479–497.

OSPREY, S.M. 2001. Climate response to a variable gravity-wave source, Ph. D. thesis, Dept. Physics, University of Canterbury, New Zealand, 175 pp.

O'SULLUVAN, D. and T.J. DUNKERTON. 1995. Generation of inertia-gravity waves in a simulated life-cycle of baroclinic instability. *J. Atmos. Sci*. **52**: 3695–3716.

PALMER, T.N. and D.A. MANSFIELD. 1986. A study of wintertime circulation anomalies during past El Niño events, using a high resolution general circulation model, I: Influence of model climatology. *Q. J. R. Meteorol. Soc.* **112**: 613–638.

———; G.J. SHUTTS and R. SWINBANK. 1986. Alleviation of a systematic westerly bias in circulation and numerical weather prediction models through an orographic gravity-wave drag parameterization. *Q. J .R. Meteorol. Soc.* **112**: 1001–1039.

PANDYA, R.E. and M.J. ALEXANDER. 1999. Linear stratospheric gravity waves above convective thermal forcing. *J. Atmos. Sci.* **56**: 2434–2446.

PAVELIN, E.; J.A. WHITEWAY and G. VAUGHAN. 2001. Observation of gravity wave generation and breaking in the lowermost stratosphere. *J. Geophys. Res*. **106**: 5173–5179.

PAWSON, S.; U. LANGEMATZ, G. RADEK, U. SCHLESE and P. STRAUCH. 1998. The Berlin troposphere – stratosphere – mesosphere GCM: Sensitivity to physical parameterizations. *Q. J. R. Meteorol. Soc*. **124**: 1343–1371.

———; K. KODERA, K. HAMILTON, T.G. SHEPHERD, S.R. BEAGLEY, B.A. BOVILLE, J.D. FARRARA, T.D.A. FAIRLIE, A. KITOH, W.A. LAHONZ, U. LANGEMATZ, E. MANZINI, D.H. RIND, A.A. SCAIFE, K. SHIBATA, P. SIMON, R. SWINBANK, L. TAKACS, R. GRANDPRÉ, R.S. ECKMAN, M. FIORINO, W.L. GROSS, H. KOIDE, J.C.R. MECHOSA, A. MOLOD, A. O'NEILL, R.B. PIERCE, W.J. RANDEL, R.B. ROOD and F. WU. 2000. The GCM-reality intercomparison project for SPARC (GRIPS): Scientific issues and initial results. *Bull. Am. Meteorol. Soc*. **81**: 781–796.

PELTIER, W.R. and T.L. CLARK. 1979. The evolution and stability of finite-amplitude mountain waves. Part II: Surface-wave drag and severe downslope windstorms. *J. Atmos. Sci.* **36**: 1498–1529.

PENG, M.S.; S.-W. LI, S.W. CHANG and R.T. WILLIAMS. 1995. Flow over mountains: Coriolis force, transient troughs and three dimensionality. *Q. J. R. Meteorol. Soc.* **121**: 593–613.

PFISTER, L.; S. SCOTT and M. LOEWENSTEIN. 1993. Mesoscale disturbances in the tropical stratosphere excited by convection: Observations and effects on the stratospheric momentum budget. *J. Atmos. Sci*. **50**: 1058–1075.

PIANI, C.; D. DURRAN, M.J. ALEXANDER and J.R. HOLTON. 2000. A numerical study of three-dimensional gravity waves triggered by deep tropical convection and their role in the dynamics of the QBO. *J. Atmos. Sci.* **57**: 3689–3702.

PIERREHUMBERT, R.T. 1986. An essay on the parameterization of orographic gravity-wave drag. *In*: Proc. Seminar/Workshop on observation, theory and modeling of orographic effects. ECMWF, Shinfield Park, Reading, U.K. 15–20 Sept. 1986, Vol. 1. pp. 251–282.

POWERS, J.G. 1997. Numerical model simulations of a mesoscale gravity wave event: sensitivity tests and spectral analyses. *Mon. Weather Rev*. **125**: 1838–1869.

PREUSSE, P.; G. EIDMANN, S.D. ECKERMANN, B. SCHAELER, R. SPANG and D. OFFERMANN. 2001. Indications of convectively generated gravity waves in CRISTA temperatures. *Adv. Space Res*. **27(10)**: 1653–1658.

PRUSA, J.M.; P.K. SMOLARKIEWICZ and R.R. GARCIA. 1996. Propagation and breaking at high altitudes of gravity waves excited by tropospheric forcing. *J. Atmos. Sci*. **53**: 2186–2216.

REEDER, M.J. and M. GRIFFITHS. 1996. Stratospheric inertia-gravity waves generated in a numerical model of frontogenesis, 2, wave sources, generation mechanisms and momentum fluxes. *Q. J. R. Meteorol. Soc*. **122**: 1175–1195.

REINKING, R.F.; J.B. SNIDER and J.L. COEN. 2000. Influences of storm-embeded orographic gravity waves on cloud liquid water and precipitation. *J. Appl. Meteorol*. **39**: 733–759.

RICCIARDULLI, L. and R.R. GARCIA. 2000. The excitation of equatorial waves by deep convection in the NCAR Community Climate Model (CCM3). *J. Atmos. Sci.* **57**: 3461–3487.

RICHARD, E.; N. CHAUMERLIAC and J.F. MAHFOUF. 1987. Numerical simulation of orographic enhancement of rain with a mesoscale model. *J. Clim. Appl. Meteorol.* **26**: 661–669.

———; P. MASCART and E.C. MICKERSON. 1989. The role of surface friction in downslope windstorms. *J. Appl. Meteorol.* **28**: 241–251.

RIND, D.; R. SUOZZO, N.K. BALACHANDRAN, A. LACIS and G. RUSSELL. 1988. The GISS Global Climate-Middle Atmosphere Model. Part I: Model structure and climatology. *J. Atmos. Sci.* **45**: 329–370.

SALBY, M.L. and R.R. GARCIA. 1987. Transient-response to localized episodic heating in the tropics, 1, excitation and short-time near-field behavior. *J. Atmos. Sci.* **44**: 458–498.

SATO, K. 1993. Small-scale wind disturbances observed by the MU radar during the passage of Typhoon Kelly. *J. Atmos. Sci*. **50**: 518–537.

———; T. KUMAKURA and M. TAKAHASHI. 1999. Gravity waves appearing in a high-resolution GCM simulation. *J. Atmos. Sci*. **56**: 1005–1018.

SATO, T. and R.F. WOODMAN. 1982. Fine altitude resolution observations of stratospheric turbulent layers by the Arecibo 430 MHz radar. *J. Atmos. Sci*. **39**: 2546–2552.

SAWYER, J.S. 1959. The introduction of the effects of topography into methods of numerical forecasting. *Q. J. R. Meteorol. Soc*. **85**: 31–43.

SCAIFE, A.A.; N. BUTCHART, C.D. WARNER, D. STAINFORTH, W. NORTON and J. AUSTIN. 2000. Realistic quasi-biennial oscillations in a simulation of the global climate. *Geophys. Res. Lett.* **27**: 3481–3484.

SCHÄR, C. and D.R. DURRAN. 1997. Vortex formation and vortex shedding in continuously stratified flows past isolated topography. *J. Atmos. Sci*. **54**: 534–554.

SCHOEBERL. M.R. and D.F. STROBEL. 1978. The zonally averaged circulation of the middle atmosphere. *J. Atmos. Sci*. **35**: 577–591.

SCINOCCA, J.F. 2002. The effect of back reflection in the parameterization of nonorographic gravity wave drag. *J. Meteorol. Soc. Jpn.* Special issue on Stratosphere-Troposphere Coupling. **80**: 939–962.

——— and R. FORD. 2000. The nonlinear forcing of large-scale internal gravity waves by stratified shear instability. *J. Atmos. Sci*. **57**: 653–672.

——— and N.A. MACFARLANE. 2000. The parameterization of drag induced by stratified flow over anisotropic topography. *Q. J. R. Meteorol. Soc*. **126**: 2353–2393.

SHARMAN, R.D. and M.G. WURTELE. 1983. Ship waves and lee waves. *J. Atmos. Sci*. **40**: 396–427.

SHEPHERD, T.G. 2000. The middle atmosphere. *J. Atmos.-Terr. Phys.* **62**: 1587–1601.

———; K. SEMENIUK and J.N. KOSHYK. 1996. Sponge layer feedbacks in middle-atmosphere models. *J. Geophys. Res*. **101**: 23447–23464.

SHUTTS, G.J. 1995. Gravity-wave drag parameterization over complex terrain: The effect of critical-level absorption in directional wind-shear. *Q. J. R. Meteorol. Soc.* **121**: 1005–1021.

———. 1998. Stationary gravity-wave structure in flows with directional wind shear. *Q. J. R. Meteorol. Soc.* **124**: 1421–1442.

SMAGORINSKY, J. 1967. The role of numerical modeling. *Bull. Am. Meteorol. Soc*. **46**: 89–93.

SMITH, R.B. 1978. A measurement of mountain drag. *J. Atmos. Sci.* **35**: 1644–1654.

———. 1979. The influence of mountains on the atmosphere. *Adv. Geophys.* **33**: 87–230.

———. 1980. Linear-theory of stratified hydrostatic flow past an isolated mountain. *Tellus,* **32**: 348–364.

———. 1989. Mountain-induced stagnation points in hydrostatic flow. *Tellus,* **41A**: 270–274.

———. 2001. Stratified flow over topography. In: Environmental Stratified Flows, Topics In Environmental Fluid Mechanics. Vol. 3, R. Grimshaw (Ed.), Kluwer, London. pp. 121–159.

——— and Y.-L. LIN. 1982. The addition of heat to a stratified airstream with application to the dynamics of orographic rain. *Q. J. R. Meteorol. Soc*. **108**: 353–378.

———; S. SKUBIS, J.D. DOYLE, A.S. BROAD, C. KIEMLE and H. VOLKERT. 2002. Mountain waves over Mt. Blanc: Influence of a stagnant boundary layer. *J. Atmos. Sci.* **59**: 2073–2092.

SMITH, S.A.; D.C. FRITTS and T.E. VANZANDT. 1987. Evidence for a saturated spectrum of atmospheric gravity waves. *J. Atmos. Sci.* **44**: 1404–1410.

SMOLARKIEWICZ, P. K.; L.G. MARHOLIN and A.A. WYSZOGRODZKI. 2001. A class of global nonhydrostatic models. *J. Atmos. Sci*. **58**: 349–364.

SURGI, N. 1989. Systematic errors of the FSU global spectral model. *Mon. Weather Rev*. **117**: 1751–1766.

SUTHERLAND, B.R. and W.R. PELTIER. 1995. Internal gravity wave emission into the middle atmosphere from a model tropospheric jet. *J. Atmos. Sci*. **52**: 3214–3235.

SWINBANK, R. 1985. The global atmospheric angular-momentum balance inferred from analyses made during the FGGE. *Q. J. R. Meteorol. Soc.* **111**: 977–992.

TAKAHASHI, M. 1996. Simulation of the stratospheric quasi-biennial oscillation using a general circulation model. *Geophys. Res. Lett*. **23**: 661–664.

——— and B.A. BOVILLE. 1992. A three-dimensional simulation of the equatorial quasi-biennial oscillation. *J. Atmos. Sci.* **49**: 1020–1035.

THOMPSON, D.W.J.; M.P. BALDWIN and J.M. WALLACE. 2002. Stratospheric connection to northern hemisphere winter weather: implications for prediction. *J. Clim*. **15**: 1421–1428.

TIBALDI, S. 1986. Envelope orography and the maintenance of quasi-stationary waves in the ECMWF model. *Adv. Geophys.* **29**: 339–374.

TSUDA, T.; Y. MURAYAMA. H. WIRYOSUMARTO, S.W.B. HARIJONO and S. KATO. 1994. Radiosonde observations of equatorial atmospheric dynamics over Indonesia 2. Characteristics of gravity waves. *J. Geophys. Res.* **99***:* 10507–10516.

———; M. NISHIDA, C. ROCKEN and R.H. WARE. 2000. A global morphology of gravity wave activity in the stratosphere revealed by the GPS occultation data (GPS/MET). *J. Geophys. Res*. **99**: 7257–7273.

UCCELLINI, L.W. and S.E. KOCH. 1987. The synoptic setting and possible energy-sources for mesoscale wave disturbances. *Mon. Weather Rev*. **115**: 721–729.

VADAS, S.L. and D.C. FRITTS. 2001. Gravity wave radiation and mean responses to local body forces in the atmosphere. *J. Atmos. Sci*. **58**: 2249–2279.

VANZANDT, T.E. 1982. A universal spectrum of buoyancy waves in the atmosphere. *Geophys. Res. Lett*. **9**: 575–578.

VINCENT, R.A. and M.J. ALEXANDER. 2000. Gravity-waves in the tropical lower stratosphere: An observational study of seasonal and interannual variability. *J. Geophys. Res*. **105**: 17971–17982.

VOSPER, S.B. and S.D. MOBBS. 1997. Measurement of the pressure field on a mountain. *Q. J. R. Meteorol. Soc.* **123**: 129–144.

——— and ———. 1998. Momentum fluxes due to three-dimensional gravity-waves: Implications for measurements and numerical modeling. *Q. J. R. Meteorol. Soc*. **124**: 2755–2769.

WALLACE, J.; S. TIBALDI and A. SIMMONS. 1983. Reduction of systematic forecast errors in the ECMWF model through the introduction of an envelope orography. *Q. J. R. Meteorol. Soc.* **109**: 683–717.

WALTERSCHEID. R.L. 2000. Propagation of small-scale gravity waves through large-scale internal wave fields: eikonal effects at low-frequency approximation critical levels. *J. Geophys. Res*. **105**: 18027–18037.

WARNER, C.D. and M.E. MCINTYRE. 1996. On the propagation and dissipation of gravity wave spectra through a realistic middle atmosphere. *J. Atmos. Sci*. **53**: 3213–3235.

——— and ———. 1999. Toward an ultra-simple spectral gravity wave parameterization for general circulation models. *Earth Planets Space,* **51**: 475–484.

——— and ———. 2001. An ultrasimple spectral parameterization for nonorographic gravity waves. *J. Atmos. Sci.* **58**: 1837–1857.

WEINSTOCK, J. 1990. Saturated and unsaturated spectra of gravity waves and scale-dependent diffusion. *J. Atmos. Sci.* **47**: 2211–2225.

WEISSBLUTH, M.J. and W.R. COTTON. 1989. Radiative and nonlinear influences on orographic gravity wave drag. *Mon. Weather Rev*. **117**: 2518–2534.

WHITEWAY, J. 1999. Enhanced and inhibited gravity wave spectra. *J. Atmos. Sci*. **56**: 1344–1352.

WOOD, N. 2000. Wind flow over complex terrain: a historical perspective and the prospect for large-eddy modeling. *Boundary-Layer Meteorol*. **96**: 11–32.

——— and P.J. MASON. 1993. The pressure force induced by neutral turbulent flow over hills. *Q. J. R. Meteorol. Soc.* **119**: 1233–1267.

———; A.R. BROWN and F.E. HEWER. 2001. Parameterizing the effects of orography on the boundary layer: An alternative to effective roughness lengths. *Q. J. R. Meteorol. Soc.* **127**: 759–777.

WORTHINGTON, R.M. 2001. Alignment of mountain lee waves viewed using NOAA AVHRR imagery, MST radar, and SAR. *Int. J. Remote Sens*. **22**: 1361–1374.

——— and L. THOMAS. 1996. The measurement of gravity wave momentum flux in the lower atmosphere using VHF radar. *Radio Sci*. **31**: 1501–1517.

WU, X. and M.W. MONCRIEFF. 2001. Sensitivity of single-column model solutions to convective parameterizations and initial conditions. *J. Clim*. **14**: 2563–2582.

WURTELE, M.G.; R.D. SHARMAN and T.L. KELLER. 1987. Analysis and simulations of a troposphere-stratosphere gravity wave model. Part I. *J. Atmos. Sci*. **44**: 3269–3281.

———; ——— and A. DATTA. 1996. Atmospheric lee waves. *Ann. Rev. Fluid Mech*. **28**: 429–476.

YAMAMOTO, M.; T. TSUDA, S. KATO, T. SATO and S. FUKAO. 1987. A saturated inertia gravity-wave in the mesosphere observed by the middle and upper-atmosphere radar. *J. Geophys. Res*. **92**: 11993–11999.

ZHANG, F.; S.E. KOCH, C. A. DAVIS AND M.L. KAPLAN. 2000. A survey of unbalanced flow diagnostics and their application. *Adv. Atmos. Sci*. **17**: 205–218.

———; ———, ——— and ———. 2001. Wavelet analysis and the governing dynamics of a large-amplitude mesoscale gravity-wave event along the east coast of the United States. *Q. J. R. Meteorol. Soc.* **127**: 2209–2245.

ZHOU, J.Y.; Y.C. SUD and K.M. LAU. 1996. Impact of orographically induced gravity-wave drag in the GLA GCM. *Q. J. R. Meteorol. Soc*. **122**: 903–927.